

Aus dem Max-Delbrück-Centrum für Molekulare Medizin –
Zelluläre Neurowissenschaften

DISSERTATION

Endogenous neural precursor cells suppress glioblastoma

Zur Erlangung des akademischen Grades
Doctor of Philosophy in Medical Neurosciences
(PhD in Medical Neurosciences)

vorgelegt der Medizinischen Fakultät
Charité – Universitätsmedizin Berlin

von

Joo-Hee Wälzlein

aus Seoul, Süd-Korea

Gutachter: 1. Prof. Dr. H. Kettenmann
2. Prof. Dr. M. Weller
3. Prof. Dr. med. M. Endres

Datum der Promotion: 29. Oktober 2007

Table of content

I.	List of figures	1
II.	List of tables	3
III.	Abbreviations	4
1.	<u>Introduction</u>	6
1.1.	Neural precursor cells	6
1.1.1.	The two stem cell niches and stem cell hierarchy	6
1.1.2.	Subtypes of neural precursor cells	8
1.1.3.	Physiology of neural precursor cells in the intact brain	9
1.1.4.	Neural precursor cells in the diseased brain	9
1.1.5.	Therapeutic perspectives	10
1.2.	Neural precursor cells are the likely cell of origin of brain tumours	10
1.2.1.	Clinical evidence for origin of glioblastoma from neural precursor cells	10
1.2.2.	Experimental evidence for origin of glioblastoma from neural precursor cells	11
1.3.	Brain tumours and their classification	11
1.3.1.	Epidemiology of gliomas	12
1.3.2.	The pathophysiology of glioblastoma	12
1.3.3.	Diagnosis and treatment of glioblastoma	14
1.4.	Cancer stem cells	15
1.4.1.	The cancer stem cell hypothesis	15
1.4.2.	Properties of cancer stem cells	16
1.4.3.	Cancer stem cells may represent novel therapeutic targets	16
1.5.	Cell death pathways	17
1.5.1.	Apoptosis	17
1.5.2.	Alternative non-apoptotic cell death pathways	18
1.6.	Aim of the study	20

2.	<u>Material and Methods</u>	21
2.1.	Material	21
2.1.1.	Devices	21
2.1.2.	Plastic ware and other material	22
2.1.3.	Chemicals	22
2.1.4.	Enzymes	24
2.1.5.	Kits	24
2.1.6.	Antibodies	25
2.1.6.1.	Primary antibodies	25
2.1.6.2.	Secondary antibodies	25
2.1.7.	Oligonucleotides (PCR primers and siRNA)	26
2.1.8.	Plasmids	26
2.1.9.	Media and buffer	27
2.1.9.1.	Cell culture media	27
2.1.9.2.	Bacteria propagation	28
2.1.9.3.	Buffers for immunolabelling	28
2.1.9.4.	Buffers for PCR	28
2.1.9.5.	Buffers and solutions for Western Blots	28
2.1.10.	Software	29
2.2.	Methods	29
2.2.1.	<i>In vivo</i> inoculation of GL261 glioma cells into the mouse brain	29
2.2.1.1.	Anaesthesia	29
2.2.1.2.	GL261 glioma cell inoculation into the mouse brain	29
2.2.1.3.	BrdU injections	30
2.2.1.4.	DiI injections	30
2.2.1.5.	Retrovirus injections	30
2.2.2.	Paraformaldehyde fixation	30
2.2.3.	Immunohistochemistry of brain sections (floating sections)	31
2.2.4.	Survival study	31
2.2.5.	TUNEL and Hoechst 33358 labelling	31
2.2.6.	Cell counting and unbiased stereology	31
2.2.7.	Explant co-cultures	32
2.2.8.	Cell culture of neural precursor cells	32

2.2.9.	Cell culture of glioma cells	33
2.2.10.	Cell co-culture experiments and cell counting	33
2.2.11.	DNA Microarray	33
2.2.11.1.	Stimulation paradigm	33
2.2.11.2.	RNA-isolation	34
2.2.11.3.	Microarray hybridization	34
2.2.11.4.	Image acquisition and data analysis	34
2.2.11.5.	Identification of differentially expressed genes and cluster analysis	35
2.2.12.	TUNEL assays	35
2.2.12.1.	The DELFIA DNA fragmentation assay	35
2.2.12.2.	The <i>In situ</i> cell death detection kit, POD	36
2.2.13.	Immunolabelling	36
2.2.14.	Microscopy	36
2.2.14.1.	Fluorescence microscopy	36
2.2.14.2.	Confocal microscopy	37
2.2.14.3.	Preparation of cryosections and electron microscopy	37
2.2.15.	BrdU assay	37
2.2.16.	Transfection methods	38
2.2.16.1.	Electroporation (Nucleofection™)	38
2.2.16.2.	Lipofectamine transfection	38
2.2.16.3.	Retroviral transfection	39
2.2.17.	Fluorescence Assisted Cell Sorting (FACS)	39
2.2.18.	Western blot	39
2.2.18.1.	Sample preparation	39
2.2.18.2.	SDS-PAGE	40
2.2.18.3.	Semi-dry transblotting	40
2.2.18.4.	Immunoblotting	40
2.2.19.	Identification of mRNA transcripts	41
2.2.19.1.	RNA-isolation (RNeasy Mini Kit)	41
2.2.19.2.	Reverse transcription (RT) - PCR	41
2.2.19.3.	Polymerase chain reaction (PCR)	42
2.2.19.4.	Gel electrophoresis of the PCR products	43

2.2.20.	Statistical analysis	43
3.	<u>Results</u>	44
3.1.	Neural precursor cells from the subventricular zone migrate towards experimental gliomas <i>in vivo</i> and <i>in vitro</i>	44
3.1.1.	Endogenous neural precursor cells accumulate around glioblastomas <i>in vivo</i>	44
3.1.1.1.	Accumulation of neural precursor cells is specifically induced by glioblastoma	45
3.1.1.2.	Nestin-GFP-positive cells around glioblastoma are genuine precursor cells	46
3.1.2.	Neural precursor cells around glioblastomas originate from the subventricular zone	47
3.1.3.	Neural precursor cells from the subventricular zone are attracted by GL261 glioma cells <i>in vitro</i>	49
3.2.	Neural precursor cells show an anti-tumourigenic response <i>in vivo</i> and <i>in vitro</i>	51
3.2.1.	Survival of experimental glioblastomas is dependent on the age-defined number of neural precursor cells at the tumour	51
3.2.2.	The anti-tumourigenic response in young and adult mice	52
3.2.2.1.	Age-related decrease of subventricular proliferation is further reduced by glioblastoma	52
3.2.2.2.	Whole cell numbers in the subventricular zone are independent of pathology	54
3.2.2.3.	Cell death rate in the subventricular zone is independent of pathology	55
3.2.2.4.	The composition of (proliferating) subventricular precursor cells in the pathological young and adult brain	56
3.2.2.5.	The proliferative response of neural precursor cells to glioma is intrinsic and stable	58
3.2.2.6.	The expression of cyclin D1 in neural precursor cells declines with increasing age	59

3.2.2.7.	Loss of D-type cyclins in the subventricular zone attenuates neural precursor cell proliferation	61
3.2.2.8.	Loss of D-type cyclins results in increased tumour size	62
3.2.3.	The anti-tumourigenic response of neural precursor cells <i>in vitro</i>	63
3.2.3.1.	Neural precursor cells reduce total GL261 glioma cell number	63
3.2.3.2.	Neural precursor cell-conditioned medium reduces total GL261 glioma cell number	64
3.2.3.3.	Neural precursor cells induce GL261 glioma cell death	65
3.2.3.4.	The influence of passage number and days of conditioning on the efficacy of neural precursor cell-conditioned medium	65
3.2.3.5.	Neural precursor cell-conditioned medium induces cell death in human glioma cells	66
3.2.3.6.	Release of GL261 glioma cell death inducing factor from neural precursor cells is age-independent	67
3.3.	Characterization of GL261 glioma cell death induced by neural precursor cells	68
3.3.1.	Neural precursor cell induced GL261 glioma cell death is not apoptosis	68
3.3.1.1.	Neural precursor cell induced GL261 glioma cell death is caspase-independent	68
3.3.1.2.	Neural precursor cell induced GL261 glioma cell death is not death-receptor mediated	70
3.3.2.	GL261 glioma cells undergo morphological changes upon stimulation with neural precursor cell-conditioned medium	71
3.3.3.	Differential gene expression in GL261 glioma cells induced by neural precursor cell-conditioned medium	72
3.3.4.	Activating transcription factor-3 is necessary and sufficient for induction of GL261 glioma cell death	74
3.3.4.1.	Activating transcription factor-3 is upregulated in GL261 glioma cells upon stimulation with neural precursor cell-conditioned medium	74

3.3.4.2.	Activating transcription factor-3 overexpression in GL261 glioma cells results in increased cell death	75
3.3.4.3.	siRNA against activating transcription factor-3 prevents GL261 glioma cell death upon stimulation with neural precursor cell-conditioned medium	76
4.	<u>Discussion</u>	78
4.1.	Neural precursor cells are attracted by experimental gliomas	78
4.1.1.	Glioma-induced attraction of subventricular neural precursor cells is an intrinsic tissue response	78
4.2.	The anti-tumourigenic response of neural precursor cells	78
4.2.1.	The age-related number of neural precursor cells around glioblastoma determines the extent of the anti-tumourigenic response	78
4.2.2.	Subventricular proliferation as the key regulator between the distinct anti-tumourigenic response of young and adult mice	79
4.2.3.	D-type cyclin expression controls the anti-tumourigenic response of neural precursor cells	80
4.2.4.	The proliferative response of neural precursor cells to gliomas is independent of p21	81
4.2.5.	The subventricular composition and the fraction of proliferating cells in young and old animals in the tumour-bearing hemisphere	82
4.2.6.	The anti-tumourigenic response of neural precursor cells is directly mediated via soluble factors	83
4.3.	The character of neural precursor cell mediated glioma cell death	83
4.3.1.	The role of activating transcription factor-3 in neural precursor cell induced glioma cell death	83
4.3.2.	Neural precursor cell mediated glioma cell death – an alternative to apoptosis	85

4.3.3.	Endoplasmic reticulum stress as the likely glioma cell death inducing pathway	85
4.4.	Neural precursor cells and their clinical relevance for gliomas	86
4.4.1.	Neural precursor cells as delivery vehicles for therapeutic substances	87
4.4.1.1.	Potential chemoattractants for neural precursor cells	87
4.5.	Regulation of neurogenesis throughout aging	88
4.5.1.	Correlation between neuronal plasticity and the anti-tumourigenic effect of neural precursor cells	88
4.5.2.	The anti-tumourigenic ability of neural precursor cells as a rescue mechanism for their likely transformation	89
5.	Summary	90
6.	References	92
	Acknowledgements	100
	Curriculum vitae	101
	List of publications	103
	Meetings with poster presentations	104
	Eidesstattliche Erklärung	105

I. List of figures

Fig. 1.1.	The two germinative centres in the adult mouse brain, the dentate gyrus and the subventricular zone (longitudinal section)	6
Fig. 1.2.	Hierarchy of stem cells	7
Fig. 1.3.	Macroscopic view of glioblastoma multiforme in a human brain	13
Fig. 1.4.	MRT of a human brain, revealing a glioblastoma multiforme	14
Fig. 1.5.	Cancer stem cell specific and conventional cancer therapy	17
Fig. 1.6.	The distinct steps of apoptosis	18
Fig. 3.1.	Endogenous neural precursor cells surround experimental glioblastoma	44
Fig. 3.2.	Time course of NPC attraction to glioblastomas or stab wounds	45
Fig. 3.3.	Nestin-GFP-positive cells around glioma are characterized as genuine neural precursor cells	46
Fig. 3.4.	Neural precursor cells around glioblastomas stem from a germinative centre	47
Fig. 3.5.	Neural precursor cells around glioblastomas stem from the SVZ	48
Fig. 3.6.	Migration of subventricular NPCs towards glioma cell aggregates <i>in vitro</i>	50
Fig. 3.7.	Attraction of NPCs towards experimental glioblastomas and development of tumour formation in P25, P100, P180 and P400 mice	51
Fig. 3.8.	Younger (P25) outlive older (P180) mice after GL261 inoculation. Exogenously applied NPCs into old (P180) animals prolong the survival of glioblastomas	52
Fig. 3.9.	Subventricular proliferation declines in the tumour-bearing hemisphere in adult compared to young mice	53
Fig. 3.10.	Whole cell numbers in the SVZ of young and of adult mice after glioma injection	54
Fig. 3.11.	The number of TUNEL-positive SVZ cells is not affected by the presence of a tumour	55
Fig. 3.12.	Numbers of total and proliferating precursor subtypes in the SVZ, ipsilaterally to the tumour in P30 and P90 animals	57

Fig. 3.13.	The diminished proliferative response of P90 NPCs towards tumours is stable under <i>in vitro</i> conditions	58
Fig. 3.14.	Cyclin D2 expression becomes predominant in subventricular NPCs during aging	59
Fig. 3.15.	Loss of cyclin D2 expression results in reduced proliferation in the SVZ	61
Fig. 3.16.	Absence of cyclin D2 leads to increased tumour sizes	62
Fig. 3.17.	Reduction of GL261 glioma cell number by neural precursor cells	63
Fig. 3.18.	Reduction of GL261 glioma cell number by neural precursor cell-conditioned medium	64
Fig. 3.19.	Induction of GL261 glioma cell death by neural precursor cell-conditioned medium	65
Fig. 3.20.	Induction of TUNEL positive GL261 by different NPC-conditioned media	66
Fig. 3.21.	Reduction of total cell number of human glioma cells by NPC-conditioned medium	67
Fig. 3.22.	NPCs from P30 and P90 animals hold an age-independent capability to induce GL261 cell death	68
Fig. 3.23.	The caspase inhibitor Z-VAD-FMK does not affect NPC-conditioned medium induced GL261 cell death	69
Fig. 3.24.	GL261 cells do not express active caspase-3 and -7 after treatment with NPC-conditioned medium	70
Fig. 3.25.	NPC-conditioned medium does not induce apoptosis in death-receptor mediated cell death sensitive tumour cells	71
Fig. 3.26.	Electron microscopy of GL261 glioma cells cultured in fresh and NPC-conditioned medium	72
Fig. 3.27.	ATF-3 distribution in GL261 glioma cells changes from cytoplasmatic localization to nuclear expression upon treatment with NPC-conditioned medium	74
Fig. 3.28.	ATF-3 overexpression in GL261 results in reduction of total cell numbers and induction of cell death	75
Fig. 3.29.	siRNA against ATF-3 prevents NPC-conditioned medium induced GL261 cell death	76

II. List of tables

Tab. 1.1.	Expression pattern of marker proteins for type B-, C- and A cells	9
Tab. 1.2.	The World Health Organization (WHO) grading system for astrocytomas	12
Tab. 2.1.	Overview of applied primary antibodies	25
Tab. 2.2.	Overview of applied secondary antibodies	25
Tab. 2.3.	Overview of used oligonucleotides	26
Tab. 2.4.	Overview of plasmids	26
Tab. 2.5.	Overview of media and buffer in cell culture	27
Tab. 2.6.	Medium for bacterial cultures	28
Tab. 2.7.	Buffers for immunolabelling	28
Tab. 2.8.	Buffers for PCR	28
Tab. 2.9.	Buffers and solutions for Western Blots	28
Tab. 2.10.	Software	29
Tab. 2.11.	Reaction mixture for the DELFIA DNA fragmentation assay	35
Tab. 2.12.	Composition of a 10 % SDS polyacrylamide gel	40
Tab. 2.13.	PCR reaction mixture	42
Tab. 2.14.	PCR-temperature profiles and number of cycles	42
Tab. 3.1.	Criteria for identifying proliferating B-, C- and A cells	57
Tab. 3.2.	Gene expression changes in GL261 cells after stimulation with NPC-conditioned medium (3d)	73

III. Abbreviation

Amp	Ampicillin resistance
BBB	Blood brain barrier
bp	Basepair
BSA	Bovine serum albumin
cDNA	Copy DNA
CMV	Cytomegalovirus
CO ₂	Carbondioxide
DMSO	Dimethyl sulfoxide
DNA	Desoxyribonucleic acid
<i>et al.</i>	<i>et alii</i> (lat.: and others)
e.g.	<i>exempli gratia</i> (lat.: for example)
EGFP	Enhanced green fluorescent protein
Eu	Europium
FACS	Fluorescence Assisted Cell Sorting
FITC	Fluorescein-5-isothiocyanate
GFAP	Glial fibrillary acidic protein
GFP	Green fluorescent protein
HRP	Horseradish peroxidase
Ig	Immunoglobulin
MAPK	Mitogen activated protein kinase
MPSV	Myeloproliferative sarcoma virus
mRNA	Messenger RNA
NPC	Neural precursor cell
PCR	Polymerase chain reaction
RNA	Ribonucleic acid
RT	Room temperature
RT-PCR	Reverse transcriptase PCR
rpm	Revolutions per minute
SDS-PAGE	Sodium dodecylsulfate polyacrylamide gel electrophoresis
SVZ	Subventricular zone

TRAIL	Tumor necrosis (TNF)-related apoptosis-inducing ligand
TRITC	Tetramethylrhodamine isothiocyanate
ON	Overnight
UV	Ultraviolet
wt	Wildtype

1. Introduction

1.1. Neural precursor cells

It was in the 1960s when neurogenesis in the adult mammalian central nervous system was first described (2). However, it took 30 years until neural stem cells were for the first time isolated from the adult mouse brain (58), which proved the existence of adult neurogenesis, a milestone in the field of neuroscience at that time. So only since that time was the “no new neuron” dogma disproven.

The two cardinal features of a stem cell are unlimited self-renewal and multipotency. The first criterion implies that cell division results in the generation of at least one identical copy of the mother cell. In case the mother cell produces two identical copies the term *symmetric cell division* is used whereas in contrast *asymmetric cell division* means that one copy of the mother cell and one more differentiated cell is generated. Multipotency describes the ability of a cell to generate at least two different cell types.

The direct progeny of a neural stem cell is the neural progenitor cell. Although the latter is more differentiated than a neural stem cell it is sometimes difficult to distinguish between these two cell developmental stages. Hence, the term *neural precursor cell* was introduced, which combines neural stem cells and neural progenitor cells and implies that the cell is undifferentiated and dividing (36).

1.1.1. The two stem cell niches and stem cell hierarchy

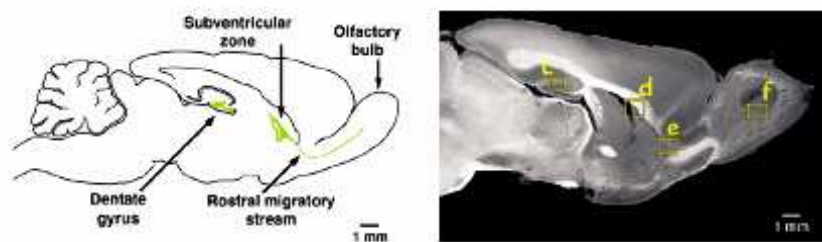


Fig. 1.1. The two germinative centres in the adult mouse brain, the dentate gyrus and the subventricular zone (longitudinal section). Also shown is the rostral migratory stream, along which the neural precursor cells from the subventricular zone migrate into the olfactory bulb (1.1.3.). Scale bar: 1 mm (29).

The adult mammalian brain contains two germinative centres (**fig. 1.1.**), the subventricular zone and the dentate gyrus, which is located inside the hippocampus (20;36). Apart from its role as a neurogenic region the dentate gyrus contains granule cells, which represent the principle excitatory neurons of the hippocampus. The development of the dentate gyrus is initiated by a primary germinative region in the wall of the lateral ventricle, which gives rise to a secondary matrix, in turn forming a third matrix, which harbours the precursor cell population in the adult animal.

The second neurogenic region, the subventricular zone (SVZ) emanates from the ventricular zone (VZ), which originates from the neuroepithelial cells along the primordial ventricles. The development of the SVZ in mice starts at around E11 (68). The embryonic VZ consists of two functional regions, the dorsal neocortical and the ventral ganglionic VZ. Whereas the first one generates the layered cortex, the latter gives rise to interneurons, astrocytes and oligodendrocytes (**fig. 1.2.**), each presenting a lineage, into which a neural stem cell can differentiate.

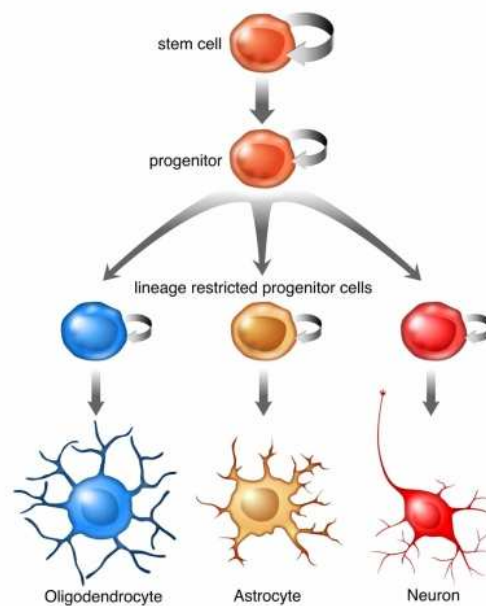


Fig. 1.2. Hierarchy of stem cells. The progeny of the neural stem cell is the neural progenitor cell, which differentiates into lineage restricted progenitor cells. These give rise to oligodendrocytes, astrocytes and neurons (http://www0.gsf.de/idg/groups/adult_neurogenesis/start.html).

Stem cell hierarchy begins with the most primitive and multipotent stem cell. The cells along the hierarchy get more and more differentiated and will finally get determined for a certain lineage. The progenitor cell already has limited potential, shows limited self-renewal and gives rise to lineage restricted progenitor cells, eventually differentiating into neurons and glia cells (20).

1.1.2. Subtypes of neural precursor cells

Doetsch *et al.* (13) investigated the composition of the subventricular zone (SVZ) and therefore established ultrastructural and immunocytochemical criteria for the identification of cell types in the adult rodent SVZ. Three main cell types were identified, which are type A, B and C cells, whereas the geneologic order is B, C and A cells. Subventricular treatment with the antimitotic substance cytosine-beta-D-arabino-furanoside resulted in elimination of type A and C cells while part of the B cells remained and started dividing soon after the treatment. Two days later, C cells reemerged, followed by type A cells, showing that type B cells are the primary precursor cells in the SVZ (12).

Type B cells represent the *astrocyte-like stem cells* of the SVZ. They can be divided into B1 and B2 cells, which refers to their exposure to the ependyma or to the striatum respectively. It has been shown that they ensheath chains of type A cells, which is thought to be trophic support and isolation from electrical and chemical influence from the surrounding parenchyma. Type B cells can be characterized by the expression of vimentin, glial fibrillary acidic protein (GFAP) and the intermediate filament nestin (**tab. 1.1.**). Cells originating from B cells, namely type C cells are the so-called *transient amplifying progenitor cells*. They show the strongest proliferative activity among the three types of precursor cells and are the fastest proliferating cells in the SVZ. They are immunopositive for nestin and the homeobox transcription factor distal-less homeobox-2 (Dlx-2). Type C cells are considered to be the precursor cells to type A cells and are not found in the rostral migratory stream (RMS, **1.1.3.**). Type A cells are migrating neuroblasts and correspond to proliferating, migrating neural precursor cells, which show positive immunolabelling for nestin, polysialylated neural cell adhesion molecule (PSA-NCAM), doublecortin (DCX) and neuronal class III β -Tubulin (Tuj1). They are considered to be the cell population, which perform chain migration from the SVZ to the olfactory bulb (**1.1.3.**).

Tab. 1.1. Expression pattern of marker proteins for type B-, C- and A-cells

Marker	B cells	C cells	A cells
Nestin	+	+	+
Glial fibrillary acidic protein (GFAP)	+	-	-
Polysialylated neural cell adhesion molecule (PSA-NCAM)	-	-	+
Doublecortin (DCX)		-	+
Neuronal Class III β -Tubulin (Tuj1)	-	-	+
Vimentin	+	-	-
Distal-less homeobox-2 (Dlx-2)	-	+	+

1.1.3. Physiology of neural precursor cells in the intact brain

In the adult murine brain, type A cells constitutively migrate from the subventricular zone (SVZ) along the rostral migratory stream (RMS), which is up to 3 mm long, into the olfactory bulb (OB, **fig. 1.1**). Thereby glial cells, identical with B cells, form a tube-like structure around the migratory stream and thus shield it against the rest of the brain. Since cells migrate as elongated aggregates of cells, the term *chain migration* is used. In general, migration occurs unidirectional towards the olfactory bulb however it is still unknown what factors are responsible for guidance of the cells (36).

Although migrating type A cells still undergo cell division, proliferation rates are reduced compared to the ones in the SVZ and their cell cycle time is lengthened. Additionally, neuronal maturation is initiated, which is accompanied by the expression of immature neuronal markers like DCX, PSA-NCAM and Tuj1.

Once the migrating type A cells reach the olfactory bulb, they disperse and migrate toward the granule cell layer and the periglomerular layers. Only upon entry of the olfactory bulb do these cells achieve neuronal maturity, detectable by altered electrophysiological properties, release of neurotransmitters and expression of mature neuronal markers (36).

1.1.4. Neural precursor cells in the diseased brain

Neural precursor cells (NPCs) are thought to play a role in the onset and progression of several neurological diseases. For example links have been made between NPC dysfunction and Alzheimer Disease, Parkinson Disease, stroke, epilepsy, schizophrenia and spinal cord injuries (36). However, functional NPCs are believed to retain therapeutic potential.

Most interesting for the present work are the connections, which have been made between NPCs and brain tumours. Apart from the theory that NPCs represent the cell of origin of brain tumours (**1.2.**) there is growing evidence that precursor cells also hold the potential to suppress glioma growth, which is the subject the present study focuses on.

1.1.5. Therapeutic perspectives

Neural precursor cells (NPCs) present a promising therapeutic tool for brain repair. They can either be endogenously recruited or exogenously expanded and implanted into the brain. For example attempts have been made to improve the outcome of stroke by inducing endogenous regeneration of lost neuronal tissue (26). Similar efforts have been undertaken for neurodegenerative and demyelinating disorders, spinal cord injury and several other neuronal pathologies.

Since it was reported that NPCs show tropism for gliomas (1) it is being discussed to use them as carriers for anti-tumourigenic drugs, which would, considering the blood brain barrier, represent an elegant way to deliver drugs to their active site. Moreover, it has been discussed that endogenous precursor cells can be used as drug carriers and as a source to repair damaged CNS tissue, caused by the tumour, at the same time (54).

1.2. Neural precursor cells are the likely cell of origin of brain tumours

1.2.1. Clinical evidence for origin of glioblastoma from neural precursor cells

As mentioned in **1.1.4.** recent findings support the theory that glioma cells arise from neural precursor cells. One indication for the stem cell origin of gliomas is that there are specific gene alterations, which occur in diversely differentiated cells within the same tumour, i.e. glioma cells with an astrocytic, oligodendrocytic (and in more rare cases even neuronal) phenotype carry identical genetic alterations. These common genetic alterations indicate the clonal origin of many tumour cells. Moreover, the diverse cellular differentiation of the progeny of that clone indicates that the originally transformed clone must have had the potential to give rise to astrocytes, oligodendrocytes and neurons. Therefore, the originally transformed cell was by definition most likely a stem cell (20).

1.2.2. Experimental evidence for origin of glioblastoma from neural precursor cells

Apart from clinical indications, there is further experimental evidence that glioblastomas can derive from neural precursor cells. The group of Holland (32) created a mouse model, which allows tissue-specific gene transfer of activated Ras and/or Akt into astrocytes and neural progenitor cells. It has been known before that frequent genetic alterations in glioblastoma multiforme (1.3.) activate common signal transduction pathways, which in all cases involve Ras and Akt. Whereas gene transfer of Ras or Akt alone was not sufficient to induce tumour formation, combined gene transfer resulted in the development of high-grade gliomas. Most interestingly, this did not occur in astrocytes but only after gene transfer into neural progenitor cells suggesting that glioma cells derive from progenitor cells, which carry mutations leading to the activation of Ras and Akt.

Although there is strong evidence that precursor cells represent the cell of origin for brain tumours, the possibility that glial tumours arise from differentiated glia cells can not be ruled out (43).

1.3. Brain tumours and their classification

Glia cells are the most common cell type in the brain and make up 90 % of the total cell number (37). They were discovered by Virchow (1856), who described them as *Nervenkitt*, a kind of glue for neurons (gr. *glia*: glue). Initially, they were considered as merely supporting cells for neurons, yet recently they were shown to fulfill a range of far more complex functions. The group of glia cells consists of astrocytes, oligodendrocytes and Schwann cells (37).

Historically, brain tumours were thought to consist of transformed glia cells and are therefore called gliomas. Different types of gliomas are astrocytomas, oligodendrogliomas and schwannomas, depending on the relevant cell type. Schwannomas often correspond to benign tumours. It is still unknown how these transformations occur and what triggers them. One theory claims that disruptions in the glial cell cycle lead to glioma formation. However, recent research provided more and more evidence that gliomas emerge from neural precursor cells (1.2.).

Gliomas are the most common group of primary tumours in the brain and make up 30 – 40 % of all brain tumours (40). The World Health Organisation (WHO) introduced a classification in 1993, which divides astrocytomas into four malignancy grades:

Tab. 1.2. The World Health Organization (WHO) grading system for astrocytomas

Grade	Example	Criteria
WHO I	Pilocytic astrocytoma Myxopapillary ependymoma/subependymoma	Low proliferating, discrete, non invasive tumour
WHO II	Diffuse astrocytoma Papillary, cellular and clear cell ependymoma	Modest proliferating, partly invasive tumour
WHO III	Anaplastic astrocytoma Anaplastic ependymoma	Fast proliferating, invasive tumour
WHO IV	Glioblastoma multiforme Highly malignant glioma-like pineoblastoma and medulloblastoma	Rapidly proliferating, highly invasive tumour

In the present work research and conclusions will be restricted to cells representing glioblastoma multiforme (GBM), i.e. a grade IV brain tumour.

1.3.1. Epidemiology of gliomas

Gliomas occur with an incidence of 5 in 100,000 (19). They make up 44 % of all primary brain tumours and 52 % of these are represented by the glioblastoma multiforme. The peak of onset of glioblastomas is around 50 - 55 years, which makes them a strongly age-related pathology. Men are slightly more prone to these neoplasms. Furthermore, the incidence is 2 - 3 times higher in white than in black people. Prognosis is poor and the median survival is 14.6 months (67); only few patients survive for three or more years. Main risk factors are high dose radiation, hereditary syndromes and increasing age. Although the last years have revealed some major approaches to develop new surgical and radiation techniques as well as multiple antineoplastic drugs, a cure for glioblastoma remains elusive (11).

1.3.2. The pathophysiology of glioblastoma

Glioblastoma multiforme (GBM) consist of a heterogenous mixture of poorly differentiated neoplastic astrocytes (31). They can occur as primary, which means *de novo* tumours but can also, although less frequent, develop from lower grade astrocytomas and thus are defined as secondary tumours. The latter typically develop in younger patients

(< 45 years) whereas *de novo* tumours arise almost solely in elderly patients (around 65 years).

The tumour as such forms a solid mass from which neoplastic cells are disseminating into the adjacent brain tissue. The tumour itself can reach a considerable size and squeeze out larger amounts of brain mass (**fig. 1.3.**), which usually leads to diverse neurological defects.

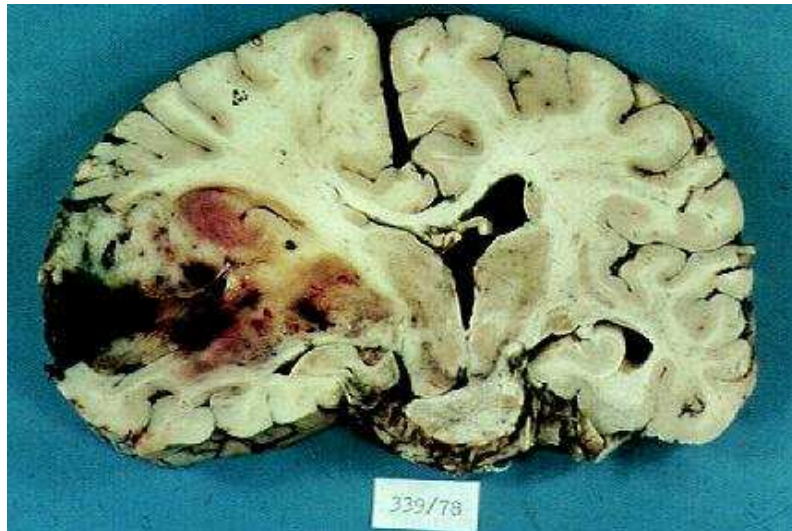


Fig. 1.3. Macroscopic view of glioblastoma multiforme in a human brain

(www.neuropat.dote.hu/jpeg/tumor/3gliobl1).

Although primary and secondary tumours differ on the genetic level in many ways, there are some common genetic abnormalities, which are considered as hallmarks of glioblastomas. One of them is the loss of heterozygosity (LOH) on chromosome 10, which seems to be specific for grade IV brain tumours. Very well known are mutations in the tumour suppressor gene p53 on chromosome 9, which also plays a pivotal role in other types of cancer. In fact, only about one third of glioblastomas carries this mutation, which corresponds to the percentage in lower grade gliomas. This suggests that the p53 gene is involved rather early in neoplastic transformation (40). In about one third of all GBMs one can find amplification of the endothelial growth factor receptor gene (EGFR), which leads to increased cell proliferation. Furthermore platelet-derived growth factor alpha (PDGF- α) and phosphatase and tensin homolog (PTEN) are two more genes, of which the expression is altered in GBMs (42;52). PDGF- α belongs to the family of growth factors and is

involved in the regulation of cell growth and cell division. It plays a particular role in angiogenesis, which is characteristically increased in cancer to provide sufficient nutrition supply for the tumour. The phosphatase PTEN is a tumour suppressor, which is related to a variety of biological functions like apoptosis, inflammation and immunity. These genetic defects have an effect on other cell proteins and finally result in tumour formation. Thus, EGFR signalling leads to the activation of Ras and PTEN mediates the negative regulation of Akt. Combined activation of Ras and Akt is able to trigger tumourigenesis. Both signalling pathways are upregulated in glioblastomas and their downstream elements have become potential therapeutic targets (56).

1.3.3. Diagnosis and treatment of glioblastoma



Fig. 1.4. MRT of a human brain, revealing a glioblastoma multiforme

(rad.usuhs.mil/rad/who/zs224248)

If a neurological examination points to a brain tumour, additional tests will be made. These mainly include scans like magnetic resonance imaging (MRI, **fig. 1.4.**), computer tomography (CT) or positron emission tomography (PET). In most cases therapy starts with surgical removal of the tumour. Due to the limited space in the brain this is much more difficult than removing a tumour in other parts of the body. Even if the surgery is

successful it has to be assumed that tumour cells have already spread throughout the brain and may be the source for tumour relapses.

One of the main properties of glioma cells is their invasive behaviour, which also signifies the biggest challenge regarding therapy (31;41). Therefore combined radiochemotherapy typically follows surgery. At present, the standard chemotherapeutic is temozolomide (Temodal®); its cytotoxicity is due to alkylation of the nucleobase guanine.

Although many efforts have been made during the last years to improve the existing therapies, the biggest problem is still the extreme invasive nature of glioblastomas. It is virtually impossible to prevent migration of tumour cells into the adjacent brain tissue, which is the cause of relapses in most cases.

1.4. Cancer stem cells

1.4.1. The cancer stem cell hypothesis

There are two hypothetical models which explain how the devolution of a single cell leads to cancer development, the stochastic and the hierarchical model. Whereas the first says that all cells within a tumour have the same tumourigenic potential, the latter states that only a small subset of cells in the tumour, namely cancer stem cells, hold the capacity to generate new tumours. Especially glioblastoma multiforme, as the name implies, is a very heterogeneous tumour and contains multiple cell types. This hypothesises that the cell, which generated them had the capacity to give rise to multiple cell types which is a hallmark of stem cells (73).

One of the many theories about the origin of cancer stem cells claims that the transdifferentiation from normal to tumour stem cells might happen by cellular fusion between healthy stem cells and differentiated cells. In addition, this could explain cellular aneuploidy and heterogeneity in cancers (6).

Another, in the meantime more supported theory claims that dividing, non-differentiated cells, in the brain primarily represented by neural stem cells, are needed for tumour formation and that cancer stem cells represent an intermediate state between healthy stem cells and transformed tumour cells. It has been shown that formation of experimental gliomas preferentially takes place in germinal regions compared to the non-proliferative brain parenchyma. Furthermore Holland *et al.* (32) showed that deletion of tumour suppressor and/or activation of oncogenes like Ras and Akt results in tumour formation

with a higher frequency in nestin-expressing cells than in GFAP-expressing astrocytes. Galli *et al.* (21) proved that cancer stem cells, isolated by CD133 expression, represent in fact cancer-initiating cells by transplanting them into the striatum of adult immunodeficient mice where they formed new tumours displaying classic features of glioblastoma multiforme. In contrast to normal tumour cells fewer cells were required to initiate a tumour even with a higher frequency.

1.4.2. Properties of cancer stem cells

The existence of cancer stem cells (CSC) was first discovered for acute myeloid leukaemia (AML). In the meantime they were also identified in breast cancer and central nervous system (CNS) malignancies. The cancer stem cell theory postulates that CSCs are the cancer initiating cells and persist in the tumour as a distinct cell population. They represent typical stem cell properties, most importantly the ability for self-renewal and differentiation into multiple cell types. They may use the same proliferation and differentiation pathways as normal stem cells, like e.g. the Notch- or sonic hedgehog (SHH)/Wnt signalling pathway. Tumour stem cells in gliomas can be identified and enriched by the expression of CD133, a 120 kDa cell surface protein, which is also a marker for human neural stem cells (73).

The origin of cancer stem cells however, still remains elusive. They might derive from true tissue originated stem cells, bone marrow stem cells or mature cells, which underwent the process of dedifferentiation.

1.4.3. Cancer stem cells may represent novel therapeutic targets

According to the cancer stem cell theory, these cells should be considered as the primary target of cancer treatment. Eliminating cancer-initiating cells would lead to tumour regression and not, though after initial decline of cancer cells, result in final tumour relapse (**fig. 1.5.**). As this very new and only recently discovered cell type is still poorly defined and not very well classified it resembles a 'moving target', for which it is hard to develop specific treatment. Another problem is that due to their similarity to normal stem cells the approach to eliminate them might also affect healthy cells. Nonetheless, they do hold novel possibilities for cancer therapy. One of the biggest challenges in tumour treatment is their resistance to drugs and toxins. Many stem cell populations show a high expression of ATP-binding cassette (ABC) drug transporters, which protect the cells against cytotoxic

agents (51). Not only is this another link between stem and tumour cells, it also suggests a combination of chemosensitizers and cytotoxic agents which alters ABC-transporter activity.

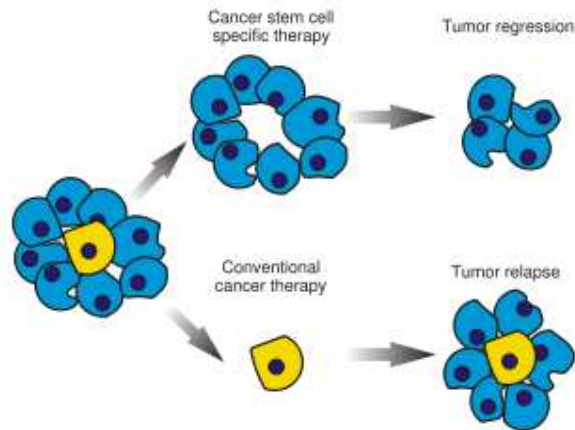


Fig. 1.5. Cancer stem cell specific and conventional cancer therapy

([http://www.healthnews-\(stat.com/primages/cancer_treatment_stem_cells_1.jpg](http://www.healthnews-(stat.com/primages/cancer_treatment_stem_cells_1.jpg))

1.5. Cell death pathways

There are many ways for a cell to die. The type of cell death, which is induced, depends on numerous factors like cell type, age of the cell, impacts from the surrounding, availability of nutrition etc. The intention of this chapter is to give a rough overview about the most common types of cell death and does not claim being complete.

1.5.1. Apoptosis

The term apoptosis (gr. *apo*: from, *ptosis*: falling) describes one of the main types of programmed cell death. It is fundamental for tissue development and plays a pivotal role for the homeostasis between mitosis and cell death in the adult organism (77). Loss of apoptotic activity results in uncontrolled cell proliferation, which in many cases leads to the development of tumours. It has therefore become an important issue in cancer research to unravel the apoptotic machinery.

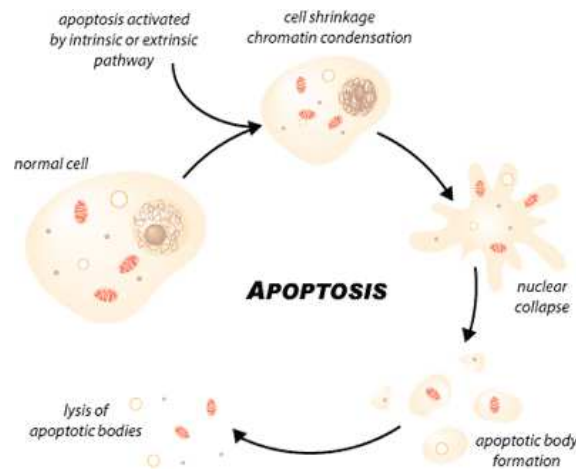


Fig. 1.6. The distinct steps of apoptosis

(<http://www.scq.ubc.ca/wp-content/uploads/2006/07/Apoptosis.gif>)

There are many initiating signals, extracellular and intracellular, which converge in the same organised apoptotic degradation procedure. The morphological features of apoptosis are cell shrinkage accompanied by membrane blebbing while simultaneously nuclear chromatin condensation occurs. Finally, the cell dissociates into several vesicles, apoptotic bodies, which are subsequently phagocytised (**fig. 1.6.**). The degradation process is mainly carried out by cysteinyl-aspartate-cleaving proteases, known as caspases, which are present in most cells in their inactive pro-form, awaiting activation by cleavage. The tumour suppressor protein p53, which is able to initiate apoptosis and is very often mutated in cancer cells, has become a central subject in cancer research.

1.5.2. Alternative non-apoptotic cell death pathways

In contrast to the programmed cell death of apoptosis, necrosis describes the pathological process, which occurs after serious physical or chemical insult caused by injury, infection, cancer, inflammation etc. Morphological features of necrosis are loss of membrane integrity and disintegration (swelling) of organelles. Cell death ends with total cell lysis, which evokes a significant inflammatory response. Regarding cancer, necrotic areas may develop due to extensive tumour growth, which leads to destruction of the affected tissue.

Autophagy, or autophagocytosis, is a lysosomal degradation pathway, which is a cellular response to stress or nutrient deprivation. In that case the cell degrades non essential cellular components in order to release missing nutrients. The autophagic process further contributes to development, growth regulation and cancer. When autophagy leads to the total degradation of a cell, it represents autophagic cell death, also known as cytoplasmic or type II cell death, another form of programmed cell death (72). Many studies have tried to investigate whether autophagy is able to suppress tumourigenesis and could possibly be considered as an alternative way to combat tumour cells since most of them are resistant to apoptosis.

A cell can also undergo cell death caused by endoplasmic reticulum (ER) stress. ER stress can be caused by unfolded proteins and other conditions which disturb the ER homeostasis. The cellular reaction to ER stress is activation of the unfolded protein response (UPR), which provokes changes in the cellular metabolism like general translation attenuation and/or transcriptional upregulation of molecular chaperone genes. ER stress can occur under both physiological and pathological conditions. Whereas physiological alterations of the ER homeostasis result in temporary translational adjustments, long-term or acute ER stress mobilizes the full UPR and often leads to cell death. ER stress has been associated with a number of diseases, among them diabetes, cardiovascular diseases, viral infections, immune response, neurodegenerative diseases and also cancer. It has been reported that hypoxia leads to an activation of the UPR. Since tumours often contain hypoxic cores, UPR activation could be a mechanism to compensate the poor growing conditions and therefore a rescue mechanism for the tumour cells. Whilst this still has to be investigated, endoplasmic reticulum stress-induced cell death has also to be considered as a novel pathway, by which tumour cells can be targeted.

1.6. Aim of the study

1. To study potential interaction of endogenous neural precursor cells with glioma
2. To specify the effect of neural precursor cells on glioma development
3. To investigate the mechanism determining the extent of the anti-tumourigenic effect
4. To examine the factors determining the differences in the anti-tumourigenic response in young and aged brains
5. To set up appropriate *in vitro* experiments in order to observe the direct interaction between neural precursor and glioma cells
6. To characterize the neural precursor cell-induced glioma cell death

2. Material and Methods

2.1. Material

2.1.1. Devices

AGFA Curix 60	AGFA, Japan
CCD camera	Proscan, Germany
Centrifuges	Eppendorf, Germany
Clean bench	Biowizard, USA
Neubauer counting chamber	LaborOptik, Germany
Cryosystem FCS	Leica Microsystems, Germany
Electron microscope 910	Zeiss, Germany
Enterprise laser	Coherent, USA
FACSVantage SE flow cytometer	Becton Dickinson, USA
Fluorescence microscope Axioplan	Zeiss
G-Box gel documentation system	Syngene, UK
Gelelectrophoresis device	BioRad, Germany
Gradient cycler	Eppendorf
Incubator	Labotect, Germany
Inverted fluorescence microscope Axiovert 100	Zeiss
Micro-infusion pump	World Precision Instruments, Germany
Microscopes	Zeiss
Nucleofector	Amaxa, Germany
Photometer	Eppendorf
Power Pack 300	BioRad
Scales	Sartorius, Germany
Spectral confocal microscope TCS SP2	Leica, Germany
Speed Vac	Bachofer, Germany
Stereotactic head holder	David Kopf Instruments, USA
Thermocycler T3000	Biometra, Germany
Trans blot SD	BioRad
Victor 1420 Multilabel Counter	Perkin Wallac GmbH, Germany
Vortex	Janke & Kunkel, Germany
Water bath	GFL, Germany

2.1.2. Plastic ware and other material

96-well plates (for DELFIA TUNEL assay)	PerkinElmer, Germany
96-/ 24-/ 6-well plates	TPP, Switzerland
Cuvettes	Eppendorf
Falcon cell culture inserts (0.4 µm) for 6-well	Becton Dickinson
Falcon tubes (15 ml, 30 ml)	TPP
Hyperfilm ECL	Amersham Biosciences, USA
Parafilm	Pechiney Plastic Packaging, USA
Saran wrap	Dow Chemical Co, USA
Tissue culture dishes (60 mm, 30 mm)	TPP
Tissue culture flasks (25 cm ² , 75 cm ²)	TPP

2.1.3. Chemicals

Acrylamide/Bisacrylamide 30 % solution	Sigma, Germany
Agarose	Roth, Germany
Ampicillin	Roche, Germany
APS (ammoniumpersulfate)	Merck, Germany
Aqua Poly/Mount	Polysciences, Inc, USA
Bio-dUTP (50 nmol)	Perkin Elmer
BrdU (5-bromo-2-deoxyuridine)	Sigma
labelling reagent	
CHAPS (3-[(3-Cholamidopropyl)	Amersham Biosciences
dimethylammonio]-1-propanesulfonate)	
Complete proteinase inhibitor	Roche
DAPI (4',6-Diamidino-2-Phenylindol-2HCl)	Sigma
DELFLIA Enhancement solution	PerkinElmer
DELFLIA Washing buffer	PerkinElmer
DiI (1,1-Dioctadecyl-6,6-di-(4-sulfophenyl)	Molecular Probes, USA
3,3,3,3-tetramethylindocarbocyanine)	
Dispase II	Roche
DNase (desoxyribonuclease)	Worthington, USA
dNTPs (desoxyribonucleosidtriphosphate)	Invitrogen, USA
dTTP (2'-deoxythymidine 5'-triphosphate)	Roche

ECL Plus (Western Blotting Detection Reagent)	Amersham Biosciences
EGF (endothelial growth factor)	Peptotech, USA
Ethanol	Roth
FCS (fetal calf serum)	Gibco
FGF (fibroblast growth factor)	Peptotech
G418 (= neomycin)	Gibco
Gel blotting paper	Roth
Glucose	Roth
Glycerol	Sigma
Hybond-P PVDF membrane	Amersham Biosciences
Isopropanol	Roth
Laminin	Invitrogen
L-Glutamine	Biochrom AG
Lipofectamine 2000 transfection reagent	Invitrogen
Matrigel	Becton Dickinson
Methanol	Roth
MgCl ₂	Invitrogen
Papain	Cell Systems, Germany
PBS (phosphate buffered saline)	Gibco
Penicillin/Streptomycin	Biochrom AG, Germany
PFA (paraformaldehyde)	Merck
Poly-L-Ornithine	Sigma
Polyvinylalcohol	Sigma
Rainbow molecular weight marker	Amersham Biosciences
Staurosporine	Sigma
Sucrose	Merck
SYBR [®] Gold	Invitrogen
TdT (Terminal deoxynucleotidyl Transferase) - buffer	Amersham Biosciences
TEMED (N,N,N',N' Tetramethyl-Ethylen- Diamine)	Amresco, USA
Tris	Roth
Triton X-100	Merck

Trypsin/EDTA (Ethylenediaminetetraacetic acid)	Biochrom AG
Tungstosilicic acid hydrate	Fluka, Germany

2.1.4. Enzymes

SuperScript II Reverse Transcriptase (200 U/ μ l)	Invitrogen
<i>Taq</i> -Polymerase	Invitrogen
<i>TdT</i> -enzyme (500 U)	Amersham Biosciences

2.1.5. Kits

BCA Protein Assay Kit	Pierce, USA
BrdU Cell Proliferation Assay	Calbiochem, Germany
Cell line C6 Nucleofector Kit	Amaxa, Germany
DELFLIA DNA fragmentation assay	Perkin Elmer
3DNA Array 50 Expression Array Detection kit	Genisphere, USA
Endo Free Plasmid Maxi Kit	Qiagen, Germany
<i>In situ</i> Cell Death Detection Kit, POD	Roche
RNeasy Mini Kit	Qiagen
QIAprep [®] Spin Miniprep Kit	Qiagen

2.1.6. Antibodies

2.1.6.1. Primary antibodies

Tab. 2.1. Overview of applied primary antibodies

Antigen	Host	Dilution	Supplier
5-Bromodeoxyuridine (BrdU)	Rat	1:500	Biozol, Germany
Caspase-3	Mouse	1:400	Cell Signaling, USA
Caspase-7	Rabbit	1:400	Cell Signaling
Cyclin D1	Mouse	1:100	BD Pharmingen, Germany
Cyclin D2	Rabbit	1:100	Santa Cruz, Germany
Cyclin D3	Mouse	1:100	Invitrogen
Distal-less homeobox (Dlx-2)	Guinea pig	1:5000	Kazuaki Yoshikawa, Osaka University, Japan (47)
Doublecortin (DCX)	Goat	1:200	Santa Cruz
Glial acidic fibrillary protein (GFAP)	Rabbit	1:500	Dako Cytomation, Denmark
Green fluorescent protein (GFP)	Goat	1:1000	Acris Antibodies, Germany
p21	Rabbit	1:100	Santa Cruz
Polysialic Acid-NCAM (PSA-NCAM)	Mouse	1:400	Chemicon, USA
Vimentin	Goat	1:400	Santa Cruz
Ki67	Rabbit	1:400	Novocastra Laboratories Ltd., UK
Musashi	Rabbit	1:400	Chemicon
NG-2	Rabbit	1:400	Chemicon

2.1.6.2. Secondary antibodies

Tab. 2.2. Overview of applied secondary antibodies

Antigen	Host	Conjugation	Dilution	Supplier
Mouse IgM	Donkey	Rhodamine Red	1:125	Jackson ImmunoResearch Laboratories, USA
Goat IgG	Donkey	Rhodamine Red	1:125	Jackson ImmunoResearch Laboratories

Rabbit IgG	Donkey	FITC	1:125	Jackson ImmunoResearch Laboratories
Rat IgG	Donkey	Biotin	1:125	Jackson ImmunoResearch Laboratories

Substrate	Conjugation	Dilution	Supplier
Streptavidin	HRP	1:10,000	Amersham Biosciences
Streptavidin	Cy5	1:200	Jackson ImmunoResearch Laboratories

2.1.7. Oligonucleotides (PCR primers and siRNA)

Tab. 2.3. Overview of used oligonucleotides

Name	Sequence (5' → 3')	Application	Source
p21 (forward)	gcc tta gcc ctc act ctg tg	PCR	MWG, Germany
p21 (reverse)	agc tgg cct tag agg tga ca	PCR	MWG
Cyclin D1 (forward)	cac agc ggt agg gat gaa at	PCR	MWG
Cyclin D1 (reverse)	ggt aat gcc atc atg gtt cc	PCR	MWG
Cyclin D2 (forward)	agt tcc gtc aag agc agc at	PCR	MWG
Cyclin D2 (reverse)	cta gtc tgc ggg ttc tcc tg	PCR	MWG
Cyclin D3 (forward)	cga gcc tcc tac ttc cag tg	PCR	MWG
Cyclin D3 (reverse)	aca gag ggc caa aaa ggt ct	PCR	MWG
β-actin (forward)	ccc tga agt acc cca ttg aa	PCR	MWG
β-actin (reverse)	gtg gac agt gag gcc aag at	PCR	MWG

2.1.8. Plasmids

Tab. 2.4. Overview of plasmids

Name	Source	Properties
pCI-ATF3	Shigetaka Kitajima, Tokyo Medical and Dental University, Japan	ATF-3 is overexpressed under the CMV promoter
pMP71GPRES-EGFP	Wolfgang Uckert, MDC, Berlin, Germany	EGFP is controlled by the retroviral MPSV promoter
pMP71GPRES-DsRed2	Wolfgang Uckert, MDC, Berlin, Germany	DsRed2 is controlled by the retroviral MPSV promoter

2.1.9. Media and buffer

2.1.9.1. Cell culture media

FCS was inactivated in the water bath for 30 min at 60°C prior to use. All media were purchased from Gibco, USA.

Tab. 2.5. Overview of media and buffer in cell culture

Cell culture medium for GL261: DMEM/10 % FCS/1 % PGS	10 % FCS 100 U/ml penicillin 100 µg/ml streptomycin 0.2 mM L-glutamine in DMEM
Cell culture medium for electroporation of GL261	10 % FCS 0.2 mM L-glutamine in RPMI
Cell culture medium for explant co-cultures	20 µg/ml human transferrin 100 µM putrescin 30 nM sodium selenite 1 nM triiodothyronine 60 U/l insulin in DMEM/F-12
Cell culture medium for NPCs: NB/B27	20 % B27 100 U/ml penicillin 100 µg/ml streptomycin 10 % L-glutamate 3 mg/ml glucose 20 ng/ml FGF 20 ng/ml EGF in Neurobasal A
Freezing medium for GL261	10 % DMSO 15 % FCS in DMEM
Freezing medium for NPCs	10 % DMSO in NB/B27
PPD solution	2.5 U/ml papain 250 U/ml DNase 1 U/ml dispase II (neutral protease) in DMEM 4.5 g/l glucose
Fixans I	8 % formaldehyde 1 % glutaraldehyde in 0.1 M phosphate buffer
Fixans II	4 % formaldehyde 0.5 % glutaraldehyde in 0.1 M phosphate buffer

2.1.9.2. Bacteria propagation**Tab. 2.6. Medium for bacterial cultures**

Luria-Bertani medium (LB)	10 g Bacto-tryptone 5 g Bacto-Yeast extract 5 g NaCl adjust pH to 7.5 with NaOH, autoclave, cool to 55°C and add antibiotics suitable for the expression plasmid
---------------------------	---

2.1.9.3. Buffers for immunolabelling**Tab. 2.7. Buffers for immunolabelling**

TBS	100 mM Tris 150 mM NaCl, pH 7.4
TBS+	0.1 % Triton X-100 3 % donkey serum in TBS

2.1.9.4. Buffers for PCR**Tab. 2.8. Buffers for PCR**

10 x loading buffer	1.7 % xylen cyanol 1.7 % bromphenolblue 80 % saccharose in H ₂ O
50 x TAE (Tris-Acetate-EDTA) buffer	242 g Tris-Base 57.1 ml acetic acid 0.5 M EDTA ad 1 l H ₂ O, pH 8.0

2.1.9.5. Buffers and solutions for Western Blots**Tab. 2.9. Buffers and solutions for Western Blots**

Sample buffer	1 % SDS 1 % Triton X-100 Complete proteinase inhibitor in TBS, pH 7.4
10 % APS	100 mg NH ₄ persulfate in 1 ml H ₂ O bidest.
Lower gel buffer	72.7 g Tris 1.6 g SDS ad 400 ml H ₂ O bidest., pH 8.8
Upper gel buffer	18.2 g Tris 1.2 g SDS ad 300 ml H ₂ O bidest., pH 6.8

10 x Running buffer	30 g Tris 140 g glycine 10 g SDS ad 1 l H ₂ O bidest.
Transfer buffer	2.93 g glycine 5.81 g Tris 0.375 g SDS ad 800 ml H ₂ O and 200 ml methanol
Washing buffer	0.5 % Tween-20 in TBS
Blocking buffer	3 % fat free milk powder in washing buffer

2.1.10. Software

Tab. 2.10. Software

Product name	Supplier
Adobe Photoshop CS	Adobe Systems Inc. USA
analySIS 3.2	Soft Imaging System, Germany
Leica Confocal Software	Leica, USA
Microsoft Office	Microsoft, USA
SPSS 11.0	SPSS, USA
Volocity 2.6.1.	Volocity, USA

2.2. Methods

2.2.1. *In vivo* inoculation of GL261 glioma cells into the mouse brain

2.2.1.1. Anaesthesia

Mice were anaesthetised with intraperitoneal injections of a 0.1 % xylazine and 1.5 % ketaminehydrochloride mixture in 0.9 % NaCl. 10 µl of the anaesthetic mixture was injected per 1 g of mouse body weight. The eyes of the mice were carefully covered with glycerin fat to avoid cornea drying.

2.2.1.2. GL261 glioma cell inoculation into the mouse brain

Anaesthetised C57/BL6 mice were immobilized and mounted onto a stereotactic head holder in the flat-skull position. The skin of the skull was dissected with a scalpel blade

and the skull surface was disinfected with a 10 % potassium iodide solution. The skull was carefully drilled with a 20 G needle tip at 1 mm anterior and 1.5 mm lateral to the bregma. Then a 1 μ l syringe with a blunt tip was inserted to a depth of 4 mm and retracted to a depth of 3 mm from the dural surface. 1 μ l of the GL261 cell suspension (2×10^4 cells/ μ l) was slowly injected over 2 min into the pre-cast hole. The needle was then slowly taken out from the injection canal and the skin was sutured with a surgical sewing cone.

2.2.1.3. BrdU injections

For BrdU labelling experiments, animals received intraperitoneal injections of 50 mg of BrdU/kg of body weight at a concentration of 10 mg/ml BrdU in sterile 0.9 % NaCl solution twice daily for three days until 24 h before the glioma cell injection.

2.2.1.4. DiI injections

Intraventricular injections of 0.2 % (w/v) DiI in DMSO were applied 0.7 mm posterior and 0.8 mm lateral to the bregma on the left side using 0.5 μ l DiI at a depth of 2.8 mm from the dural surface. Tumour cell injections into the right hemisphere were performed as described above. Twenty nestin-GFP mice with or without glioblastomas were used to prove the reliability of the DiI injection technique and were sacrificed after six hours and one, four and seven days to observe the intensity and distribution of DiI.

2.2.1.5. Retrovirus injections

The open reading frames for DsRed2 and EGFP were subcloned from pDsRed2-N1 and pEGFP-N1 vectors into the vector pMP71GPRE via the NotI and EcoRI restriction sites. Stable producer cell clones were generated by co-transfection of 293-10A1 packaging cells with either of the retroviral vector plasmids and the plasmid pWLneo (15).

Retroviruses ($6 - 8 \times 10^6$ cfu/ml) were delivered at a speed of 0.5 μ l/5 min with a micro-infusion pump 0 mm posterior and 0.8 mm lateral to the bregma at a depth of 2.0 mm from the dural surface.

2.2.2. Paraformaldehyde fixation

The mice were killed by a 10 % ketamin intraperitoneal injection and perfused with an intracardiac injection of freshly prepared 4 % paraformaldehyde (PFA) solution (30 ml per animal). The PFA perfusate was replaced by a 0.9 % NaCl solution. After that, the skull

was opened and the brain was carefully removed and postfixed overnight in 4 % PFA. Finally, the brains were cryopreserved in 30 % sucrose (minimum incubation for 48 h).

2.2.3. Immunohistochemistry of brain sections (floating sections)

The PFA perfused cryoprotected brains were rapidly frozen in dry ice and mounted onto a sliding microtome. 40 µm thick sections were collected into a CPC-cryoprotecting solution (25 % glycerol and 25 % ethylenglycol in 0.05 M phosphate buffer). Before immunolabelling, the sections were washed three times with TBS and subsequently blocked by incubating them in 3 % H₂O₂ (in 50 % methanol) for 30 min at room temperature on a shaker. The sections were again washed three times with TBS and incubated in TBS+ for 30 min for permeabilisation. Then, the sections were incubated for 48 - 72 h at 4°C with relevant primary antibodies. Sections were washed three times with TBS and incubated with the fluorescence conjugated secondary antibodies (1:125) for 3 h at room temperature. After a final wash they were mounted onto microscope glass slides, covered with coverslips and stored at 4°C until used for microscopical analysis.

2.2.4. Survival study

Wild-type mice (C57/BL6) of P25 and P180 received GL261 glioma cell injections alone. Another group of P180 animals obtained a mixture of GL261 cells plus adult neural precursor cells. The application of the cells was performed as described under **2.2.1**. Injections of tumour cells alone contained 2×10^4 cells/5 µl and of mixed cell suspensions 6×10^4 NPCs/4 µl plus 2×10^4 GL261 cells/1 µl with a total volume of 5 µl.

2.2.5. TUNEL and Hoechst 33358 labelling

After performing immunohistochemistry for BrdU, Hoechst 33358 (50 ng/ml in TBS) was applied to the slides for 15 min. Thereafter, slides were mounted and used for whole cell counts. TUNEL labelling for DNA 3'-strand breaks have been performed as previously described (22).

2.2.6. Cell counting and unbiased stereology

In every 12th axial section 1.8 – 4.2 mm from dural surface, the area that was primarily infiltrated by the tumour was being sampled. Anteriorly, the olfactory bulb was excluded

and posteromedially, the hippocampal formation, at the dorsal end of which we cut laterally toward the surface of the hemisphere. Cell counts were determined in an unbiased approach using an optical fractionator procedure. Tumour volume was quantified according to the Cavalieri principle by determining the tumour area in every sixth 40 μm brain slice and then multiplying by 6 x 40 μm . For further phenotypic analysis of nestin-GFP-positive cells, 100 cells nearby the tumour were randomly selected per section. Six different tissue sections were analysed and tissue from three different mice was used.

2.2.7. Explant co-cultures

Subventricular zones (SVZs) were microdissected from 250 μm brain slices of P0 nestin-GFP-transgenic mice. These were co-cultured with three-dimensional GL261-DsRed cell aggregates, containing 50,000 cells. Tissues were put next to each other on a transwell, embedded in matrigel (1:10 diluted in DMEM) and co-cultured for seven days in chemically defined serum-free medium. The medium was changed every third day. As controls, SVZ explants were co-cultured with cortical tissue.

2.2.8. Cell culture of neural precursor cells

Mice were decapitated and skin and skull were removed. The brain was dissected from the brain stem and transferred into cold PBS/Glucose (4.5 g/l). The cerebellum and olfactory bulb were taken off and cross sections of the brain containing the subventricular zone (SVZ) were made. The lateral ventricles of the SVZ were microdissected, collected in a 15 ml tube and centrifuged (500 g, 5 min, 4°C). The collected tissue was incubated with occasional mixing in PPD solution (5 ml/animal) for 40 min at 37°C. The tissue was washed three times with PBS to remove the PPD. Cells were plated in 10 cm dishes in NB/B27 (two to three animals per dish). Cultures were incubated at 37°C, 5 % CO₂ and medium was changed on the next day. The cells were cultured until they formed semi-adherent neurospheres. For splitting, NPCs were collected by centrifugation (500 g, 5 min, 4°C) and dissociated by pipette-mixing for 35 times. The cells were counted and seeded in a clonal density of 500,000 per 10 cm dish in NB/B27.

For adherent cultivation, cells were put on dishes coated with poly-L-ornithine and laminin. These dishes were coated by first incubating them with poly-L-ornithine solution (10 $\mu\text{g}/\text{ml}$ in H₂O) overnight at room temperature. On the next day they were rinsed twice with sterile H₂O and incubated with a laminin solution (5 $\mu\text{g}/\text{ml}$ in PBS) overnight at 37°C.

2.2.9. Cell culture of glioma cells

The GL261 cell line was purchased from the National Cancer Institute, NCI-Frederick (MD, USA). GL261 glioma cells were grown in DMEM/10 % FCS/1 % PGS in T 25 tissue culture flasks. The mouse GL261 cell line was selected for its isogenity to the mouse strain C57/BL6, which was used for the animal experiments. The medium was changed every two days and cells were passaged when the cell density in the flask reached confluency. Cell cultures were maintained in the incubator at 37°C in a humidified and by 5 % CO₂ conditioned atmosphere.

2.2.10. Cell co-culture experiments and cell counting

GL261-DsRed cells (10^4) were co-cultured on coverslips with NPCs isolated from nestin-GFP transgenic mice in ratios of 1:1 and 1:3. After 72 h, the cells were fixed with 4 % PFA and the nuclei were stained with DAPI. The total cell number was determined using a fluorescence microscope. Cells labelling for DsRed and DAPI were counted per randomly selected optical field. On each coverslip, 10 non-overlapping areas were counted. One experimental group consisted of cell counts from three coverslips and each series of experiments was repeated three times. Control groups consisted of co-cultures of GL261 cells with fibroblasts and astrocytes in the ratio 1:3.

To establish adherent cell cultures of GL261 in NPC-conditioned medium, 2×10^4 glioblastoma cells were initially seeded in serum-containing medium. After one day, this medium was removed, the cells were washed three times with PBS and cultured in the NPC-conditioned medium for 72 h. As controls, GL261 cells were cultured in fibroblast- and astrocyte-conditioned medium for 72 h.

2.2.11. DNA Microarray

2.2.11.1. Stimulation paradigm

GL261 glioma cells were seeded in DMEM/10 % FCS/1 % PGS into T75 culture flasks. The next day, medium was replaced with fresh NB/B27 (control group) and NPC-conditioned medium (treated group) respectively. Gene expression of the treated group was analysed after 72 h compared to the control group.

2.2.11.2. RNA isolation

Cells were washed with PBS and harvested by scraping them off in a volume of 5 ml PBS. They were centrifuged at 800 rpm, 10 min, 4°C (GL261) and 500 g, 5 min, 4°C (NPC), respectively. The pellet was resuspended in 10 ml Trizol and incubated at room temperature for 5 min. 2 ml chloroform was added, mixed and incubated for two to three minutes. Cells were then centrifuged, this time at 5,000 rpm for 20 min. The supernatant was split in 750 µl aliquots, to which 750 µl isopropanol was added. After another centrifugation (12,000 rpm, 10 min, 4°C), 500 µl ethanol was added to the pellet, which was centrifuged again (7,500 rpm, 5 min, 4°C). The pellet was dried in a SpeedVac for 5 min with heating and finally dissolved in 100 µl DEPC-H₂O. It was then incubated for 10 min on ice and afterwards for 5 min at 65°C. The RNA concentration was quantified and the RNA was loaded onto a 1 % agarose gel, where the two typical RNA bands appeared.

2.2.11.3. Microarray hybridization

Microarray labelling and hybridization reactions were performed using the 3DNA Array 50 Expression Array Detection kit. Total RNA (20 µg) of the cells treated with neural precursor cell-conditioned medium and of untreated control cells was reverse transcribed with primers each containing a specific capture sequence. The two cDNA samples were pooled and hybridized to microarray slides containing 20,000 cDNA clones in a humidified chamber at 42°C for 16 h. Dye-swap repeats were performed. Slides were washed in 2 x SSC/0.2 % SDS for 10 min, 2 x SSC for 10 min and 0.2 x SSC for 10 min at room temperature. Visualization of bound cDNA was carried out by hybridization with 3DNA in a humidified chamber at 42°C for 3 h. The dendrimers contained Cy3 or Cy5 and bound to the respective specific capture sequences. Subsequently, slides were again washed as before.

2.2.11.4. Image acquisition and data analysis

Fluorescence intensities of Cy3 and Cy5 were analyzed with a laser scanner at a wavelength of 532 and 635 nm. The obtained 16-bit data files were transferred into the Microarray Suite image analysis software. Raw spot intensities of Cy3 and Cy5 were locally background subtracted. Empty spots and spots holding sequences for plant genes were excluded from further analysis. Variance stabilization was applied using the

vsn package of bioconductor ((33) <http://bioconductor.org>). For further analysis means of normalized log-products and log-ratios of each dye swap experiment pair were used. For normalization procedures R (<http://cran.R-project.org>) was applied.

2.2.11.5. Identification of differentially expressed genes and cluster analysis

The dataset was first reduced to clones, which showed an estimated fold change of at least 1.5. The threshold of estimated 1.5-fold change was acquired by statistical analysis aiming at minimizing the percentage of false positives (59). All genes above a 1.5-fold change were considered as relevant. A false positive rate was therefore between 2 and 5 %, which was considered as tolerable. Clones, which were present only once on the array were sequence-verified, those, which were represented by more clones on the array with comparable expression changes were not sequence-verified. Cluster analysis of the differentially expressed genes was carried out according to Gurok *et al.* (27).

2.2.12. TUNEL assays

2.2.12.1. The DELFIA DNA fragmentation assay

GL261 glioma cells (10^4 /well) were seeded in DMEM/10 % FCS/1 % PGS on a 96-well plate. The next day the medium was removed and replaced by NPC-conditioned NB/B27 medium (unconditioned NB/B27 and 10 μ M staurosporine served as negative and positive controls). After 72 hours of incubation cells were fixed and treated with the following reagents from the DELFIA DNA fragmentation assay:

Tab. 2.11. Reaction mixture for the DELFIA DNA fragmentation assay

Reagent	Final concentration
CHAPS	0.01 %
Bio-dUTP	5 μ M
dTTP	15 μ M
TdT-buffer (5 x)	1 x
TdT-enzyme	5.5 U
H ₂ O	ad 50 μ l

After 30 min incubation at 37°C cells were washed six times with DELFIA washing buffer. Then, Europium-labelled streptavidin (100 ng/ml) was added to the cells for one hour at room temperature. Again, cells were washed six times and 200 µl of Enhancement solution was added to each well. After 5 min incubation on the shaker at room temperature, the time-resolved fluorescence was measured using a VICTOR™ Multilabel Counter at a wavelength of 613 nm.

2.2.12.2. The *In situ* cell death detection kit, POD

To quantify dying glioblastoma cells in co-cultures with neural precursor cells, astrocytes and fibroblasts, cells were fixed after the co-culture period with 4 % PFA for 10 min and washed three times with PBS. Cell death was detected with a fluorescent cell death detection kit (*In situ* cell death detection kit, POD) according to the manufacturer's instructions. The samples were analysed under a fluorescence microscope at a wavelength in a range of 450 – 500 nm. TUNEL-positive nuclei of DsRed-expressing cells were counted as described above (2.2.10.).

2.2.13. Immunolabelling

Cells on coverslips were fixed with 4 % PFA for 10 min and then washed three times with PBS. To permeabilise the cell membrane, cells were incubated in TBS+ for 30 min. The primary antibody was applied overnight at 4°C while cells were kept in a wet chamber. The next day, cells were washed three times with PBS and incubated with the fluorescence conjugated secondary antibody for three hours at room temperature. Cells were finally washed three times with PBS and mounted onto microscope glass slides.

2.2.14. Microscopy

2.2.14.1. Fluorescence microscopy

Immunohistochemical preparations were visualized with a fluorescence microscope. Fluorescence microscopy was further used to evaluate transfection rates. Live cultures were analysed for fluorescence using an inverted fluorescence microscope.

2.2.14.2. Confocal microscopy

Confocal microscopy was performed using a spectral confocal microscope. Immunohistochemical preparations were visualized using three different laser channels for FITC (485 nm/535 nm), TRITC (555 nm/575 nm) and Cy5 (650 nm/665 nm). Appropriate gain and black level settings were determined on control tissues stained with secondary antibodies alone. All confocal images were taken with a 40 x magnification objective with a keyhole aperture between 45 μm and 85 μm . Overview images were processed with Photoshop CS and co-localization images were processed with Volocity 2.6.1.

2.2.14.3. Preparation of cryosections and electron microscopy

Two hours before fixation, the culture medium was changed. Freshly prepared fixans was added in equal amount to the growing medium. After 2 min this mixture was replaced by the second fixans and left for two hours at 4°C. Cells were washed with 0.1 M phosphate buffer, harvested with a rubber policeman and centrifuged at 3000 rpm for 5 min. After two washing steps with phosphate buffer, cells were embedded in 10 % gelatine in 0.1 M phosphate buffer, cut into small blocks, infiltrated with 2.3 M sucrose overnight at 4°C and frozen in liquid nitrogen. Ultrathin cryosections (70 nm) were obtained according to Tokuyasu *et al.* (70;71) using an ultramicrotome attached to a cryosystem FCS. Cryosections were contrasted and stabilized with a mixture of 3 % tungstosilicic acid hydrate and 2.5 % polyvinylalcohol (M_r 10000) according to Kargel *et al* (34). Samples were examined with an electron microscope at an acceleration voltage of 80 kV. Digital images were taken with a 1k x 1k high speed slow scan CCD camera and the analySIS 3.2 software.

2.2.15. BrdU-assay

Neural precursor cells (5×10^3 /well) were seeded on a poly-L-ornithine-/laminin-coated 96-well plate. The next day, the medium was removed and replaced by GL261-conditioned NB/B27 and unconditioned NB/B27 as a negative control. Cells were incubated for three days. BrdU label was added to the cells 18 h prior to fixation. The next day, cells were fixed with 200 μl fixative/denaturing solution for 30 min. After that, 100 μl of the anti-BrdU antibody (1:100 in antibody dilution buffer) was added to the cells for one hour at room temperature. Cells were washed three times with 1 x wash buffer and 100 μl of peroxidase goat anti-mouse IgG HRP conjugate was added for 30 min at room

temperature. Cells were again washed three times with wash buffer and the plate was entirely flooded with dH₂O. After complete H₂O removal, cells were incubated with 100 µl substrate solution for 15 min at room temperature in the dark. The reaction was stopped with 100 µl of stop solution. The absorbance was measured using a spectrophotometric plate reader at dual wavelengths of 450 – 540 nm.

2.2.16. Transfection methods

2.2.16.1. Electroporation (Nucleofection™)

Cells were passaged two to three days before transfection and were growing in their logarithmic growth phase. They were washed once with PBS and harvested by trypsinization. The reaction was stopped by adding serum containing culture medium and cells were centrifuged (800 rpm, 10 min, 4°C). After counting, the required number of cells ($1 \times 10^6 - 5 \times 10^6$ per sample) was centrifuged at 200 x g for 10 min at 4°C. The pellet was resuspended in 100 µl room temperature Nucleofector™ solution and 1 – 5 µg of the relevant DNA was added. The sample was transferred into an Amaxa cuvette, which was inserted into the cuvette holder and the appropriate programme was started. Then, 500 µl of pre-warmed culture medium was added and the sample was transferred into plates, which were pre-incubated with medium. The cells were put back to 37°C and the gene expression was detectable after 6 – 24 h.

2.2.16.2. Lipofectamine transfection

10^6 cells/well were plated one day prior to the experiment in a 6-well plate so that they reached 90 - 95 % confluency at the time of transfection. For one transfection reaction 4 µl of Lipofectamine 2000 was mixed with 250 µl OptiMEM and incubated for 5 min at room temperature. Meanwhile, 4 µg of plasmid DNA was diluted in 250 µl OptiMEM. Then, 250 µl of diluted DNA was added to each vial containing Lipofectamine 2000 and incubated for 30 min. In the meantime, the normal growth medium of the plated cells was exchanged for 2 ml/well of OptiMEM. The transfection mixture of Lipofectamine 2000 and plasmid DNA (500 µl per well) was added to the cells. After six hours, the reagents were exchanged for normal growth medium. After two to three days, cells were trypsinised, pelleted and plated in an appropriate format.

2.2.16.3. Retroviral transfection

For retroviral transduction, 100 μ l of viral supernatant (5×10^6 to 1×10^7 cfu/ml, **2.2.1.5.**) was added to 70 % confluent GL261 cells in a 6-well plate. Cells were centrifuged at 2000 rpm for 90 min, 32°C. After one day, the medium was exchanged for fresh growth medium and cells were propagated until a number of 5×10^6 was reached. Transduced cells were purified by FACS sorting and cultured as described. No decline in the number of GFP-expressing cells was observed after five passages.

2.2.17. Fluorescence Assisted Cell Sorting (FACS)

To prepare the cells for FACS-sorting, they were trypsinised or mechanically dissociated, centrifuged (800 rpm, 10 min or 500 g, 5 min, 4°C) and thoroughly resuspended in 1 ml PBS. To eliminate cell clumps, the cell suspension was filtered through a cell strainer with a 40 μ m mesh. Then, the single-cell suspension was subjected to FACS. Flow cytometric experiments were carried out using a FACSVantage SE flow cytometer. Sorting was done using a 70 micron nozzle. Excitation of the sample was performed by a standard 488 nm water cooled Enterprise laser. Forward scatter (FSC), side scatter (SSC) and fluorescence were collected by a 539/40 nm band pass filter. The sorted cells were gated by the dotplot FSC versus SSC and positive fluorescent compared to non fluorescent cells. The positive, i.e. fluorescent cells were collected and further cultured in their original culture medium.

2.2.18. Western blot

2.2.18.1. Sample preparation

Cells were washed two times with ice-cold PBS before the sample buffer was applied (10 μ l/cm²). Cells were scraped with a rubber policeman and the cell lysates were collected in 1.5 ml tubes and incubated on ice for 15 min. Then, the samples were centrifuged at 13,000 rpm for 20 min. The pellet was discarded and the supernatant collected; the protein concentration was determined using the BCA protein assay kit. The protein concentrations of all samples were equalised with sample buffer. Mercaptoethanol (5 %) and glycerol (15 %) was added to the samples and they were incubated at 95°C for 15 min.

2.2.18.2. SDS-PAGE

The gels were cast in glass plates. The composition of the gels is shown in **tab. 2.12**. Gels were loaded with 10 μ l molecular weight marker and 20 μ l of each sample. Then, electrophoresis was performed at 100 V for 10 min and at 150 V for approximately 45 min.

Tab. 2.12. Composition of a 10 % SDS polyacrylamide gel

Separating gel (lower gel)

Lower gel buffer	2.5 ml
Acrylamide	3.3 ml
12 % glycerol (in H ₂ O)	4.17 ml
10 % APS	30 μ l
TEMED	15 μ l

Stacking gel (upper gel)

Upper gel buffer	1.25 ml
Acrylamide	750 μ l
12 % glycerol (in H ₂ O)	3.0 ml
10 % APS	20 μ l
TEMED	10 μ l

2.2.18.3. Semi-dry transblotting

Gels were carefully removed from the glass plates and equilibrated in transfer buffer for 10 min. Meanwhile, a PVDF membrane was activated by incubation in methanol for 5 min and afterwards equilibrated in transfer buffer for 5 min. At the same time, blotting paper was soaked in transfer buffer and placed on the lower electrode (anode). The PVDF membrane and the separating gel were placed between two pieces of moist blotting paper. The sandwich was covered with the upper electrode (cathode) and blotted at 15 V for 60 min.

2.2.18.4. Immunoblotting

The membrane was incubated in methanol for 5 min, washed once in TBS for 5 min and then blocked with blocking buffer for 30 min. The primary antibody was then added in blocking buffer for an overnight incubation at 4°C on a shaker. On the next day, the membrane was washed three times in washing buffer and incubated with the HRP

conjugated secondary antibody for one hour at room temperature. After three more washing steps, each for 20 min, the ECL reagent was applied for 5 min. The membrane was dried from excess ECL reagent and placed on a transparent foil. It was exposed in a film cassette to ECL films (in the dark room) for various time periods (e.g. 15 s, 30 s, 1 min, 5 min) and the films were developed in the film developing machine.

2.2.19. Identification of mRNA transcripts

2.2.19.1. RNA isolation (RNeasy Mini Kit)

The microdissected SVZ tissue (2.2.8.) was disrupted and the lysate was homogenized in 600 µl RLT buffer. After centrifugation (14,000 rpm, 3 min, 4°C) 600 µl of 70 % ethanol was added to the supernatant. The sample was applied to a RNeasy mini column placed in a 2 ml tube and centrifuged at 10,000 rpm, 15 s, 4°C. The flow-through was discarded and 700 µl of buffer RW1 was added to the column. The tube was again centrifuged and transferred into a new collection tube. 500 µl of RPE buffer was added twice onto the column to wash the sample. After transfer of the column to a new 1.5 ml tube, 40 µl of RNase-free water was added onto the membrane. After 5 min incubation the tube was centrifuged at 10,000 rpm for 1 min to elute the RNA. Finally, the RNA concentration was quantified using a photometer.

2.2.19.2. Reverse transcription (RT) – PCR

To obtain cDNA, which can be used for a PCR reaction, RT-PCR was performed. Therefore the following mixture was prepared:

Oligo-dT	1 µl
dNTP Mix (10 mM each dATP, dCTP, dGTP, dTTP)	1 µl
Total RNA	1 µg
DEPC-H ₂ O	ad 20 µl

This was heated up to 65°C for 5 min and quickly chilled on ice. Then, the following mixture was added:

5 x First-Strand buffer	4 µl
DTT (0.1 M)	2 µl
RNase OUT Recombinant ribonuclease inhibitor (49 u/µl)	1 µl

The mixture was incubated at 42°C for 2 min and 1 µl Superscript II (200 U) was added. Hereon, another incubation at 42°C followed for 50 min and the reaction was inactivated at 70°C for 15 min. The cDNA concentration was quantified using a photometer.

2.2.19.3. Polymerase chain reaction (PCR)

To amplify certain segments of the yielded DNA, PCR reactions were performed. Therefore the following reaction was mixed:

Tab. 2.13. PCR reaction mixture

10 x PCR buffer	5 µl
MgCl ₂	1.5 µl
dNTP mix	1 µl
Primer 1	1 µl
Primer 2	1 µl
<i>Taq</i>	0.4 µl
cDNA	5 µl
H ₂ O	35.1 µl

Tab. 2.14. PCR-temperature profiles and number of cycles

1. Hot start	94°C	1 min
2. Denaturation	94°C	30 s
3. Primer annealing	Annealing temperature	30 s
4. Elongation	72°C	1 min; 35 cycles
5. End	72°C	8 min
6. Pause	4°C	∞

	Annealing temperature
β-actin	55°C
Cyclin D1	56.5°C
Cyclin D2	55°C
Cyclin D3	59.5°C
p21	53.5°C

2.2.19.4. Gel electrophoresis of the PCR products

The PCR products were loaded onto an agarose gel in order to visualize them under UV-light using a fluorescence dye. The 3 % agarose gel (in 1 x TAE buffer) was cast and pre-stained in SybrGold (1:10,000) for 40 min in the dark. 10 μ l of each PCR product was mixed with 5 μ l loading buffer and loaded into the gel slots; a 1 kb DNA ladder was also loaded. Electrophoresis was carried out at a voltage of 90 V for approximately 45 min. The DNA bands were visualized using the gel documentation facility G-Box.

2.2.20. Statistical analysis

Statistical significance was determined at the $p < 0.05$ level. The results are expressed as mean values \pm standard errors of the mean (SEM). Comparisons among the groups were performed with the Student's t test.

3. Results

3.1. Neural precursor cells from the subventricular zone migrate towards experimental gliomas *in vivo* and *in vitro*

3.1.1. Endogenous neural precursor cells accumulate around glioblastomas *in vivo*

Endogenous neural precursor cells (NPCs) are attracted towards experimental glioblastomas *in vivo* (24). To distinguish between NPCs and GL261 glioma cells, transgenic mice were used expressing enhanced green fluorescent protein (GFP) under the control of the nestin promoter. Although nestin is not only expressed in NPCs, this specific promoter construct largely restricts GFP expression to NPCs. It was shown that a short, evolutionarily conserved region of the nestin promoter is sufficient to drive nestin gene expression in CNS progenitor cells whereas reactive astrocytes and endothelial cells require the whole promoter sequence to express nestin (50). The GFP fluorescence therefore served as a marker for NPCs (nestin-GFP-positive cells). GL261 glioma cells were stably transfected to express DsRed. They were injected into the caudate putamen of 25 days old mice (P25), which resulted in tumour formation after two weeks (**fig. 3.1.**).

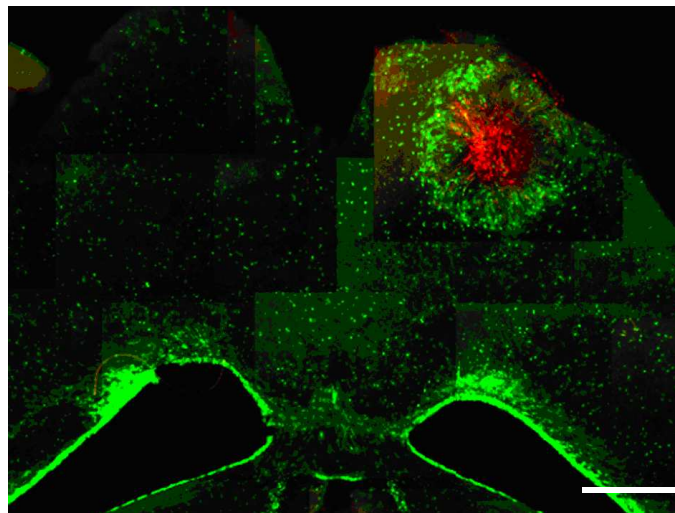


Fig. 3.1. Endogenous neural precursor cells surround experimental glioblastoma. Fluorescence microscope composite image of a horizontal section through the brain. GL261-DsRed glioblastoma cells were inoculated into the right forebrain of a transgenic nestin-GFP mouse (P25). Within two weeks nestin-GFP cells (green) accumulated around the tumour (red). Scale bar: 1 mm.

3.1.1.1. Accumulation of neural precursor cells is specifically induced by glioblastoma

To distinguish whether nestin-GFP-positive cells are generally attracted by injured tissue or specifically by a tumour, nestin-GFP distribution was analysed in animals after inoculation of tumour cells and in animals after sham operations (stab wounds). Seven days after application of the lesion accumulation of nestin-GFP-positive cells reached its peak (**fig. 3.2f**). 14 days after sham operation, the nestin-GFP-positive cells displayed the star-shaped morphology of activated astrocytes and were scattered throughout the hemisphere (**fig. 3.2g**). After 30 days, only few nestin-GFP-positive cells were left in the injured hemisphere (**fig. 3.2h**).

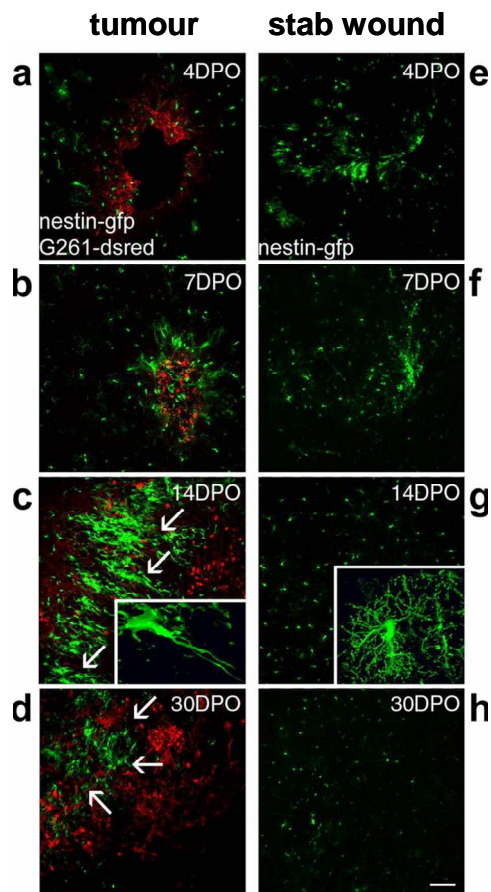


Fig. 3.2. Time course of NPC attraction to glioblastomas or stab wounds. **a, e:** At 4 d postoperatively (4 DPO), the injection canals were still visible; later they were identified stereotactically. At 4 DPO and 7 DPO, tumour formation started (red, **a, b**) but nestin-GFP cells accumulated both around tumours and controls (green, **e, f**). At 14 DPO and 30 DPO no nestin-GFP-positive cells remained at the stab wound (**g, h**). Cells scattered throughout the lesioned hemisphere displayed a star-shaped morphology (**g, inset**). GL261-induced gliomas reached a diameter of >1 mm, encircled by NPCs forming a layer of at least 200 μm (the tumour border is indicated by arrows in **c**). These nestin-GFP-positive cells showed a bipolar morphology (**c, inset**). At 30 DPO, the tumour cells had practically overgrown the layer of nestin-GFP-positive cells (the tumour border is indicated by arrows in **d**). Scale bar: 120 μm .

3.1.1.2. Nestin-GFP-positive cells around glioblastoma are genuine precursor cells

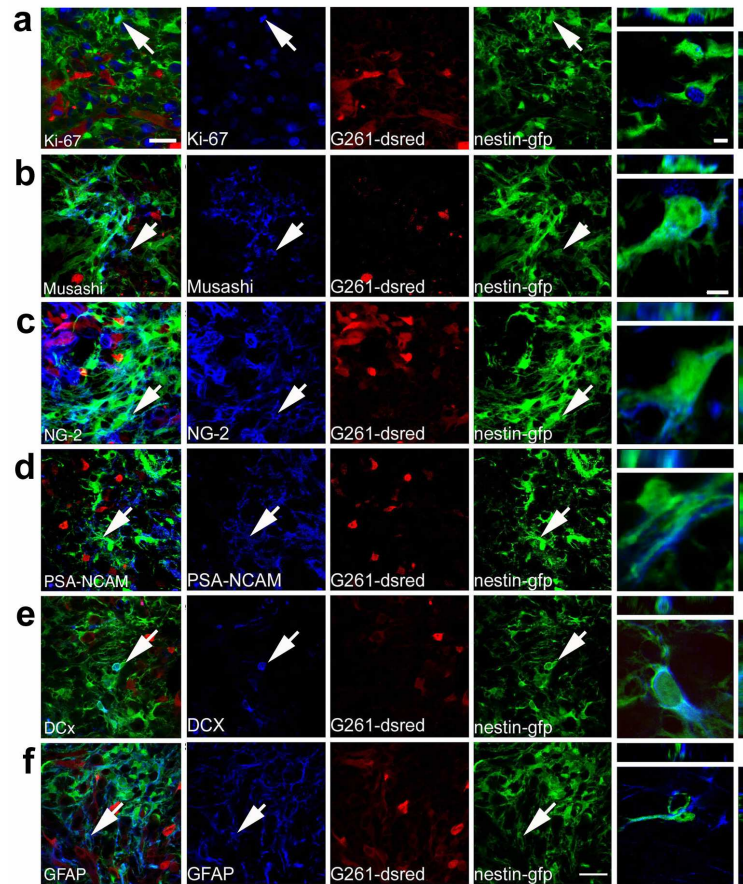


Fig. 3.3. Nestin-GFP-positive cells around glioma are characterized as genuine neural precursor cells. GL261-DsRed glioma cells (red) inoculated into the caudate putamen of P25 nestin-GFP (green) mice. Expression of cell type-specific markers in blue at 14 DPO. Co-localization of these markers with nestin-GFP cells is indicated by arrows in the micrographs and by 3D reconstructions of single cells. **a:** The cell cycle protein Ki67, a proliferation marker, labelled nuclei of many tumour cells and numerous nestin-GFP cells. **b:** The neural precursor marker Musashi 1 exclusively labelled nestin-GFP-positive cells. **c:** NG-2, marking neoplastic cells, was abundant on the plasma membranes and in the cytosol of nestin-GFP-positive and glioma cells. **d:** Staining for the neural precursor cell marker PSA-NCAM was almost exclusively positive for nestin-GFP-positive cells and was not found on tumour cells. **e:** Immunolabelling for DCX, which controls migration in neural precursors, was only detected in the cytoplasm of nestin-GFP-positive cells. **f:** The intermediate filament GFAP, which is present in neural stem cells, radial glia and astrocytes, primarily co-labelled with nestin-GFP in areas close to tumour. Few cells expressing only GFAP but not nestin-GFP were observed in the glioma bearing area. Scale bars: **overviews:** 25 μm ; **3D reconstructions:** 6 μm .

Nestin-GFP-positive cells accumulating around gliomas expressed cell type-specific markers, which allowed their characterization as precursor cells (**fig. 3.3**). About 30 % of nestin-GFP-positive cells expressed Ki67 (**fig. 3.3a**), indicating that they were actively dividing. Musashi, a RNA-binding protein (55) which is restricted to precursor cells was expressed in about 35 % of nestin-GFP-positive cells (**fig. 3.3b**). Staining with NG-2, a chondroitin sulfate proteoglycan, which marks glial precursors and neoplastic cells (62), was also positive for approximately 35 % of nestin-GFP-positive cells. Interestingly, NG-2 co-localized with both nestin-GFP-positive cells and the GL261 glioma cells (**fig. 3.3c**). Immunolabelling with markers for migrating neural precursor cells (9;69), PSA-NCAM (**fig. 3.3d**) and doublecortin (DCX, **fig. 3.3e**) was positive for ca. 30 % (PSA-NCAM) and 10 % (DCX) of nestin-GFP-positive cells. GFAP is a classic marker for astrocytes but also identifies stem cells by co-labelling with nestin within neurogenic regions of the adult brain (25). About 60 % of nestin-GFP-positive cells showed GFAP expression (**fig. 3.3f**).

3.1.2. Neural precursor cells around glioblastomas originate from the subventricular zone

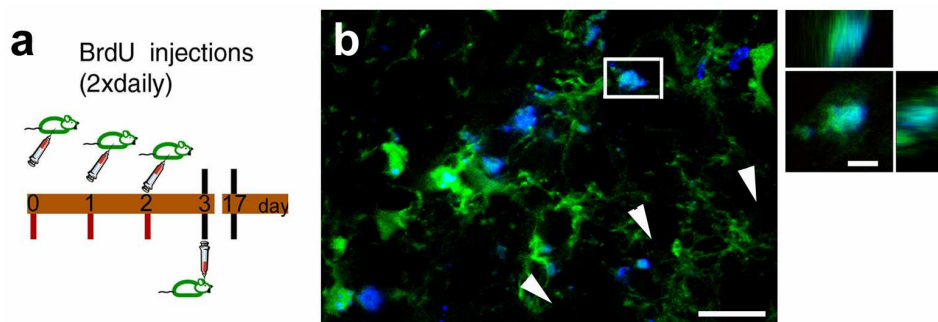


Fig. 3.4. Neural precursor cells around glioblastomas stem from a germinative centre. **a:** Animals received intraperitoneal BrdU injections prior to the GL261 glioma cell inoculation. **b:** Many nestin-GFP cells at the tumour border (arrowheads) are labelled for BrdU (blue). The cell, which is highlighted by a rectangle displays co-labelling for nestin-GFP and BrdU, which was confirmed by 3D reconstruction. Scale bar: **b:** 20 μm ; **3D reconstruction:** 5 μm .

Under physiological conditions, neural precursor cells (NPCs) are restricted to the germinative centres (1.1.1.). This suggests that they may also derive from these sites under pathological conditions. Precursor cells were preoperatively labelled with the thymidine analogue BrdU. Since proliferation only takes place in the stem cell niches, tracing BrdU-positive cells ensures tracing cells from these niches. Two weeks after the GL261 glioma cell injection cells could be observed, which were immunopositive for both nestin-GFP and BrdU (fig. 3.4.). No DsRed fluorescence is visible because it was lost by the immunostaining procedure for BrdU.

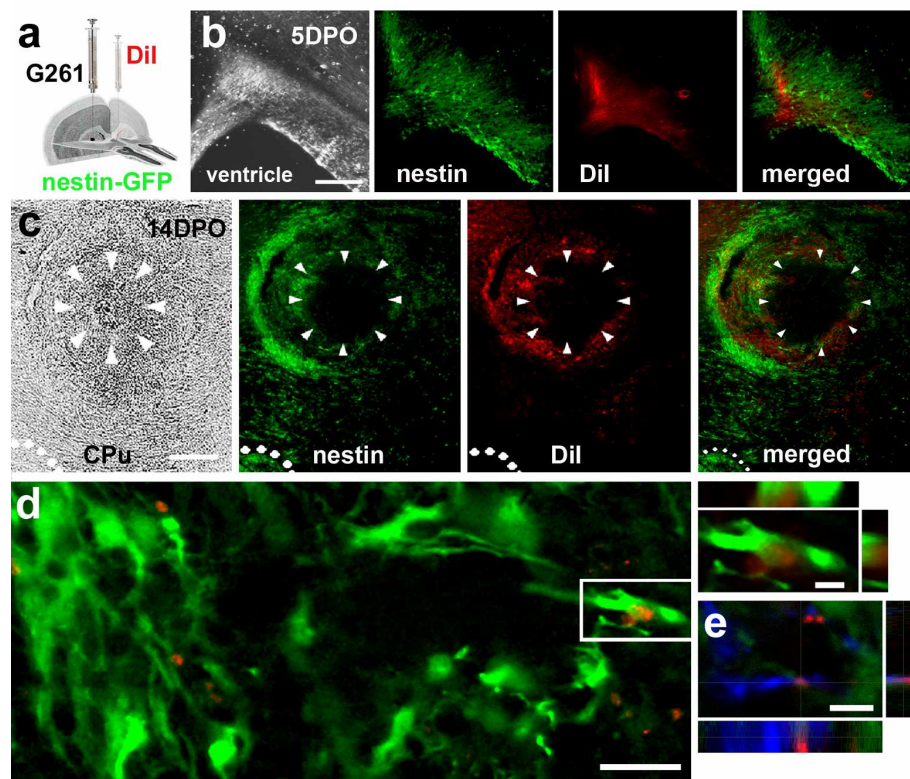


Fig. 3.5. Neural precursor cells around glioblastomas stem from the SVZ. a: Scheme of the location for injections of GL261 and DiI. **b:** Five days postoperatively (5 DPO), DiI (red) co-localises with nestin-GFP (green) and is distributed throughout the ventricular and subventricular zones. **c:** At 14 DPO, a tumour has developed in the caudate-putamen (CPu). Nestin-GFP-positive (green) neural precursors from the SVZ (indicated by dots) accumulate around the tumour (arrowheads). The glioma is surrounded by DiI-positive cells (red). Nestin-GFP-fluorescence co-localised with the DiI labelling. **d:** At the single cell level, DiI almost solely co-localises with nestin-GFP (3D reconstruction). **e:** Triple-positive labelling for doublecortin (blue), nestin-GFP and DiI. Scale bars: **b,c:** 400 μm ; **d:** 20 μm ; 3D reconstructions: 6 μm .

Since there are two germinative regions in the brain, the subventricular zone (SVZ) and the dentate gyrus, it was necessary to identify from which stem cell niche the migrating neural precursor cells (NPCs) originated from. Considering the fact that NPCs, which migrate along the rostral migratory stream are of subventricular origin it is likely that the precursors around the tumour are also derived from this brain region. The fluorescent dye DiI was applied into the ventricle of the left brain hemisphere ensuring labelling of those cells, which were in direct contact to the fluid continuum of the ventricular system (ependymal and stem cells of both hemispheres). Following the dye application, GL261 glioma cells were injected into the right hemisphere (**fig. 3.5a**). Injecting the dye into the left ventricle and glioma cells into the right hemisphere should demonstrate whether NPCs are able to migrate from one hemisphere to the other towards the tumour. Two weeks after the operation, both DiI- and nestin-GFP-positive cells were detected around the tumour mass. DiI-positive cells were almost exclusively nestin-GFP-positive, implying that they had migrated from the subventricular zone towards the tumour (**fig. 3.5d**, 3D reconstruction).

Triple positive labelling for nestin-GFP, DiI and doublecortin, a marker for migrating neural precursors, indicates that the experimental glioma had attracted proliferating NPCs from the subventricular zone.

3.1.3. Neural precursor cells from the subventricular zone are attracted by GL261 glioma cells *in vitro*

After having observed the migratory behaviour of neural precursor cells (NPCs) *in vivo* it was interesting to know if the cells show the same properties independent of the surrounding brain tissue. Therefore, an *in vitro* migration assay with microdissected tissue samples from the subventricular zone (SVZ) seemed to be an appropriate model. To perform this assay, microdissected SVZ explants from 250 μm brain slices of P0 nestin-GFP-transgenic mice were placed onto a transwell placed in a 6-well plate, which allowed free cell migration on the surface but ensured sufficient nutrition supply. The SVZ explants were put next to three-dimensional GL261-DsRed aggregates, containing 50,000 cells and embedded in matrigel. As controls, cultures of SVZ explants and cortical tissue were performed.

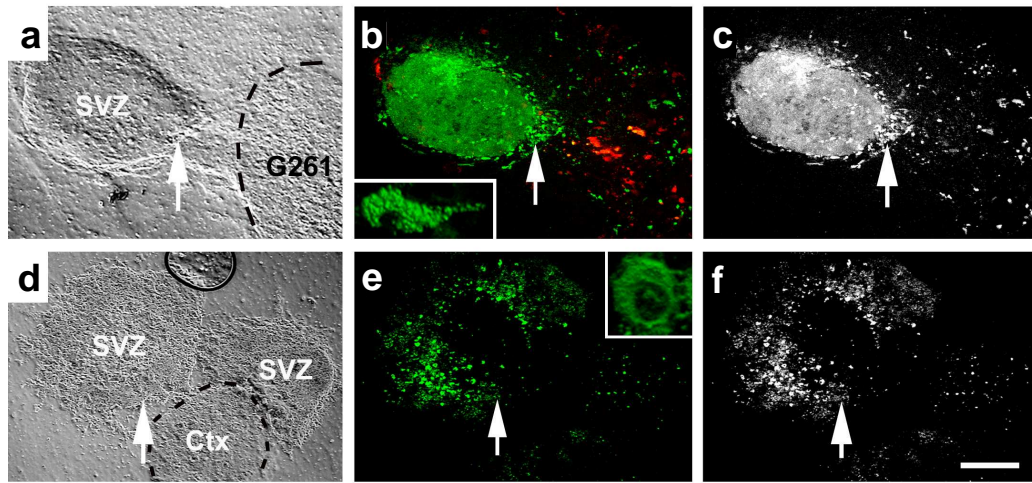


Fig. 3.6. Migration of subventricular NPCs towards glioma cell aggregates *in vitro*. A SVZ explant from a nestin-GFP mouse was exposed to a three-dimensional cell aggregate of GL261-DsRed glioma cells. The outline of the tumour is indicated by a dashed line (**a**). **b**: After 7 d of incubation, many GFP-expressing NPCs have migrated with a tropism towards the tumour; these migrating NPCs (indicated by an arrow) display a bipolar morphology. **c**: Single-channel micrograph indicating that neural precursors are exclusively attracted by the glioma cells. **d**: Two explants from the SVZ were exposed to each other and to cortical tissue (Ctx; indicated by a dashed line) for a period of 7 d; all tissues were derived from nestin-GFP mice. **e**: NPCs, which were exposed to SVZ- and cortex tissue stayed stationary and held a round cell morphology (indicated by an arrow). **f**: Single-channel micrograph showing absence of any precursor cell migration. Scale bar: 150 μm .

Analysis by confocal microscopy showed that after seven days, NPCs have left the explant and have migrated specifically towards the GL261 aggregate but not towards the opposed side. I also did not observe any migration towards the control tissue (**fig. 3.6**). Analysing the cells in higher magnification indicated that the migrating NPCs possessed a bipolar morphology (**fig. 3.6b**) whereas the stationary cells kept a round morphology (**fig. 3.6d, g**). Since the SVZ explants and the GL261 aggregates were in no direct contact to each other, this experiment suggests that it is a soluble factor, secreted by the tumour cells, which attracts NPCs.

3.2. Neural precursor cells show an anti-tumourigenic response *in vivo* and *in vitro*

3.2.1. Survival of experimental glioblastomas is dependent on the age-defined number of neural precursor cells at the tumour

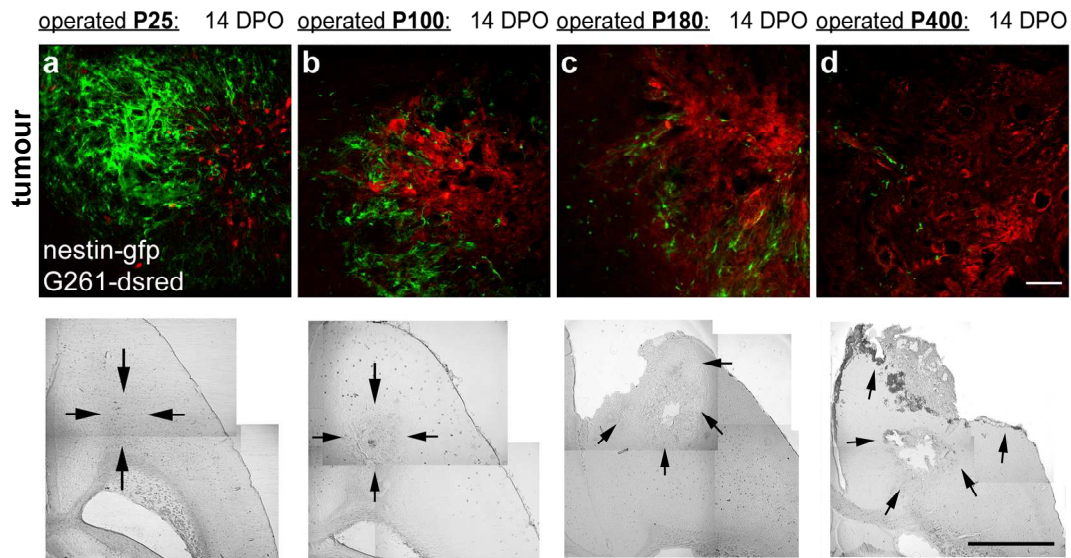


Fig. 3.7. Attraction of NPCs towards experimental glioblastomas and development of tumour formation in P25, P100, P180 and P400 mice (a-d). GL261-DsRed glioma cells were injected into nestin-GFP mice. At 14 DPO, notably less NPCs have accumulated around the glioma in the P100 compared to the P25 animals; the amount of NPCs declines even further in the P180 and P400 animals. The diminished number of NPCs corresponds to a more severe pathology of the brain caused by the tumour. Scale bar: **fluorescence images:** 50 μ m; **phase contrast composites:** 1 mm.

Mice of different age were compared regarding the accumulation of nestin-GFP expressing cells around the glioma and the tumour development 14 days after GL261 glioma cell inoculation. Whereas glioblastomas were quite small and confined in 25 days old animals (P25, **fig. 3.7a**), they increased in size proportionally to the age of the mice and the tumour itself became more and more jagged. At P400, the tumour spread over most of the brain hemisphere, often displayed necrotic areas and also contained local bleedings. In contrast to the P25 animals there was a considerably lower number of neural precursor cells (NPCs) around the tumour in the P100 mice. The decline of NPCs at the site of the tumour became more evident in the P180 mice and there were only few cells left in the P400 brain

(**fig. 3.7d**). This implies that the tumour growth inversely correlates with the amount of attracted NPCs, which in turn diminishes with increasing age.

To quantify how the survival of a glioblastoma depends on the age of the animal and on the amount of neural precursor cells in the brain I compared survival times of animals of different age after inoculation of GL261 glioma cells. Recipients consisted of a group of young (P25) and a group of adult (P180) mice. A third group obtained a mixture of cultured adult NPCs and GL261 glioma cells in the ratio 3:1. As **fig. 3.8**. shows, the survival of younger mice significantly exceeded that of older animals after GL261 cell inoculation. However, when exogenous NPCs were administered together with the GL261 cells, the older animals survived as long as the young ones.

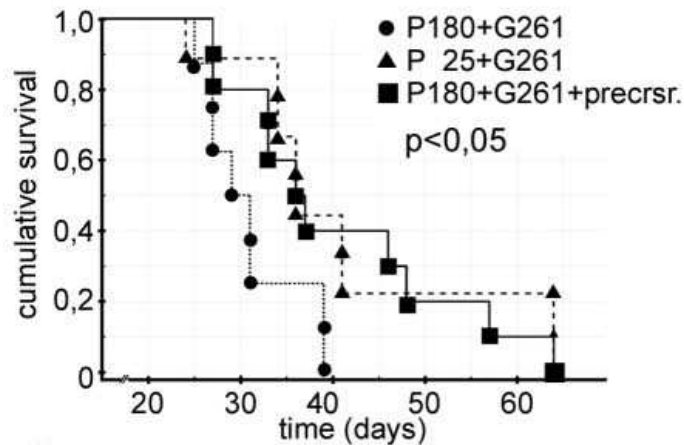


Fig. 3.8. Younger (P25) outlive older (P180) mice after GL261 inoculation. Exogenously applied NPCs into old (P180) animals prolong the survival of glioblastomas. P25 + GL261, $n = 8$; P180 + GL261; $n = 9$ and P180 + GL261 + NPCs, $n = 10$.

3.2.2. The anti-tumourigenic response in young and adult mice

3.2.2.1. Age-related decrease of subventricular proliferation is further reduced by glioblastoma

I had observed that the number of neural precursor cells (NPCs), which are recruited to the tumour, diminishes with increasing age of the animal, which in turn results in a shorter survival time. Next, I examined whether the reduced number of NPCs around the tumour in adult animals was due to lower subventricular proliferation in response to the tumour.

Thus, young (P30) and adult (P90) mice received intraperitoneal injections of BrdU, a marker for proliferation, two hours before killing.

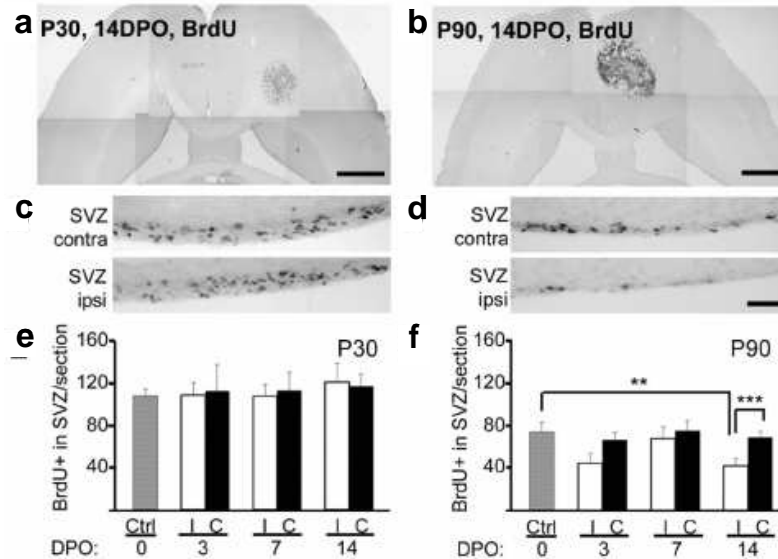


Fig. 3.9. Subventricular proliferation declines in the tumour-bearing hemisphere in adult compared to young mice. Horizontal sections through mouse brains of P30 (a) and P90 (b) reveal strong labelling for BrdU in the tumour and in the SVZ at 14 DPO. Higher magnification of the BrdU labelling in the SVZ contra- and ipsilateral to the tumour (SVZ contra, SVZ ipsi) in P30 (c) and P90 (d) animals. Proliferation in the P90 is generally lower than in the P30 mouse (contralateral SVZ) and even more reduced on the tumour-bearing hemisphere. **e:** Quantification of subventricular proliferation in untreated controls (Ctrl., 0 DPO) and 3, 7 and 14 DPO after GL261 inoculation. The proliferation in mice of P30 is maintained at a constant level both ipsi- (I, white bars) and contralaterally (C, black bars) over the whole time course. **f:** Proliferation in P90 mice stays relatively constant on the contralateral side over two weeks, though on a lower level than in the younger group. However, ipsilaterally, proliferation decreases rapidly 3 DPO, returns to control levels at 7 DPO and significantly declines again (14 DPO). Scale bars: **a,b:** 1 mm; **d:** 50 μ m

The gliomas in young mice were consistently smaller than in adult mice (**fig. 3.9a,b**). Young animals displayed a constant level of BrdU-positive cells in the SVZ over a period of 14 days. The number of dividing cells in the tumour-bearing brains did not differ from the untreated control sections (**e**). Yet, proliferation rates in adult animals were different. At 3 DPO, the number of BrdU labelled cells in the ipsilateral SVZ reached only about 60 % of the untreated control group (0 DPO) and about 70 % on the contralateral side. Seven days after GL261 glioma cell inoculation, proliferation returned to the level of

untreated controls on the ipsi- and contralateral side. However, 14 DPO ipsilateral SVZ cell proliferation had again declined by approximately 40 % compared to the contralateral side and to the untreated control SVZ. BrdU labelling in the contralateral SVZ and in control brains remained at a constant level (f).

In summary, I observed that young animals displayed a steady state of proliferating cells in the SVZ both ipsi- and contralaterally to the tumour. There is a reduction of the total number of dividing cells in the adult SVZ (c,d) and a further significant decline of BrdU labelling in the tumour-bearing hemisphere.

3.2.2.2. Whole cell numbers in the subventricular zone are independent of pathology

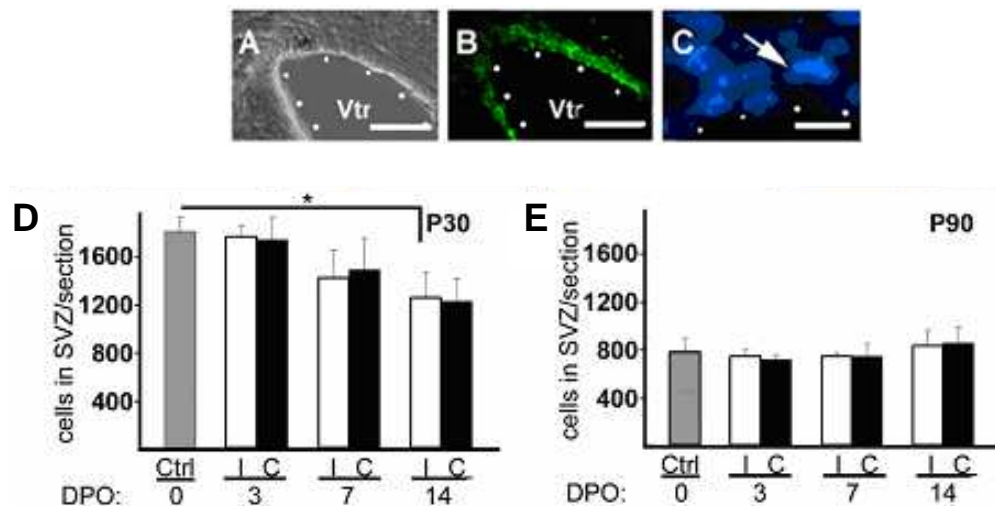


Fig. 3.10. Whole cell numbers in the SVZ of young and of adult mice after glioma injection. **A:** Phase contrast image of a horizontal section through a nestin-GFP mouse brain. **B:** The corresponding fluorescence micrograph, the ventricle is indicated by dots. **C:** Single cell nuclei (arrow) in the SVZ after Hoechst labelling. **D:** The total number of cells in the SVZ of P30 animals declines over a period of 14 days but remains on the same level in the site ipsilateral (I, white bars) and contralateral (C, black bars) to the tumour. **E:** The total SVZ cell number of P90 mice stays at a constant level lower than in the P30 group and does not vary between the ipsi- and contralateral side. Statistical significance: $p < 0.05$ (*). Scale bars: **A, B:** 500 μ m; **C:** 5 μ m.

Having quantified the number of proliferating subventricular cells in response to a tumour, whole cell numbers in young (P30) and adult (P90) subventricular zones (SVZs) were analysed. Quantification of subventricular whole cell numbers should clarify the question, whether altered numbers of total cells in the SVZ are responsible for the diminished number of neural precursor cells (NPCs) around the tumour in adult animals or if adult subventricular proliferation is further reduced by the presence of a tumour.

Stereological cell counting of nuclei in the SVZ, visualized with Hoechst 33358 was performed. Young animals revealed a diminishing total SVZ cell number within 14 days after tumour application both on the ipsi- and contralateral side (**fig. 3.10D**). The total number of cells in the adult SVZ was about 50 % lower compared to that in P30 mice (**E**). However, cell numbers remained at a constant level over the time course of 14 days on both hemispheres, thus independent of the tumour.

3.2.2.3. Cell death rate in the subventricular zone is independent of pathology

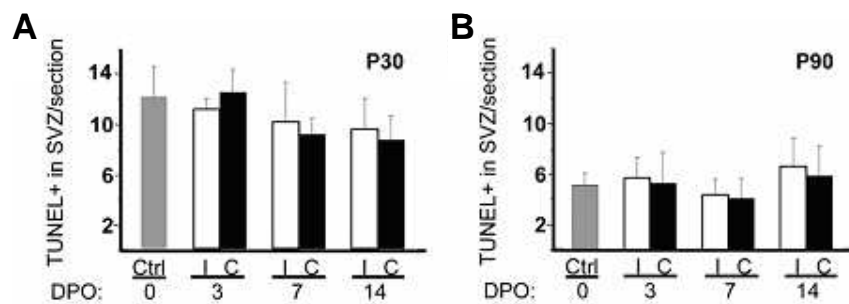


Fig. 3.11. The number of TUNEL-positive SVZ cells is not affected by the presence of a tumour. GL261 glioma cells were inoculated into P30 (**A**) and P90 (**B**) mice. TUNEL-positive cells were quantified after 3, 7 and 14 DPO. Values remained on the same level within one group and did not differ in the site ipsilateral (I, white bars) and contralateral (C, black bars) to the tumour. Non-operated animals represented 0 DPO.

To further investigate the different tumour response in young and adult mice, cell death rates in young (P30) compared to adult (P90) subventricular zones (SVZs) were determined. I used TUNEL labelling of nestin-GFP expressing cells to quantify the total number of dying cells. The amount of TUNEL-positive cells in the SVZ of young and of adult mice did not change within each group over the time course of 14 days after glioma inoculation and was not affected by the presence of the tumour (**3.11A, B**). The group of adult animals displayed a 50 % reduction of total TUNEL-positive cells compared to the P30 animals. However, this seems to be related to the decline in total cell number in the adult SVZ, which was also reduced by 50 %.

3.2.2.4. The composition of (proliferating) subventricular precursor cells in the pathological young and adult brain

In order to get more information about the nature of the proliferating cells in a tumour-bearing brain, the composition of the subventricular zone (SVZ) was investigated over a timecourse of 14 days. Therefore, type B, C and A cells were labelled with specific immunohistochemical markers. Type B cells were identified by labelling for nestin, vimentin and GFAP, type C cells were stained for nestin and DLX2 but were negative for PSA-NCAM. Type A cells were labelled for nestin, DLX2 and PSA-NCAM. Having identified each cell type, the relative fraction of each precursor cell type of all nestin-positive cells was quantified. Finally, the percentage of type B, C and A cells, which underwent cell cycling, was determined. **Tab. 3.1.** shows the scheme which was used for quantifying proliferating cells. The obtained data (for non-operated animals) are in good agreement with the ones published by Doetsch *et al.* (13).

Young animals displayed a relatively constant level of type B and C cells over the timecourse of 14 d of glioma development (**fig. 3.12A**), which was comparable to the condition in non-operated animals (0 DPO). The relative amount of type A cells gradually declined, which corresponds to the decline in whole cell numbers in the SVZ (**fig. 3.10A**). Precursor cell proliferation in young animals did not change between 0 DPO and 14 DPO. However, adult (P90) mice showed a rapid decline of both cell numbers and proliferation rates after 14 days (**fig. 3.12B**). The proliferation levels of type A cells may explain the biphasic course of BrdU labelling in operated P90 mice determined by stereological cell counting (**fig. 3.9f**).

Tab. 3.1. Criteria for identifying proliferating B-, C- and A cells

B cells	C cells	A cells
Nestin+ BrdU+ GFAP+ Vimentin+	Nestin+ BrdU+ DCX- PSA-NCAM- Vimentin- GFAP-	Nestin+ BrdU+ PSA-NCAM+

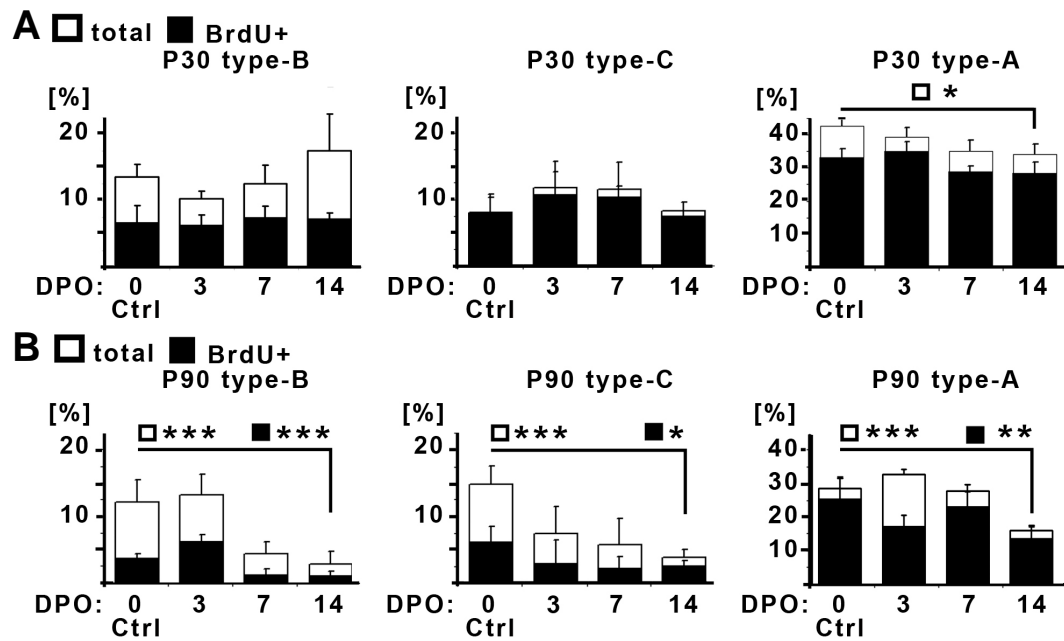


Fig. 3.12. Numbers of total and proliferating precursor subtypes in the SVZ, ipsilaterally to the tumour in P30 and P90 animals. **A:** In young mice, the relative fraction of each precursor cell type to the group of all nestin-positive cells (white bars) and the percentage of type B, C and A cells (black bars) is maintained at a constant level from 0 DPO until 14 DPO. **B:** Adult mice reveal a decline in the number of NPCs and of proliferation. Statistical significance: $p < 0.05$ (*), $p < 0.01$ (**), $p < 0.005$ (***)

3.2.2.5. The proliferative response of neural precursor cells to glioma is intrinsic and stable

It could be shown that subventricular proliferation in the pathological brain was reduced during the process of aging. Thus, it was of interest if neural precursor cells (NPCs) of different aged animals also show different proliferative responses upon stimulation with GL261 glioma cell conditioned medium *in vitro*. NPCs isolated from young (P30) and adult (P90) mice were therefore treated with GL261-conditioned medium and proliferation rates were quantified by BrdU labelling. NPCs from P30 mice showed a 75.3 % increase in BrdU incorporation after treatment with GL261-conditioned medium. In contrast, cell division in NPCs from P90 animals was induced by only 32.6 % (fig. 3.13A). Interestingly, extended passaging did not affect the proliferative response of NPCs, neither in cultures from P30 nor from P90 animals (fig. 3.13B). The response seems to be inheritable and therefore a stable cell-intrinsic effect.

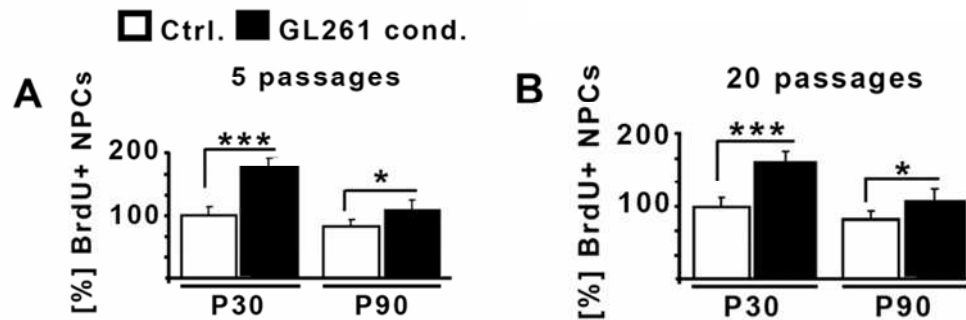


Fig. 3.13. The diminished proliferative response of P90 NPCs towards tumours is stable under *in vitro* conditions. Cultured NPCs of P30 and P90 mice were stimulated with GL261-conditioned medium for 3 d. Proliferation was quantified by BrdU labelling. NPCs of P30 animals were strongly induced to proliferate whereas cells of P90 mice only revealed modest proliferation (A). NPCs from P30 animals maintained their high proliferative response over 15 passages and NPCs from P90 mice maintained their moderate cell division rates (B). Statistical significance: $p < 0.05$ (*), $p < 0.005$ (***).

3.2.2.6. The expression of cyclin D1 in neural precursor cells declines with increasing age

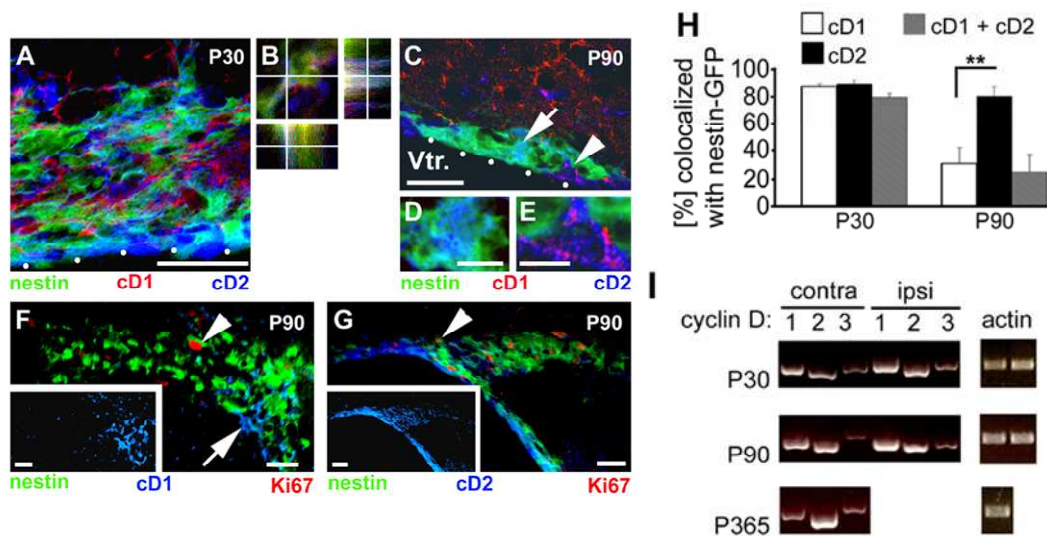


Fig. 3.14. Cyclin D2 expression becomes predominant in subventricular NPCs during aging. 14 DPO after GL261 inoculation into P30 and P90 mice the expression of D-type cyclins was examined by immunohistochemistry of the NPCs in the SVZ. **A:** P30 NPCs mostly co-label for cyclin D1 (red) and D2 (blue) (**B:** co-labelling cell in 3D reconstruction). **C:** P90 NPCs mainly express cyclin D2 (arrow, magnified in **D**); note that some nestin-GFP negative cells in the SVZ (arrow, magnified in **E**) and cells outside the SVZ label for cyclin D1. **F:** Nestin-GFP negative and cyclin D1 expressing cells in the P90 SVZ (arrow, magnified in insert) do not co-label for Ki67 (red) whereas nestin-GFP positive, cyclin D1 negative cells are still dividing (arrowhead). **G:** Strong expression of cyclin D2 in the P90 SVZ (insert) and co-labelling of Ki67 and cyclin D2 (arrowhead). **H:** In NPCs of the P30 SVZ cyclin D1 and nestin-GFP co-labelling cells additionally co-label for cyclin D2 and vice versa. NPCs of the P90 SVZ mainly express cyclin D2 but cyclin D1 labelled cells still co-express cyclin D2. **I:** RT-PCRs for cyclin D1, D2 and D3 were performed from microdissected SVZs. The amount of cyclin D1 mRNA gradually declines from P30 to P365 on the contralateral side of the tumour (contra) and untreated P365 SVZ, respectively. Cyclin D2 becomes predominantly expressed. Cyclin D1 expression in P90 on the ipsilateral side (ipsi) results from non-subventricular cells. Very little cyclin D3 expression was observed under all conditions. Equal amounts of DNA was used (actin). Scale bars: **A, C, F, G:** 30 μ m; **D, E:** 5 μ m. Statistical significance: $p < 0.01$ (**).

It was shown that subventricular proliferation is diminished by the presence of a glioma in adult but not in young animals. Since D-type cyclins regulate G1-progression and therefore play a crucial role for proliferation and are moreover age-dependently differentially expressed, it was of major interest how the expression of D-type cyclins develops during

the process of aging in response to the tumour. Cyclin D1 promotes entry into S-phase in neural precursor cells (NPCs) in young but is missing in adult animals. In contrast, cyclin D2 expression also remains in adult mice; cyclin D2 knockout animals therefore lack adult neurogenesis (45).

Based on this knowledge it was investigated whether cyclin D1 is also lost in adult mice under pathological conditions. 14 days after glioma inoculation, nestin-GFP positive subventricular NPCs of P30 and P90 animals were labelled for D-type cyclins ipsi- and contralateral to the tumour. Young animals showed abundant expression for cyclin D1 and cyclin D2 on both the ipsi- and contralateral side (**fig. 3.14A, B**). In contrast, P90 NPCs expressed cyclin D1 only on a very low level in the ipsi- and contralateral SVZ (**C**) whereas cyclin D2 expression was still strongly present (**C, D**). Cyclin D1 expression was also detected in nestin-GFP negative cells in the P90 SVZ (**E**). P30 animals co-expressed cyclin D1 and cyclin D2 in almost all nestin-GFP positive cells. At P90, cyclin D1 expression was significantly reduced and cyclin D2 became predominant in subventricular NPCs (**H**). Performing immunolabelling with the proliferation marker Ki67 revealed that only few P90 cyclin D1 expressing cells underwent cell-cycling (**F**) whereas cyclin D2 expressing cells also co-labelled for Ki67 (**G**).

To investigate the mRNA expression of cyclin D1, D2 and D3 throughout aging under pathological conditions, semi-quantitative RT-PCRs were performed. Additionally, D-type cyclin expression was analysed in non-operated one year old mice. Young (P30) ipsi- and contralateral subventricular NPCs displayed equal expression of cyclin D1 and D2. However, adult NPCs (P90) showed a stronger expression of cyclin D2 compared to cyclin D1 on the contralateral side. The one year old animals demonstrated only faint bands for cyclin D1, which makes cyclin D2 predominant. The strong band indicating cyclin D1 expression in the ipsilateral P90 NPCs is most probably generated by neurons outside the SVZ, which were dissected together with the SVZ tissue. Under all experimental conditions cyclin D3 was very weakly expressed.

In summary, the data show that NPCs in the tumour-bearing P30 SVZ co-express cyclin D1 and D2 and that P90 mice have lost large parts of cyclin D1 expression in their subventricular NPCs.

3.2.2.7. Loss of D-type cyclins in the subventricular zone attenuates neural precursor cell proliferation

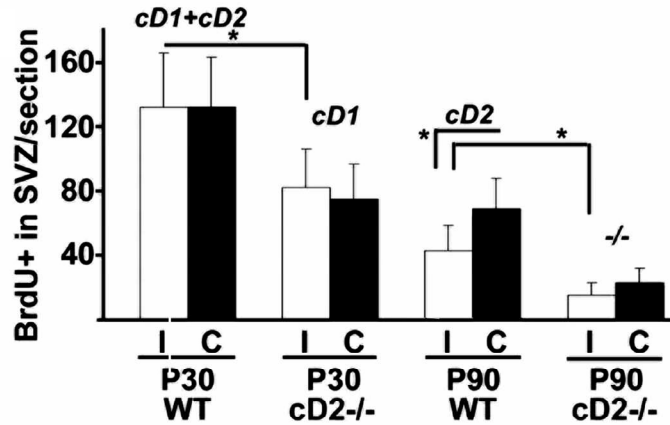


Fig. 3.15. Loss of cyclin D2 expression results in reduced proliferation in the SVZ. GL261 cells were inoculated into the caudate putamen of the right hemisphere of P30 and P90 cyclin D2 deficient mice (cD2^{-/-}) and their wild type (WT) littermates. Proliferation in the ipsi- and contralateral SVZ was quantified. The number of dividing cells in P90 mice is significantly lower on the ipsi- compared to the contralateral side than in P30 mice. P30 (cD2^{-/-}) displayed a similar proliferation rate as the P90 WT. Proliferation was most radically reduced in P90 (cD2^{-/-}). Indicated in italics are those cyclins, which mainly remained expressed at each age and under each genetic condition. Statistical significance: $p < 0.05$ (*).

It was shown that only adult animals (P90) show a decline of cyclin D1 in the tumour-exposed subventricular zone whereas cyclin D2 remains stably expressed. Since cyclin D1 knockout animals display developmental abnormalities (23) cyclin D2 knockout mice were used to investigate the effect of absent cyclin D2 expression on proliferation in the subventricular zone (SVZ) after glioma inoculation. Neurogenesis in adult cyclin D2 knockout mice is drastically reduced but does not have major anatomical effects on the embryonic or early postnatal development of the forebrain (45). Since neurogenesis is affected, loss of cyclin D2 should also have an effect on neural precursor cell (NPC) proliferation in the subventricular zone. A glioma was injected and proliferation rates were quantified by BrdU labelling of NPCs in wild type (WT) and cyclin D2-deficient cD2^{-/-} mice ipsi- and contralateral to the tumour at 14 days after the operation. In comparison to wild type animals, proliferation in the P30 SVZ of cD2^{-/-} mice was reduced by 40 %.

NPCs in the contralateral side of P90 WT mice displayed the same level of proliferation as P30 cD2(-/-) animals. WT P90 mice showed diminished cell division in the ipsi- compared to the contralateral SVZ. Only very little proliferation was left in the P90 cD2(-/-) animals (fig. 3.15.).

3.2.2.8. Loss of D-type cyclins results in increased tumour size

To further investigate how the proliferation of subventricular neural precursor cells (NPCs) affects glioma development, tumour sizes in WT and cD2(-/-) mice 14 DPO were quantified (fig. 3.16A-D). The data show that P30 and P90 cyclin D2 knockout animals developed gliomas, which were about 100 % increased in size compared to their age matched WT littermates. In absolute numbers the respective tumour volumes were as follows: P30 WT: 1.96 mm³; P30 cD2(-/-): 3.96 mm³; P90 WT: 3.4 mm³; P90 cD2(-/-): 6.39 mm³.

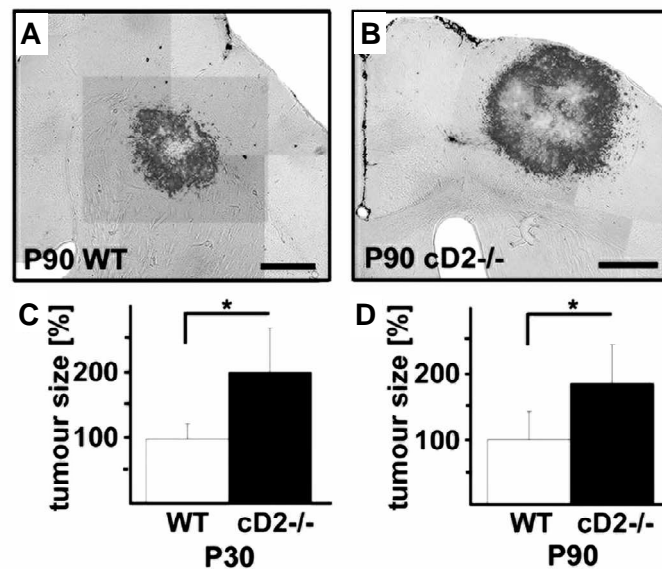


Fig. 3.16. Absence of cyclin D2 leads to increased tumour sizes. A,B: Micrographs of horizontal sections of mouse brains. Tumours in P90 (cD2(-/-)) have grown bigger after 14 DPO than in P90 WT. C: Quantification of the tumour volumes in WT and (cD2(-/-)) at P30 and P90. Tumours are significantly bigger in the knockout animals than in the WT littermates. Scale bars: A,B: 1 mm. Statistical significance: p<0.05 (*).

3.2.3. The anti-tumourigenic response of neural precursor cells *in vitro*

3.2.3.1. Neural precursor cells reduce total GL261 glioma cell number

It was shown that the proliferating pool of neural precursor cells (NPCs) in the subventricular zone (SVZ) and the accumulation of these cells around the glioblastoma correlates with a decreased tumour size *in vivo* and thereby significantly prolongs the survival of the animals (24). In order to investigate whether this effect is mediated only between glioma and precursor cells or if there are other cell types required to obtain the anti-tumourigenic response, tumour cells and NPCs were analysed under *in vitro* conditions. Therefore, co-cultures of adherent neural precursor cells (NPCs) isolated from a P14 nestin-GFP mouse and GL261 glioma cells-DsRed were set up. (Unless otherwise mentioned, all NPCs, which are used for *in vitro* experiments are isolated from P14 animals.) After three days cell nuclei were stained with DAPI, which allowed quantifying the GL261 cell number by counting DsRed-DAPI co-localising cells. For each group cells were counted in ten non-overlapping optical fields of the microscope, the quantification for each group was repeated three times.

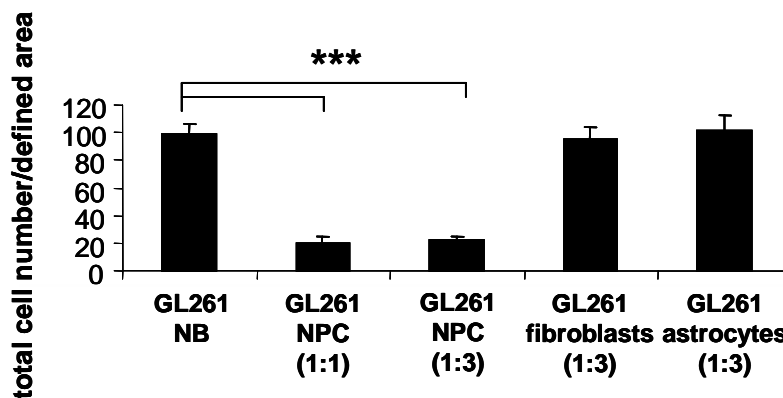


Fig. 3.17. Reduction of GL261 glioma cell number by neural precursor cells. GL261-DsRed cells were co-cultured with NPCs-GFP in different ratios (1:1 and 1:3) for 72 h. Co-cultures of GL261 with fibroblasts and astrocytes served as controls. Quantification of the total GL261 cell number was determined by counting cells co-labelling for DAPI and DsRed per defined area. Ten optical fields were counted per group, counting was repeated three times. NB: non-conditioned NB/B27, NPC: neural precursor cells. Statistical significance: $p < 0.005$ (***)

In comparison to the controls, in which GL261 glioma cells were co-cultured with astrocytes and fibroblasts, GL261 cell numbers were significantly reduced in the presence of NPCs (**fig. 3.17.**). Average total GL261 cell number per defined area (i.e. per optical field under the microscope) was 99 and decreased to 20 (in the ratio 1:1) and 22 (in the ratio 1:3) when cells were co-cultured with NPCs. After co-cultures with fibroblasts and astrocytes (both in the ratio 1:3) total cell numbers were 95 and 101, respectively. Thus, NPCs seem to have a direct impact on glioma cell numbers.

3.2.3.2. Neural precursor cell-conditioned medium reduces total GL261 glioma cell number

To examine whether direct cell contact is necessary or if a soluble factor is sufficient to provoke the observed anti-tumourigenic response by neural precursor cells (NPCs), GL261 glioma cells were cultivated in NPC-conditioned medium instead of growing them in co-cultures. After three days, cells were stained with DAPI and the total GL261 cell number was determined. **Fig. 3.18.** shows that NPC-conditioned medium drastically reduced GL261 cell numbers whereas fibroblast- and astrocyte-conditioned medium did not have such an effect.

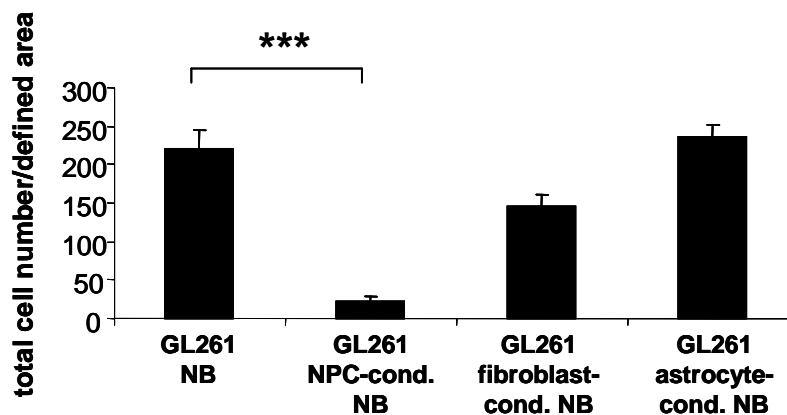


Fig. 3.18. Reduction of GL261 glioma cell number by neural precursor cell-conditioned medium.

GL261 cells were cultured on coverslips in NPC-conditioned medium. Cells were fixed after 72 h and stained with DAPI. Quantification of the total GL261 cell number was determined by counting DAPI-stained nuclei per defined area. Ten optical fields were counted per group, counting was repeated three times. NB: non-conditioned NB/B27, NPC-cond. NB: neural precursor cell-conditioned NB/B27. Statistical significance: $p < 0.005$ (***).

3.2.3.3. Neural precursor cells induce GL261 glioma cell death

In order to characterize the mechanisms, which lead to the reduced GL261 glioma cell number, GL261 were co-cultured with neural precursor cells (NPCs) and subjected to TUNEL analysis. TUNEL positivity indicates active cell death. I observed that GL261 cells were TUNEL-positive after co-culturing them with NPCs for three days. In comparison, co-cultures of GL261 cells with fibroblasts and astrocytes resulted in significantly less TUNEL-positive glioblastoma cells (fig. 3.19.).

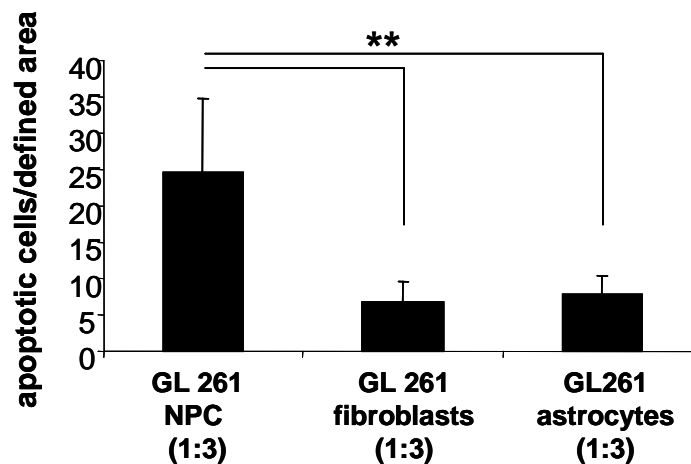


Fig. 3.19. Induction of GL261 glioma cell death upon co-culture with neural precursor cells. GL261 cells were co-cultured with NPCs, fibroblasts and astrocytes in the ratio 1:3. After 72 h, cells were fixed and a TUNEL reaction was performed. TUNEL-positive cells were quantified using a fluorescence microscope. Ten optical fields were counted per group, counting was repeated three times. NPC: neural precursor cell. Statistical significance: $p < 0.01$ (**).

3.2.3.4. The influence of passage number and days of conditioning on the efficacy of neural precursor cell-conditioned medium

The properties of neural precursor cell (NPC) neurosphere cultures change with continuous passaging. Therefore, I wanted to investigate how these different culture properties influence the ability of NPC-conditioned medium to induce TUNEL positive GL261 glioma cells. Cells, which have undergone different numbers of passaging (p10-25, > p25) were used to generate NPC-conditioned medium. The medium was collected after one, two and three days of conditioning and added to GL261 for 72 hours. After that, cells were

fixed and tested on induction of cell death by a TUNEL reaction. Subsequently, cells were stained with DAPI and quantified by counting. The data show that the most potent medium was the one obtained from NPCs, which were growing between passage 10 and passage 25 and which was conditioned for three days. Cells, which were cultivated for more than 25 passages were still able to induce TUNEL positive GL261, yet longer conditioning did not result in a significant increase but even displayed a slight decrease of efficacy (**fig. 3.20.**). Obviously, NPCs secrete less of the death inducing factor(s) after being cultivated for more than 25 passages. Since NPCs need some passages after isolation to reach the clonal density in which they grow later on, medium was not used from these early cultures (p0-p10).

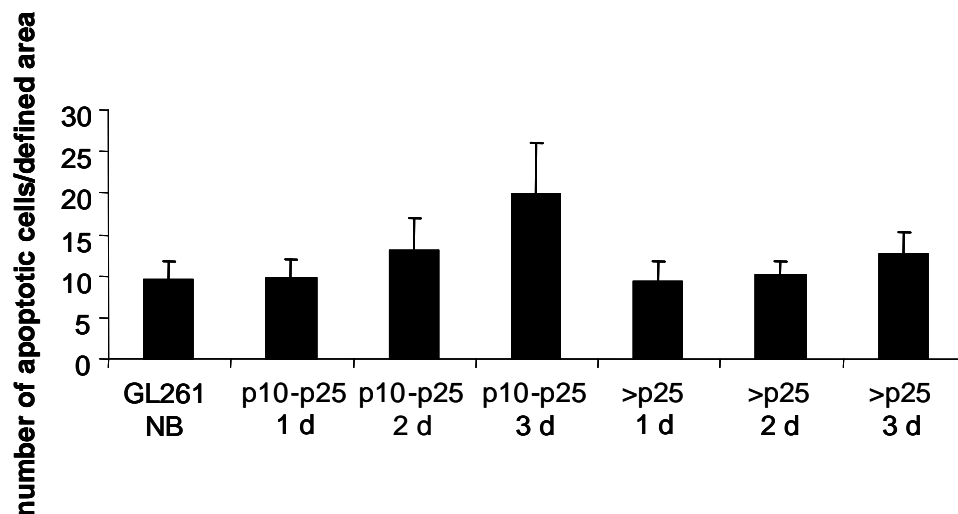


Fig. 3.20. Induction of TUNEL positive GL261 by different NPC-conditioned media. Media were obtained from cells with different passage numbers (p10-25, > p25), each conditioned for 1 d, 2 d and 3 d. GL261 were cultivated in these media for 72 h. Cells were fixed and a TUNEL reaction was performed. Cells were labeled with DAPI and nuclei were counted per defined area. Ten optical fields were counted per group, counting was repeated three times. NB: non-conditioned NB/B27, p: passage.

3.2.3.5. Neural precursor cell-conditioned medium induces cell death in human glioma cells

Having observed that neural precursor cell (NPC)-conditioned medium provokes an anti-tumourigenic response in GL261 cells, a murine glioma cell line it was interesting to know whether this medium also affects viability of human glioblastoma cells. Therefore, human

glioma cells derived from a grade III astrocytoma were cultivated in NPC-conditioned medium on coverslips for a period of 72 h. Cells were labelled with DAPI and the total cell number was determined by counting the cells under a fluorescence microscope. The number of cells, which were cultivated in NPC-conditioned medium, was significantly reduced compared to the number of cells, which were incubated in non-conditioned medium (**fig. 3.21.**). Additionally, a TUNEL assay was performed. TUNEL positive cells were quantified using a fluorescence microscope. The number of TUNEL positive cells was significantly higher in the group, which was cultured in NPC-conditioned medium compared to the control group. Thus, it can be assumed that NPC-conditioned medium also induces cell death in human glioma cells.

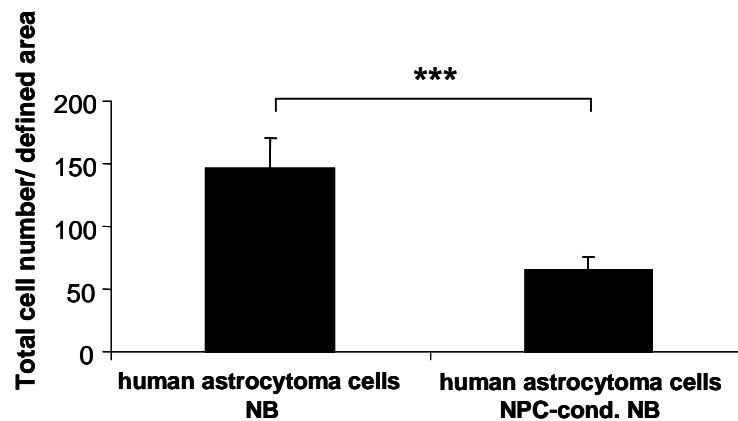


Fig. 3.21. Reduction of total cell number of human glioma cells by NPC-conditioned medium. Cells were cultivated on coverslips in non-conditioned and NPC-conditioned medium respectively. After 72 h cells were fixed and stained with DAPI. Total cell numbers were quantified by counting DAPI stained nuclei. Ten optical fields were counted per group, counting was repeated three times. NB: non-conditioned NB/B27, NPC-cond. NB: neural precursor cell-conditioned NB/B27. Statistical significance: $p < 0.005$ (***)

3.2.3.6. Release of GL261 glioma cell death inducing factor from neural precursor cells is age-independent

I observed that neural precursor cells (NPCs) in young subventricular zones (SVZ) had an increased proliferative potential compared to NPCs in adult SVZs. Due to this enhanced proliferation more NPCs could accumulate around the tumour, which enabled young animals (P30) to display a stronger anti-tumourigenic response than adult animals (P90). The question was therefore whether the distinct anti-tumourigenic response of young NPCs is due to their higher cell division rates or whether they are more anti-tumourigenic as

such. GL261 cells were treated with NPC-conditioned medium from P30 and P90 NPCs for three days and tested by TUNEL regarding induced cell death. Additionally, P90 hippocampal NPCs were used to generate NPC-conditioned medium, which was also used for GL261 treatment. **Fig. 3.22.** displays that all media induced GL261 cell death with roughly the same fold induction rate. Non-conditioned medium and staurosporine served as negative and positive controls.

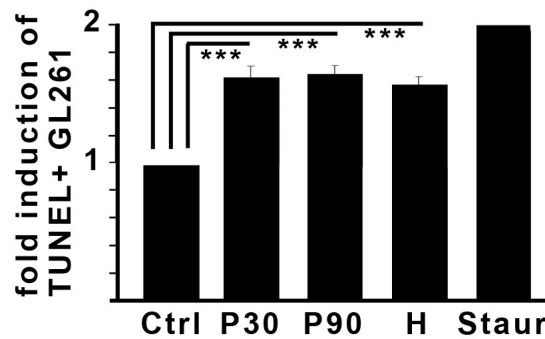


Fig. 3.22. NPCs from P30 and P90 animals hold an age-independent capability to induce GL261 cell death. Non-conditioned medium served as a negative control (Ctrl.) whereas staurosporine represented a positive control (Staur) with a 2-fold induction of GL261 cell death. Conditioned medium from NPCs of P30 and P90 SVZs as well as from P90 hippocampal NPCs (H) had equal potency to induce glioma cell death. Statistical significance: $p < 0.05$ (*).

3.3. Characterization of GL261 glioma cell death induced by neural precursor cells

3.3.1. Neural precursor cell induced GL261 glioma cell death is not apoptosis

3.3.1.1. Neural precursor cell induced GL261 glioma cell death is caspase-independent

Apoptosis, one type of programmed cell death is probably the most studied type of cell death mechanism. To investigate whether neural precursor cell (NPC)-conditioned medium induced GL261 cell death is apoptosis or some alternative cell death mechanism, I examined if caspases, the key enzymes of apoptotic reactions were involved. GL261 cells were cultivated in non-conditioned and NPC-conditioned medium. Additionally, GL261 cells were incubated in NPC-conditioned medium containing the caspase-inhibitor

Z-VAD-FMK (20 μ M). After three days, cell death rate in each group was quantified by performing the DELFIA TUNEL (DNA fragmentation) assay, which demonstrated that the rate of GL261 cell death, induced by NPC-conditioned medium was not affected by the presence of the caspase inhibitor (**fig. 3.23.**). Hence, caspases do not seem to be involved in NPC-conditioned medium induced glioma cell death.

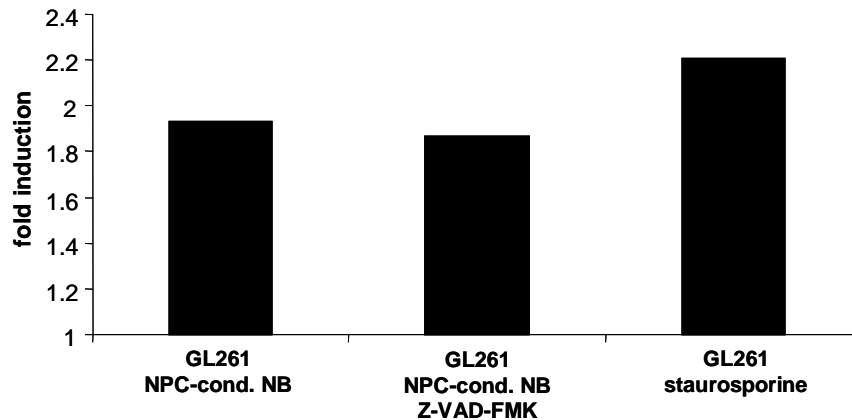


Fig. 3.23. The caspase inhibitor Z-VAD-FMK does not affect NPC-conditioned medium induced GL261 cell death. GL261 were cultivated in NPC-conditioned medium alone (NPC-cond. NB) and NPC-conditioned medium containing the caspase-inhibitor Z-VAD-FMK (20 μ M) for 3 d. Non-conditioned medium served as a negative (baseline) and staurosporine (10 μ M) as a positive control. GL261 cell death rates were determined by the DELIFA TUNEL assay.

In addition, I studied the involvement of caspases in GL261 cell death by performing western blot for caspase-3 and -7. GL261 glioma cells were cultured in non-conditioned and NPC-conditioned medium and harvested after three days. Cells were lysed according to the protocol and the western blot was performed using antibodies against cleaved caspase-3 and -7. Only upon activation of initiator caspases like for example caspase-8 the pro-form of caspase-3 and -7 will be cleaved and induce the further cascade in the apoptotic cell death machinery. The blot revealed that neither cleavage of caspase-3 nor of caspase-7 occurred (**fig. 3.23.**) As a positive control, cell extracts from C6 rat glioma cells were used, which were treated with the CK2-inhibitor ZKK-1 (50 μ M). Two independent samples of non-conditioned and NPC-conditioned NB/B27 were used.

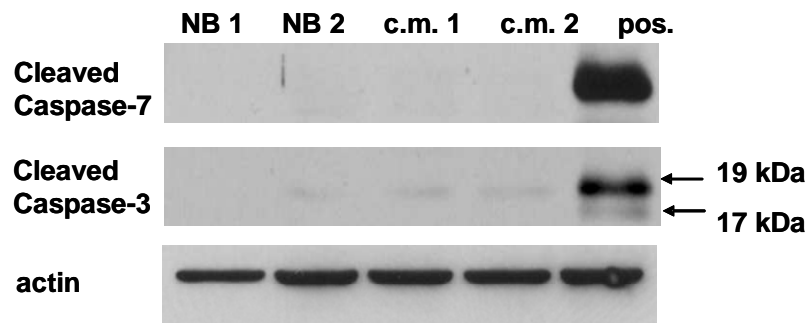


Fig. 3.24. GL261 cells do not express active caspase-3 and -7 after treatment with NPC-conditioned medium. GL261 cells were cultivated in non-conditioned NB/B27 (NB) and NPC-conditioned medium (c.m.). Cells were lysed and a western blot was performed. There was no activation of caspase-3 or -7 in either sample visible. The positive control (pos.) consisting of C6 cells treated with ZKK-1 (50 μ M) revealed two clear bands indicating cleavage of caspase-3 and -7. Equal amounts of protein lysates were used (actin).

3.3.1.2. Neural precursor cell induced GL261 glioma cell death is not death-receptor mediated

Fas-ligand (FasL), one of the members of the TNF superfamily of ligands, is known as a death ligand and mediates apoptosis. Upon binding of the ligand to its receptor formation of a death inducing signaling complex (DISC) occurs, which is comprised of death receptors, adaptor molecules and initiator caspases. The assembly of a DISC leads to the activation of caspase-8 which can activate downstream executing caspases leading to apoptosis.

To test whether this happens in GL261 glioma cells, which die upon treatment with neural precursor cell (NPC)-conditioned medium, this medium was applied to tumour cells (LN18), which are extremely sensitive to death-receptor mediated apoptosis; recombinant TNF-related apoptosis-inducing Ligand (TRAIL) served as a positive control. The number of cells, which turned apoptotic, was quantified by FACS-analysis. As shown in **fig. 3.25.**, neither of the two independent samples of NPC-conditioned medium induced apoptosis, suggesting that the conditioned medium does not induce death-receptor mediated cell death in GL261 glioma cells.

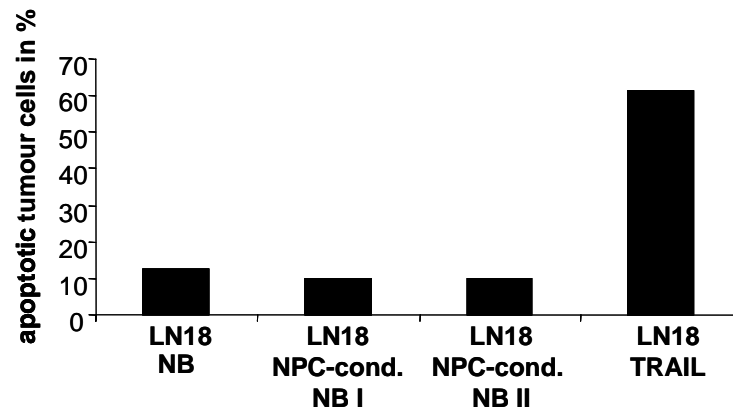


Fig. 3.25. NPC-conditioned medium does not induce apoptosis in death-receptor mediated cell death sensitive tumour cells. Tumour cells, which are extremely sensitive for death-receptor mediated apoptosis (LN18) were treated with two charges of non-conditioned NB/B27 (NB) and NPC-conditioned medium (NPC-cond. NB) for 72 h. Quantification of apoptotic tumour cells was performed by FACS-analysis. Recombinant TRAIL served as a positive control.

3.3.2. GL261 glioma cells undergo morphological changes upon stimulation with neural precursor cell-conditioned medium

Altered cell functions are often accompanied by changed cell morphology. To acquire more information about the GL261 cell death mechanism, induced by neural precursor cell (NPC)-conditioned medium, cells were analysed by electron microscopy. After three days of cultivation in fresh and NPC-conditioned medium respectively, cells were fixed, harvested and embedded in gelatine. After the overnight incubation in sucrose they were frozen in liquid nitrogen. Ultrathin cryosections were made, which were contrasted and stabilized. Samples were examined with an electron microscope, pictures were taken and analysed with the software analySIS 3.2. **Fig. 3.26.** demonstrates that the cytoplasm of GL261 cells, which were cultured in fresh medium appears homogenously grey, indicating a healthy status of the cell. The endoplasmic reticulum (ER) appears normal in contrast to the ER of the GL261 cells, which were cultivated in NPC-conditioned medium. In those cells, the ER membrane displays extreme swelling presenting so-called ER enlargement, which is a morphological indicator of ER stress.

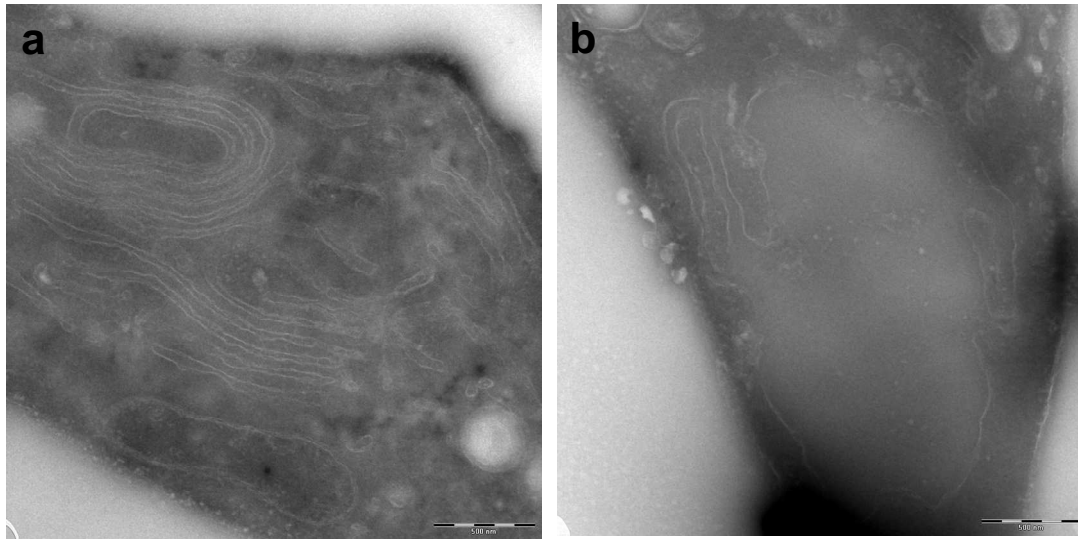


Fig. 3.26. Electron microscopy of GL261 glioma cells cultured in fresh and NPC-conditioned medium. **a:** GL261 cells, which were cultivated in non-conditioned medium display a homogenous grey cytoplasm. The ER presents a normal morphology. **b:** The ER of GL261 cells, which were treated with NPC-conditioned medium, exhibits large areas of membrane swelling. Scale bar: 500 nm.

3.3.3. Differential gene expression in GL261 glioma cells induced by neural precursor cell-conditioned medium

Neural precursor cell (NPC)-conditioned medium induced cell death of GL261 glioma cells can be observed after three days. This relatively long period for cell death induction suggests that cell death is based on (post)-transcriptional changes of the cell. Therefore differential gene expression in GL261 glioma cells was investigated and a cDNA microarray was performed. Tumour cells were cultivated in NPC-conditioned medium and non-conditioned medium as a control respectively for three days. Cells were harvested and three co-hybridizations were performed. The obtained datasets were subjected to further analysis, which involved normalization (2.2.11.4.). For identification of relevant differentially expressed genes, each clone with a more than 1.5-fold difference in expression was considered for further evaluation. **Tab. 3.1.** contains the genes, which were differentially expressed (+: upregulation, -: downregulation) in all three arrays.

Tab. 3.2. Gene expression changes in GL261 cells after stimulation with NPC-conditioned medium (3d)

Gene title	Clone ID	Ratio 1	Ratio 2	Ratio 3
Transcription factor-like protein ODA-10	AB012276 BF321641 BF020914	+2.671240427	+2.262598741	+1.781127655
ESTs Highly similar to isopentenyl-diphosphate delta-isomerase <i>Schizosaccharomyces pombe</i>	BG311324 AA763802 BG093481	-1.560838788	-2.457469698	-2.822011173
Cyclin-dependent kinase inhibitor 1A P21	W82380 AW048937 BF228138	+1.540065547	+1.715015758	+1.566748616
Ceruloplasmin	BF137253 AW209037 BE370729	+1.83335753	+1.574804634	+1.560214722
SEC23A <i>S. cerevisiae</i>	BF152874 BF139876 BE309389	+1.559004001	+1.623743462	+1.902765328
<i>Mus musculus</i> FN5 protein mRNA complete cds	AF197136 BF714169 AA562014	+1.815823034	+1.513886108	+1.569352245
UDP-glucuronosyltransferase 1 family member	AI043114 AI036348 AI043065	+1.513293723	+1.776750423	+1.580958099
Olfactomedin related ER localized protein	D78264 NM_019498 D78262	-1.86218235	-2.061057707	-1.618463408
p21 CDKN1A activated kinase 1	BF456404 BE945109 AW045634	+1.503105863	+3.086052368	+1.870096345
ESTs Weakly similar to Y053_human hypothetical protein KIAA0053 <i>H. sapiens</i>	BE980945 AW456462 BG228919	+1.713053008	+2.039771479	+1.740704979
Activating transcription factor 3	U19118 BE199676 BG067364	+1.72427926	+2.41265722	+2.025507903
Myeloid differentiation primary response gene 116 (MyD 116 or GADD34)	BF017433 NM_008654 X51829	+2.473003345	+2.695526118	+1.673508867
RIKEN cDNA 1200015M12 gene	AA174873 AA175210 C85726	+2.386765288	+3.514794935	+1.502894293
RIKEN cDNA 1110017I16 gene	BE950971 AK003750 AI413224	-1.683435126	-2.892604681	-1.713246751
<i>Mus musculus</i> clone MGC 11758 mRNA complete cds	AI429734 AW743686 BF323428	+1.515854246	+1.891053383	+1.506231193
Expressed sequence AW120568	BC004709 BF730769 AW911184	-1.538416179	-1.79185828	-1.510652671
RIKEN cDNA 1810063P04 gene	BC004729 BE952795 BG175638	-1.808061554	-1.945448558	-1.537807977
ESTs	BE650884 AI504979 BB126077	-1.867165877	-1.852181068	-1.56249436
RIKEN cDNA 1500005G05 gene	AK005159	+1.744043097	+2.199663063	+1.919558003

	BG066520 C79462			
Macrophage stimulating 1 receptor c-met-related tyrosine kinase	U65949 NM_009074 X74736	-1.539121641	-1.813239245	-1.546742904
a disintegrin and metalloproteinase domain 12 meltrin alpha	BF227082 BF117283 AA174290	-2.505233888	-2.445476081	-1.618707776
Expressed sequence AI413331	AW908976 AW909135 AA607513	-2.119992439	-1.779051239	-1.559792036
RIKEN cDNA 2410008J01 gene	BI078181 BF319575 BG094315	-2.037577027	-3.036647913	-1.528874349
ESTs Moderately similar to S64718 formin-binding protein 17 - mouse <i>M. musculus</i>	AA034800 AA276943 BG144432	-1.700533814	-1.581804345	-1.665947864

3.3.4. Activating transcription factor-3 is necessary and sufficient for induction of GL261 glioma cell death

3.3.4.1. Activating transcription factor-3 is upregulated in GL261 glioma cells upon stimulation with neural precursor cell-conditioned medium

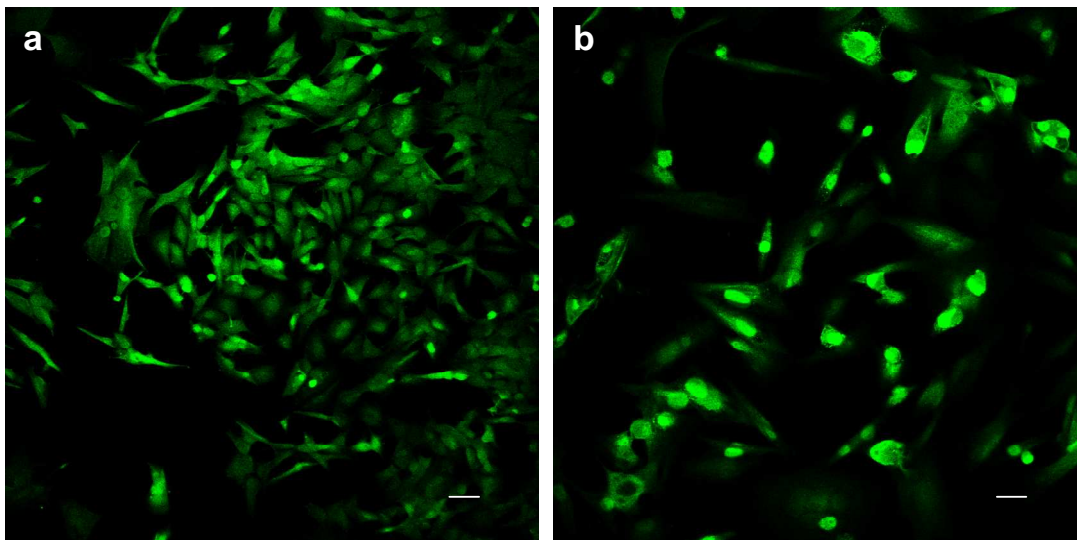


Fig. 3.27. ATF-3 distribution in GL261 glioma cells changes from cytoplasmic localization to nuclear expression upon treatment with NPC-conditioned medium. GL261 cells were cultivated in non-conditioned (a) and NPC-conditioned medium (b) for three days and stained against ATF-3. The secondary antibody is FITC-conjugated. Scale bar: 40 μ m.

Data from the gene array experiment revealed an upregulation of activating transcription factor-3 (ATF-3) in GL261 glioma cells upon treatment with neural precursor cell (NPC)-conditioned medium. This result could be validated by immunolabelling for ATF-3. Cells were cultured in non-conditioned (NB) and NPC-conditioned medium for three days and stained for ATF-3. GL261 cells, incubated in NB predominantly showed cytoplasmatic expression of the transcription factor whereas cells, treated with NPC-conditioned medium mainly displayed nuclear expression of ATF-3 (**fig. 3.27**).

3.3.4.2. Activating transcription factor-3 overexpression in GL261 glioma cells results in increased cell death

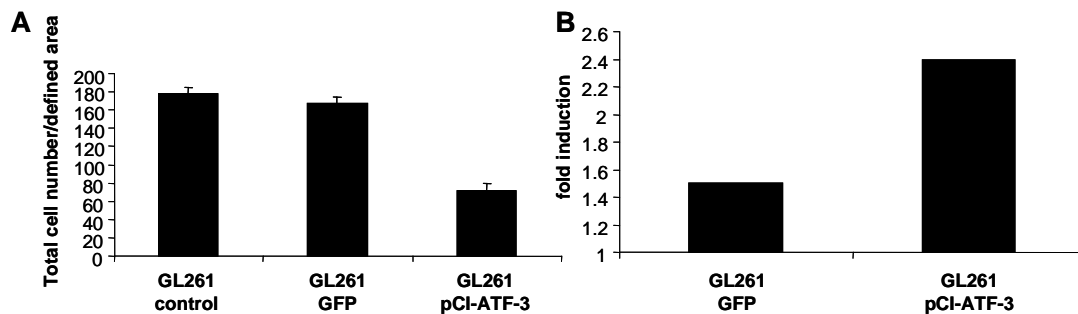


Fig. 3.28. ATF-3 overexpression in GL261 results in reduction of total cell numbers and induction of cell death. GL261 cells were transfected with the vector pCI-ATF-3 inducing overexpression of ATF-3. **A:** ATF-3 overexpression lead to a reduction of total cell number per defined area. Cell numbers of GL261, which were transfected with GFP were not affected. Ten optical fields were counted per group, counting was repeated three times. **B:** GL261 cell death rates, determined by TUNEL were increased by overexpression of ATF-3 compared to GL261, transfected with GFP.

To examine whether induction of activating transcription factor-3 (ATF-3) is sufficient to induce glioma cell death, ATF-3 overexpression was induced in GL261 cells. Cells were transfected with an ATF-3 overexpressing vector (pCI-ATF-3). Following the transfection, cells were stained with DAPI and quantified by counting the DAPI-stained nuclei under a fluorescence microscope. Cells from each group were counted in ten non-overlapping optical fields of the microscope. Quantification was performed three times for each group. The number of cells per defined area was significantly reduced after ATF-3 overexpression (**fig. 3.28**). Cells, which were transfected with DNA, encoding for GFP were not affected in total cell numbers. Additional performance of a TUNEL assay of the transfected cells

ensured that the observed reduced GL261 cell number after NPC-conditioned medium is due to increased cell death rates. Glioma cells, transfected with GFP displayed a cell death induction of 1.5 compared to the basal level, which consisted of non-transfected GL261. Overexpression of ATF-3 resulted in a 2.4-fold increase in cell death compared to the basal level.

3.3.4.3. siRNA against activating transcription factor-3 prevents GL261 glioma cell death upon stimulation with neural precursor cell-conditioned medium

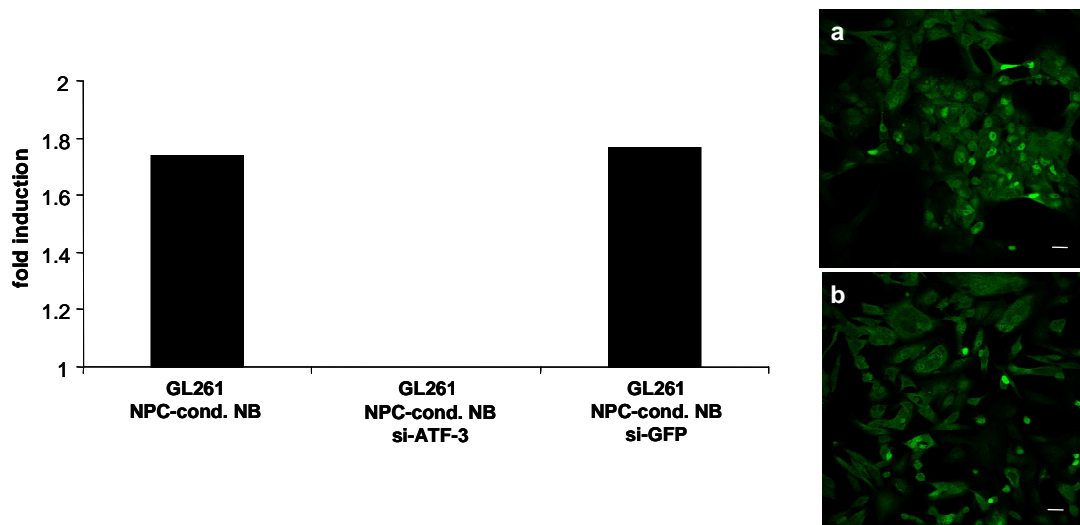


Fig. 3.29. siRNA against ATF-3 prevents NPC-conditioned medium induced GL261 cell death. GL261 were transfected with siRNA against ATF-3 and cultivated in non-conditioned and NPC-conditioned medium for 3 d. Cell death rates were quantified by TUNEL and are displayed as the fold induction compared to the basal level, consisting of non-transfected cells. Control cells, which were transfected with siRNA against GFP did not show altered values of TUNEL positive cells. However, ATF-3-siRNA transfected cells did not undergo cell death.

Immunolabelling of GL261 against ATF-3. **a:** GL261 were transfected with siRNA against ATF-3 and cultured in NB-medium. **b:** GL261 were transfected with siRNA against ATF-3 and cultured in NPC-conditioned medium. Cytoplasmic expression of ATF-3 demonstrates that NPC-conditioned medium does not induce activation of ATF-3 anymore.

I observed that overexpression of activating transcription factor-3 (ATF-3) in GL261 glioma cells results in reduced total cell numbers and increased cell death. Activation of ATF-3 therefore seems to be sufficient to induce glioma cell death. To further investigate the role of ATF-3 and to demonstrate whether ATF-3 is also necessary to induce glioma cell death, mediated by neural precursor cell (NPC-) conditioned medium, siRNA against ATF-3 was used. Glioma cells were transfected with siRNA against ATF-3 whereas control cells were transfected with siRNA against GFP. After transfection, cells were stimulated with non-conditioned and NPC-conditioned medium for three days and cell death was analysed by TUNEL. Whereas cells, which were transfected with siRNA against GFP displayed equal cell death rates as the non-transfected cells (2-fold and 1.8-fold induction respectively compared to the basal level), GL261, which were transfected with siRNA against ATF-3 did not show TUNEL positive cells at all (0.9-fold induction, **fig. 3.29**).

4. Discussion

4.1. Neural precursor cells are attracted by experimental gliomas

4.1.1. Glioma-induced attraction of subventricular neural precursor cells is an intrinsic tissue response

In the present study it was demonstrated that neural precursor cells (NPCs) show tropism towards glioblastomas *in vivo*. It was further shown that these migrating precursor cells stem from one of the germinative centres, the subventricular zone (SVZ). This tropism seems to be specific for gliomas since neither a stab wound nor non-tumourigenic cells were able to mimic NPC attraction (24). Similar observations could be made under *in vitro* conditions, where SVZ explants were cultivated next to GL261 glioma cell aggregates. Single NPCs left the explant and migrated exclusively into the direction where the tumour cells were placed.

Tumour development was observed until 14 days after glioma inoculation because it has been shown that the accumulation of neural precursor cells (NPCs) around the tumour peaks at about this time point and declines later at around 30 days after operation (30 DPO). This could be due to progressive differentiation of NPCs around the tumour induced by secretion of growth factors by the tumour (24).

4.2. The anti-tumourigenic response of neural precursor cells

4.2.1. The age-related number of neural precursor cells around glioblastoma determines the extent of the anti-tumourigenic response

Having observed that neural precursor cells (NPCs) accumulate around gliomas, the impact was studied, which those NPCs have on the tumour cells.

Inoculation of glioma cells into mice of different age revealed that younger animals significantly outlive older ones with the same amount of tumour cell load. Identification of precursor cells demonstrated that the number of NPCs accumulating around the tumour declines proportionally to the age of the animal. Accordant to that, tumour sizes were increased in old animals and the brain pathology grew more severe the less NPCs were present at the site of the tumour, which included more local bleedings and a bigger extent of tissue destruction. This inverse correlation between the number of NPCs and the glioma

size was the first indication for an anti-tumourigenic role of precursor cells during glioma development. The second indication for the tumour suppressive role of neural precursors derived from the observation that these cells can prolong the survival of glioma bearing mice. Apparently, neural precursors hold the potential to inhibit glioma growth.

4.2.2. Subventricular proliferation as the key regulator between the distinct anti-tumourigenic response of young and adult mice

To investigate why adult animals recruit less neural precursor cells (NPCs) towards gliomas, subventricular proliferation was examined under pathological conditions. While whole cell numbers in young (P30) animals declined in the subventricular zone (SVZ), absolute numbers of BrdU labelled cells in the SVZ were maintained at a constant level during a timecourse of 14 days of tumour development. Thus, the relative number of proliferating subventricular cells, which was calculated by dividing the total number of cells through the number of proliferating cells, was increased within the two weeks. In contrast, adult mice were not able to gain this relative increase in proliferating cells. On the side ipsilateral to the tumour relative numbers of BrdU labelled cells even declined. Since this decrease of proliferating cells could not be observed on the contralateral hemisphere, it seems to be specifically mediated by the tumour. The altered relative number of proliferating cells between young and adult mice suggests that precursors in the P30 SVZ are more receptive for growth signals, derived from the tumour, than NPCs in the P90 brain. Alternatively, cell cycle length could be shortened in NPCs of young mice. However, there is enrichment for proliferating cells in P30 animals compared to P90 mice. Thus, the diminished number of accumulating NPCs around the tumour in adult animals is due to a reduced pool of proliferating subventricular cells. This reduction occurs exclusively in fully adult animals (P90) and is initiated by the tumour.

It appears likely that precursor cells obtain the information to which extent they should respond to tumour-derived growth signals in the subventricular zone. Once the cell has gained this information, which is dependent on the age of the animal, it retains it also independent of the surrounding tissue, which was shown under *in vitro* conditions. Neural precursor cells isolated from young SVZs displayed a higher level of proliferation upon stimulation with GL261 glioma cell conditioned medium compared to NPCs isolated from adult SVZs and this difference did not change over many platings. This indicates that a neural precursor cell, once programmed to have a phenotype according to a certain age,

will keep this phenotype *in vitro* and will not sense its own aging over many generations. This also means that it is mainly the stem cell microenvironment, i.e. the SVZ, which determines the age-related phenotype.

Since neither whole cell numbers nor numbers of dying cells in the SVZ were affected by the presence of a tumour in both young and adult animals, it can be assumed that the tumour mainly affects neural precursor cell physiology by having an impact on their proliferation. The fact that P30 mice, in contrast to P90 animals, displayed a decline in whole cell numbers over the timecourse of 14 days on both the ipsi- and contralateral side of the tumour suggests that this reduction occurred physiologically, i.e. due to aging of the animal.

4.2.3. D-type cyclin expression controls the anti-tumourigenic response of neural precursor cells

Mammalian cells use the cell cycle restriction point at the end of G1 phase to control responsiveness to exogenous growth signals. Primary regulators of the G1/S transition are the D-type cyclins, which consist of cyclin D1, D2 and D3 (61). Growth stimuli provoke expression of D-type cyclins, which are the regulatory subunits of cyclin dependent kinases (CDKs). Synthesis of D-type cyclins and subsequently CDK 4 or 6 leads to the phosphorylation of the retinoblastoma protein and subsequently entry into S-phase. As reported by Ferguson *et al.* (18), induction of this pathway is crucial for proliferation of neural precursor cells (NPCs). Kowalczyk *et al.* (45) reported that cyclin D2 is the only D-type cyclin expressed in neural precursor cells (NPCs) derived from the adult hippocampus, whereas young mice displayed expression of all three D-type cyclins. Moreover, knock out of cyclin D2 completely abrogated adult neurogenesis. Therefore cyclin D2 seems to control adult neurogenesis whereas cyclin D1 influences early neuronal development.

Under pathological conditions expression of cyclin D1 gradually declines in animals older than P30 and is not re-expressed in response to glioma growth. Quantification of precursor cell proliferation in cyclin D2 knockout animals demonstrated that D-type cyclins play an essential role for the proliferation of NPCs in the presence of a tumour. Proliferation rates in the P30 subventricular zone (SVZ) were much lower in the knockout animals compared to their wildtype littermates. The diminished amount of proliferating cells in these knockout mice was comparable to proliferation in aged animals, indicating that both loss of

cyclin D1, which ensues naturally by aging, and loss of cyclin D2, induced by mutation of the cyclin D2 gene, results in great reduction of proliferation. Loss of cyclin D1 and D2, which was the situation in the aged knockout mice, resulted in even larger reduction of dividing subventricular cells.

Not only did the elimination of cyclin D expression restrict subventricular proliferation, it also had major effects on tumour growth. Cyclin D2 deficient P30 mice developed tumours twice as big as the ones in P30 wildtype animals; P90 knockout mice generated tumours, which were 80 % increased in size compared to wildtype mice. These data point out that attenuation of NPC proliferation, either by aging or by knockout of cyclin D2, results in enhanced tumour growth and hence a more severe pathology.

The expression of cyclin D2 is strictly limited to the germinative centres (14) and germ line mutations of cyclin D2 only have an impact on adult neurogenesis and do not harm forebrain development (45). Peripheral impacts in cyclin D2 knockout animals are female infertility and cerebellar defects (10), which do not interfere with glioma development. Although decline of cyclin D1 throughout aging was observed, no use of cyclin D1 deficient animals was made because this cyclin affects more or less all cell types in the brain during pathology. This has been shown for microglia and astrocytes (35), neurons (4) and endothelia (17) while none of these effects have been observed for cyclin D2.

4.2.4. The proliferative response of neural precursor cells to gliomas is independent of p21

The tumour suppressor p21, also known as p21^{cip1/waf1} or cyclin dependent kinase inhibitor (CDKN) 1A, is a cell cycle inhibitor. Study of p21 expression in young (P30) and old (P90) tumour-bearing animals revealed that the older mice slightly lost p21 compared to the younger ones. This matches the decline of whole cell numbers in the subventricular zone in adult animals compared to younger ones. However, there was no difference in expression between the ipsi- and contralateral subventricular zones (SVZ) in young or old mice observable (Wälzlein *et al.*, submitted).

There are studies which show that p21 is required to prevent proliferative exhaustion specifically of stem cells in the brain during aging (39). It has further been reported that p21 contributes to the restriction of neural stem cell reactivity specifically to pathology (57). Yet, the observations made in our mouse model indicate that NPC proliferation in the

presence of a tumour occurs independently of p21 and is therefore probably unrelated to any changes in neural stem cell division.

The fact that the proliferative response of NPCs to gliomas seems to be controlled independent of p21 points out that the reduction of proliferation in the tumour-bearing hemispheres of old animals is also mediated p21 independently. The tumour suppressor protein p21 is a downstream effector of TGF- β mediated anti-growth signals and is abundantly secreted by the tumour (63;75). Since p21 knockout did not change subventricular proliferation in glioma bearing mice of P90, I conclude that the decrease of proliferation in the P90 SVZ is not mediated by tumour derived anti-growth signals like TGF- β .

4.2.5. The subventricular composition and the fraction of proliferating cells in young and old animals in the tumour-bearing hemisphere

Precursor cells in the subventricular zone (SVZ) can be divided into three subtypes, migrating neuroblasts (type A cells), type B cells and transient amplifying cells (type C cells). Type B cells can be further subdivided into slowly dividing cells, which are referred to as type B1 cells and represent the stem cells and into fast proliferating type B2 cells. I had ruled out that subventricular stem cells are differentially regulated with respect to the proliferation during tumour growth (see above, experiments in p21(-/-) mice). In the following I investigated the contribution of type B2 cells to proliferation in the SVZ in response to glioma. Like in all other BrdU labelling experiments, the animals received one BrdU pulse 2 h before killing, which should predominantly label the fast dividing cells (44).

The identified relative fraction of each precursor cell type to the group of all nestin-positive cells corresponds to the data reported by Doetsch *et al.* (13).

Young animals preserved a constant level of type B and C cells during the timecourse of tumour development. Only the relative amount of type A cells progressively declined within two weeks of tumour growth. It is therefore likely that they are responsible for the observed regression of whole cell numbers in the SVZ.

In adult animals (P90) all fast proliferating cells (type B2, type C and type A cells) showed a significant decline in whole cell numbers and level of proliferation. Interestingly, type A cells showed the same biphasic trend in proliferation during glioma growth, which was already observed for the whole cell population. Since type A cells are the largest fraction

of neural precursor cells in the SVZ they may have the strongest impact on the behaviour of the whole cell population. However, all adult precursor cells, probably with exception of the stem cells, are similarly affected by the cell division attenuating action of a glioma.

4.2.6. The anti-tumourigenic response of neural precursor cells is directly mediated via soluble factors

Both co-cultures of neural precursor cells (NPCs) with glioma cells and precursor cell-conditioned medium are able to kill glioblastoma cells. Therefore there is evidence that NPCs secrete one or more soluble factors, which induce(s) glioma cell death. This result also implies that glioma cell death is directly mediated from the precursor cell or from the NPC-conditioned medium independent from other cell types or tissue substances.

Importantly, the anti-tumourigenic ability of single neural precursor cells does not decline with aging. This was demonstrated by administration of conditioned medium from P30 and P90 neural precursors to GL261 cells, which could induce glioma cell death to a similar extent. However, in the aged animal much less neural precursors accumulated at the tumour since decreased proliferation in the SVZ makes less precursors available. Hence, this appears to be the main reason for the decline in the intrinsic anti-tumourigenic response in the fully adult brain.

Since precursor cell-conditioned medium also interferes with the rapid expansion of human grade III astrocytoma cells, the anti-tumourigenic response does not seem to be restricted to one species. This result could be of particular importance for future therapeutic development.

4.3. The character of neural precursor cell mediated glioma cell death

4.3.1. The role of activating transcription factor-3 in neural precursor cell induced glioma cell death

It was reported by some other groups that stem cells exert an anti-tumourigenic effect. For example Khakoo *et al.* (38) showed that human mesenchymal stem cells (MSCs) migrate to sites of tumourigenesis in an *in vivo* model of Kaposi's sarcoma and effectively inhibit tumor growth. They further show that human MSCs are able to prevent activation of the Akt protein kinase in tumour cells. Since the present work reports that neural precursor cells induce upregulation of activating transcription factor-3 (ATF-3) in glioma cells,

inhibition of Akt could be involved. Little is known about the interplay of ATF-3 and Akt but concurrent ATF-3 induction and Akt inactivation has been described (46). However, the identification of the death-inducing factor(s) still remains elusive.

Activating transcription factor-3 (ATF-3) belongs to the mammalian ATF/cAMP responsive element binding protein (CREB) family of transcription factors, which contains proteins with the basic region-leucine zipper (bZip) DNA binding domain. Activation of ATF-3 has been discussed as a response to stress signals, like for example ischemia, wounding, toxicity *in vivo* and cytokines, cell death-inducing agents etc. *in vitro* (28). There is evidence that the mitogen-activated protein kinases (MAPK) Erk, JNK and p38 are involved in the regulation of ATF-3, although the detailed regulatory signal pathways as well as the biological significance still have to be elucidated.

It was shown that ATF-3 is activated in GL261 glioma cells upon stimulation with neural precursor cell (NPC)-conditioned medium. It has further been demonstrated that ATF-3 induction is necessary and sufficient to induce NPC-mediated glioma cell death. Therefore, precursor cells or rather factors, which are released by these cells into the medium seem to represent a stress signal for glioma cells leading to activation of ATF-3 and eventually resulting in cell death.

It is known that ATF-3 receives feedback inhibition by the bZip protein Gadd153/Chop 10 (76). On the other hand, Gadd153/Chop 10 is a downstream target of ATF-3, which is interesting considering that Gadd153/Chop 10 was also differentially expressed in GL261 cells upon treatment with NPC-conditioned medium (albeit scored to be significant only in 2 out of 3 microarrays). However, the ATF-3 downstream effector Gadd34 was significantly upregulated in all three arrays. Since the transcription of these proteins (ATF-3, Gadd153/Chop10 and Gadd34) has been related to endoplasmic reticulum (ER) stress (48) and ATF-3 is also ER stress inducible (8), it is a strong argument that NPC-conditioned medium provokes induction of ER stress in glioma cells.

Fan *et al.* (16) reported that overexpression of ATF-3 is able to abate progression of cells from G1 to S phase, indicating that ATF-3 might slow down proliferation. Apparently, activation of ATF-3 can interfere with both cell cycle progression and cell viability, which was shown by *in vitro* overexpression of the ATF-3 protein in glioma cells, which resulted in an increase of TUNEL positive cells.

4.3.2. Neural precursor cell mediated glioma cell death – an alternative to apoptosis

One of the biggest obstacles in fighting glioblastomas is their insensitivity for apoptosis. Like in most neoplastic cells, essential pathways regulating apoptosis are disrupted in malignant gliomas; radiation or chemotherapy do also not result in activation of the extrinsic death receptor-dependent apoptotic pathway. It is assumed that increased expression of anti-apoptotic compared to pro-apoptotic proteins and a high level of inhibitor-of-apoptosis protein (IAP) might be the reason for the inability of tumour cells to induce the caspase-cascade upon apoptotic stimulation (52).

It was therefore not very surprising that GL261 glioma cells did not reveal caspase activity after treatment with neural precursor cell (NPC)-conditioned medium. The cell death inducing stimuli of NPC-conditioned medium generally do not seem to represent apoptotic signals since it also did not induce death-receptor mediated apoptosis in cells, which are very sensitive to this pathway. Yet, it is even more striking that cell death did occur. Electron microscopy of GL261 glioma cells, treated with NPC-conditioned medium did not display features typical for a specific type of cell death. Cells revealed general signs of bad condition like an inhomogeneous cytoplasm and a number of vacuoles. Since some of these vacuoles were filled with a substance resembling condensed protein, there was reason to discuss autophagic processes and autophagy as a possible cell death pathway. There are studies, which show that glioma cells are less resistant to type II programmed cell death (autophagy) than to type I programmed cell death (apoptosis) and therefore consider autophagic activity as an alternative tumour treatment (42). However, glioma cells were negative for specific markers for autophagy after treatment with NPC-conditioned medium (data not shown).

4.3.3. Endoplasmic reticulum stress as the likely glioma cell death inducing pathway

Since activating transcription factor-3 (ATF-3), a stress response gene, was induced in GL261 cells after treatment with neural precursor cell (NPC)-conditioned medium, stress-induced cell death has to be considered. There are numerous studies linking endoplasmic reticulum (ER) stress to mainly apoptosis but also to other, caspase-independent types of cell death. Disruption of the ER homeostasis leads to an evolutionarily conserved cell stress response, the unfolded protein response (UPR), which is thought to restore cell damage but can eventually cause cell death if dysfunctions are prolonged or serious (60).

Electron microscopy of the glioma cells treated with NPC-conditioned medium revealed cells displaying endoplasmic reticulum (ER) enlargement, which is characterized by protuberances of the ER membrane and is a morphological sign for ER stress.

The expression of other ER stress markers like for example translation of ATF-4 and phosphorylation of eIF2 α (74) has to be further examined. However, based on the presented data there is strong evidence that NPC-conditioned medium induces ER stress in glioma cells, leading to ATF-3 activation and finally resulting in cell death.

4.4. Neural precursor cells and their clinical relevance for gliomas

Neural precursor cells (NPCs) can give rise to glioblastomas by misregulated proliferation or differentiation (32). Moreover, more recent studies reported the existence of cancer stem cells, the most potent tumour initiating fraction of cells, which have been discovered in leukaemias and gliomas (21;30;64;65).

In addition to the theory that neural precursor cells give rise to gliomas, the present work reports that these precursor cells hold the capacity to provoke host-beneficial effects in response to existing tumours. It remains to be determined if neural precursors can have a specific anti-tumourigenic effect against these tumour initiating glioma stem cells, too.

Anti-tumourigenic responses (regarding classic tumour cells) have previously been described for exogenously applied, immortalised precursors from new born mice (5;66). This knowledge is now extended by the data showing that also endogenous, non-immortalised NPCs are able to combat gliomas. Since they are endogenous cells and already mediate an anti-tumourigenic response without exogenous manipulation, they occupy remarkable therapeutic potential. The fact that they also own migratory properties, which allows using them as vehicles for therapeutic substances, makes them even more appropriate for therapeutic purposes.

Attempts have been made before to use stem cells and their progeny for brain repair (29). However, models for stroke or cortical lesions for example did not succeed in recruiting enough precursor cells to the lesion to make sound conclusions about precursor cell activation (3;53;57).

The peak of onset of gliomas is between 55 and 65 years in humans, which makes age one of the main risk factors for this disease. Considering this, the data is of great clinical interest, which showed that older animals, which had a much shorter survival of gliomas than young mice, revealed reduced precursor cell proliferation, which turned out to be

regulated by D-type cyclins. Precursor cells might be genetically modified to re-express D-type cyclins, lost by aging to increase proliferation NPC proliferation and thus enhancing the anti-tumourigenic effect.

4.4.1. Neural precursor cells as delivery vehicles for therapeutic substances

While it is also still unknown what particular factor or combination of factors, released by the tumour, finally leads to the attraction of neural precursor cells (NPCs), Aboody *et al.* (1) showed that exogenous NPCs, which were implanted intracranially at a site distant from the tumour are able to migrate through normal tissue and track down glioma. At the same time these cells maintained their stable expression of a foreign gene, namely cytosine deaminase (CD), which was retrovirally transduced into the precursor cells. The target-orientated expression of this oncolytic drug led to the induction of tumour cell death. This promising finding suggests that NPCs could be used as delivery vehicles for therapeutic genes. The most challenging property of glioma cells is their extreme invasiveness, which makes it still impossible to cure higher grade gliomas because single cells can infiltrate the whole brain and lead to tumour relapses. Considering this, NPCs could be used in order to locate these disseminated tumour cells and erase them by expressing lethal genes. Since the present work reports the attraction of endogenous NPCs by gliomas, genetic modification of endogenous cells could even save the implantation of exogenous NPCs, which implies another risk factor.

4.4.1.1. Potential chemoattractants for neural precursor cells

It is one of the intrinsic properties of neural precursor cells to migrate. Under physiological conditions they migrate from the SVZ along the rostral migratory stream to the olfactory bulb, where they differentiate into interneurons. Although it is still unknown how this directed migration of NPCs is controlled on the molecular level, several candidates have been discussed to hold either repellent activity for neurons or to function as attractants for stem cells. One of these substances is the polysialylated form of the neural cell adhesion molecule (PSA-NCAM), a glycoprotein, which allows global modulation of cell-cell attachment and therefore also acts as a regulator in cell migration (7). It has been shown that the migration of neural precursor cells (NPCs) towards the olfactory bulb appears as a mechanism described as chain migration. Cells migrate in a stream and use each other as a substrate (49). Thus, PSA-NCAM is also used as a marker for type A cells, representing

migrating neuroblasts. It has further been shown that the vascular endothelial growth factor (VEGF), also a glycoprotein, acts as a chemoattractant for neural progenitor cells, which in turn express the VEGF-receptor 1 and 2 (78).

Whilst the process of migration of NPCs under physiological conditions still has to be investigated on the molecular level, it is also of strong interest, regarding therapeutic aspects, how this migration is regulated in the diseased brain. Substances, which are discussed as chemoattractants under physiological conditions, have to be taken into account in the pathological brain. Since tumour cells often signal via growth factors (e.g. VEGF), in an autocrine fashion, it is likely that NPCs are attracted by substances, secreted by the tumour. It was possible to show that NPCs leave SVZ tissue and migrate towards glioma cell aggregates, which were put next to the SVZ tissue. The tissue and cell aggregates were in no direct contact to each other. The fact that no direct cell-cell contact is required to induce migration implies that the attractant must be one or more soluble factor(s).

4.5. Regulation of neurogenesis throughout aging

4.5.1. Correlation between neuronal plasticity and the anti-tumourigenic effect of neural precursor cells

It is known that neurogenesis declines with increasing age (36). The present work reports that neurogenesis, i.e. dividing neural precursor cells (NPCs) mediate an anti-tumourigenic effect. Thus, young animals which are equipped with a larger number of NPCs, show improved survival of a glioblastoma compared to adult animals. If neurogenesis has such beneficial impacts on the brain, why is there a decline in adult animals, which obviously makes them more prone to the onset of glioblastoma? A possible presumption is that there is need for cellular plasticity at an early stage of development, which is provided by a large pool of precursor cells. Since these precursors have been extensively discussed as the cell of origin for brain tumours (1.2.), a bigger amount of NPCs also increases the chance that one of these cells undergoes a mutation and thereby gives rise to a glioma. It could well be that consequently neurogenesis is decreased at a timepoint when cellular plasticity is not required to a great extent anymore. A decrease in proliferating NPCs would reduce the risk that these dividing cells eventually transform (which likely occurs with aging) and may give rise to a tumour. However, the consequence of a decline in neurogenesis is also that

once a glioma has emerged, the anti-tumourigenic effect of the precursor cells is not effective anymore.

4.5.2. The anti-tumourigenic ability of neural precursor cells as a rescue mechanism for their likely transformation

Another issue is why do neural precursor cells (NPCs) have anti-tumourigenic abilities at all? As mentioned before, a neural precursor is the cell, which is at present seen as the most likely cell of origin for brain tumours. Since a proliferating cell is always a target for mutation and therefore transformation, it would be extremely beneficial for the animal if this cell is equipped with a protection mechanism. The observed anti-tumourigenic effect could therefore be seen as a rescue mechanism, provided by the precursor cell itself in case another cell experiences a mutation, which eventually results in the rise of a tumour.

The characterization of the induced glioma cell death, which is presented in this work, could be of big interest for further studies regarding glioma therapy and might make contributions in order to get more insight into stem cell biology.

5. Summary

Neural precursor cells (NPCs) migrate towards glioblastoma *in vivo* and *in vitro*. They are attracted by glioma cells independent of other cell types or surrounding tissue.

Young animals display prolonged survival after glioma inoculation compared to older animals due to the larger amount of precursors, which accumulate around the tumour. Young animals are naturally equipped with a greater number of NPCs. Additionally subventricular proliferation is even more restrained by the presence of a tumour only in adult animals. This further reduction of dividing precursors in adult mice solely refers to diminished proliferation rates since whole cell number and cell death rate was not affected by glioblastoma. Survival times of old animals can be aligned to the one of young mice by applying exogenous precursor cells.

Proliferative capacity of NPCs is determined by the age of the subventricular zone and is an intrinsic and stable attribute.

Neural precursors as well as NPC-conditioned medium directly induce glioma cell death. The transcription factor activating transcription factor-3 (ATF-3) is necessary and sufficient for the induction of cell death. Differential gene expression and morphological changes after administration of NPC-conditioned medium point to glioma cell death induced by endoplasmic reticulum stress.

Neuronale Vorläuferzellen migrieren spezifisch zu Glioblastomen *in vivo* und *in vitro*. Dieser Prozess findet unabhängig von anderen Zelltypen oder umgebendem Gewebe statt. Junge Mäuse verfügen nach Inokulierung von Gliomzellen über eine längere Überlebenszeit im Vergleich zu adulten Tieren. Dies lässt sich auf die erhöhte Anzahl von Vorläuferzellen, die um den Tumor herum akkumulieren, zurückführen. Junge Tiere besitzen von Natur aus eine höhere Anzahl von neuronalen Vorläuferzellen. Dazu kommt, dass die subventrikuläre Proliferation nur in adulten Tieren zusätzlich durch den Tumor negativ beeinflusst wird. Diese Reduktion von sich teilenden subventrikulären Vorläuferzellen in adulten Mäusen beruht ausschließlich auf einer verminderten Proliferationsrate da sowohl Gesamtzellzahl und Zelltodrate vom Tumor unbeeinflusst blieben. Es zeigte sich, dass adulte Tiere nach Gabe von exogenen Vorläuferzellen die Überlebenszeit junger Tiere erreichen.

Das proliferative Potential von neuronalen Vorläuferzellen wird durch das Alter der subventrikulären Zone determiniert und stellt eine intrinsische und stabile Eigenschaft dar. Neuronale Vorläuferzellen sowie Vorläuferzell-konditioniertes Medium induzieren Gliomzelltod unabhängig von äußeren Faktoren *in vitro*.

Der Transkriptionsfaktor *activating transcription factor-3* (ATF-3) ist für die Induktion von Gliomzelltod notwendig und hinreichend. Differentielle Genexpression und Morphologieänderung in Gliomzellen, induziert durch Vorläuferzell-konditioniertes Medium, lassen Zelltod durch endoplasmatischen Stress vermuten.

6. References

1. **Aboody,K.S., Brown,A., Rainov,N.G., Bower,K.A., Liu,S., Yang,W., Small,J.E., Herrlinger,U., Ourednik,V., Black,P.M. et al.** 2000. Neural stem cells display extensive tropism for pathology in adult brain: evidence from intracranial gliomas. *Proc.Natl.Acad.Sci.U.S.A* 97:12846-12851.
2. **Altman,J.** 1962. Are new neurons formed in the brains of adult mammals? *Science* 135:1127-1128.
3. **Arvidsson,A., Collin,T., Kirik,D., Kokaia,Z., and Lindvall,O.** 2002. Neuronal replacement from endogenous precursors in the adult brain after stroke. *Nat.Med.* 8:963-970.
4. **Bauer,S. and Patterson,P.H.** 2005. The cell cycle-apoptosis connection revisited in the adult brain. *J.Cell Biol.* 171:641-650.
5. **Benedetti,S., Pirola,B., Pollo,B., Magrassi,L., Bruzzone,M.G., Rigamonti,D., Galli,R., Selleri,S., Di Meco,F., De Fraja,C. et al.** 2000. Gene therapy of experimental brain tumors using neural progenitor cells. *Nat.Med.* 6:447-450.
6. **Bjerkvig,R., Tysnes,B.B., Aboody,K.S., Najbauer,J., and Terzis,A.J.** 2005. Opinion: the origin of the cancer stem cell: current controversies and new insights. *Nat.Rev.Cancer* 5:899-904.
7. **Bruses,J.L. and Rutishauser,U.** 2001. Roles, regulation, and mechanism of polysialic acid function during neural development. *Biochimie* 83:635-643.
8. **Cai,Y., Zhang,C., Nawa,T., Aso,T., Tanaka,M., Oshiro,S., Ichijo,H., and Kitajima,S.** 2000. Homocysteine-responsive ATF3 gene expression in human vascular endothelial cells: activation of c-Jun NH(2)-terminal kinase and promoter response element. *Blood* 96:2140-2148.
9. **Chazal,G., Durbec,P., Jankovski,A., Rougon,G., and Cremer,H.** 2000. Consequences of neural cell adhesion molecule deficiency on cell migration in the rostral migratory stream of the mouse. *J.Neurosci.* 20:1446-1457.

-
10. **Ciemerych,M.A. and Sicinski,P.** 2005. Cell cycle in mouse development. *Oncogene* 24:2877-2898.
 11. **DeAngelis,L.M.** 2001. Brain tumors. *N.Engl.J.Med.* 344:114-123.
 12. **Doetsch,F., Caille,I., Lim,D.A., Garcia-Verdugo,J.M., and Alvarez-Buylla,A.** 1999. Subventricular zone astrocytes are neural stem cells in the adult mammalian brain. *Cell* 97:703-716.
 13. **Doetsch,F., Garcia-Verdugo,J.M., and Alvarez-Buylla,A.** 1997. Cellular composition and three-dimensional organization of the subventricular germinal zone in the adult mammalian brain. *J.Neurosci.* 17:5046-5061.
 14. **Easterday,M.C., Dougherty,J.D., Jackson,R.L., Ou,J., Nakano,I., Paucar,A.A., Roobini,B., Dianati,M., Irvin,D.K., Weissman,I.L. et al.** 2003. Neural progenitor genes. Germinal zone expression and analysis of genetic overlap in stem cell populations. *Dev.Biol.* 264:309-322.
 15. **Engels,B., Noessner,E., Frankenberger,B., Blankenstein,T., Schendel,D.J., and Uckert,W.** 2005. Redirecting human T lymphocytes toward renal cell carcinoma specificity by retroviral transfer of T cell receptor genes. *Hum.Gene Ther.* 16:799-810.
 16. **Fan,F., Jin,S., Amundson,S.A., Tong,T., Fan,W., Zhao,H., Zhu,X., Mazzacurati,L., Li,X., Petrik,K.L. et al.** 2002. ATF3 induction following DNA damage is regulated by distinct signaling pathways and over-expression of ATF3 protein suppresses cells growth. *Oncogene* 21:7488-7496.
 17. **Fasanaro,P., Magenta,A., Zaccagnini,G., Cicchillitti,L., Fucile,S., Eusebi,F., Biglioli,P., Capogrossi,M.C., and Martelli,F.** 2006. Cyclin D1 degradation enhances endothelial cell survival upon oxidative stress. *FASEB J.* 20:1242-1244.
 18. **Ferguson,K.L., Callaghan,S.M., O'Hare,M.J., Park,D.S., and Slack,R.S.** 2000. The Rb-CDK4/6 signaling pathway is critical in neural precursor cell cycle regulation. *J.Biol.Chem.* 275:33593-33600.

-
19. **Friese,M.A., Steinle,A., and Weller,M.** 2004. The innate immune response in the central nervous system and its role in glioma immune surveillance. *Onkologie.* 27:487-491.
 20. **Gage,F.H.** 2000. Mammalian neural stem cells. *Science* 287:1433-1438.
 21. **Galli,R., Binda,E., Orfanelli,U., Cipelletti,B., Gritti,A., De Vitis,S., Fiocco,R., Foroni,C., Dimeco,F., and Vescovi,A.** 2004. Isolation and characterization of tumorigenic, stem-like neural precursors from human glioblastoma. *Cancer Res.* 64:7011-7021.
 22. **Gavrieli,Y., Sherman,Y., and Ben Sasson,S.A.** 1992. Identification of programmed cell death in situ via specific labeling of nuclear DNA fragmentation. *J.Cell Biol.* 119:493-501.
 23. **Geng,Y., Yu,Q., Sicinska,E., Das,M., Bronson,R.T., and Sicinski,P.** 2001. Deletion of the p27Kip1 gene restores normal development in cyclin D1-deficient mice. *Proc.Natl.Acad.Sci.U.S.A* 98:194-199.
 24. **Glass,R., Synowitz,M., Kronenberg,G., Walzlein,J.H., Markovic,D.S., Wang,L.P., Gast,D., Kiwit,J., Kempermann,G., and Kettenmann,H.** 2005. Glioblastoma-induced attraction of endogenous neural precursor cells is associated with improved survival. *J.Neurosci.* 25:2637-2646.
 25. **Goldman,S.** 2003. Glia as neural progenitor cells. *Trends Neurosci.* 26:590-596.
 26. **Goldman,S.A. and Windrem,M.S.** 2006. Cell replacement therapy in neurological disease. *Philos.Trans.R.Soc.Lond B Biol.Sci.* 361:1463-1475.
 27. **Gurok,U., Steinhoff,C., Lipkowitz,B., Ropers,H.H., Scharff,C., and Nuber,U.A.** 2004. Gene expression changes in the course of neural progenitor cell differentiation. *J.Neurosci.* 24:5982-6002.
 28. **Hai,T., Wolfgang,C.D., Marsee,D.K., Allen,A.E., and Sivaprasad,U.** 1999. ATF3 and stress responses. *Gene Expr.* 7:321-335.

-
29. **Hallbergson,A.F., Gnatenco,C., and Peterson,D.A.** 2003. Neurogenesis and brain injury: managing a renewable resource for repair. *J.Clin.Invest* 112:1128-1133.
 30. **Hemmati,H.D., Nakano,I., Lazareff,J.A., Masterman-Smith,M., Geschwind,D.H., Bronner-Fraser,M., and Kornblum,H.I.** 2003. Cancerous stem cells can arise from pediatric brain tumors. *Proc.Natl.Acad.Sci.U.S.A* 100:15178-15183.
 31. **Holland,E.C.** 2001. Gliomagenesis: genetic alterations and mouse models. *Nat.Rev.Genet.* 2:120-129.
 32. **Holland,E.C., Celestino,J., Dai,C., Schaefer,L., Sawaya,R.E., and Fuller,G.N.** 2000. Combined activation of Ras and Akt in neural progenitors induces glioblastoma formation in mice. *Nat.Genet.* 25:55-57.
 33. **Huber,W., von Heydebreck,A., Sultmann,H., Poustka,A., and Vingron,M.** 2002. Variance stabilization applied to microarray data calibration and to the quantification of differential expression. *Bioinformatics.* 18 Suppl 1:S96-104.
 34. **Kargel,E., Menzel,R., Honeck,H., Vogel,F., Bohmer,A., and Schunck,W.H.** 1996. Candida maltosa NADPH-cytochrome P450 reductase: cloning of a full-length cDNA, heterologous expression in Saccharomyces cerevisiae and function of the N-terminal region for membrane anchoring and proliferation of the endoplasmic reticulum. *Yeast* 12:333-348.
 35. **Kato,H., Takahashi,A., and Itoyama,Y.** 2003. Cell cycle protein expression in proliferating microglia and astrocytes following transient global cerebral ischemia in the rat. *Brain Res.Bull.* 60:215-221.
 36. **Kempermann,G.** 2006. Adult Neurogenesis. Stem Cells and Neuronal Development in the Adult Brain. Oxford University Press.
 37. **Kettenmann,H. and Ransom,B.** 1995. Neuroglia. Oxford University Press.

-
38. **Khakoo,A.Y., Pati,S., Anderson,S.A., Reid,W., Elshal,M.F., Rovira,I.I., Nguyen,A.T., Malide,D., Combs,C.A., Hall,G. et al.** 2006. Human mesenchymal stem cells exert potent antitumorigenic effects in a model of Kaposi's sarcoma. *J.Exp.Med.* 203:1235-1247.
 39. **Kippin,T.E., Martens,D.J., and van der Kooy,D.** 2005. p21 loss compromises the relative quiescence of forebrain stem cell proliferation leading to exhaustion of their proliferation capacity. *Genes Dev.* 19:756-767.
 40. **Kleihues,P., Burger,P.C., and Scheithauer,B.W.** 1993. The new WHO classification of brain tumours. *Brain Pathol.* 3:255-268.
 41. **Kleihues,P., Soylemezoglu,F., Schauble,B., Scheithauer,B.W., and Burger,P.C.** 1995. Histopathology, classification, and grading of gliomas. *Glia* 15:211-221.
 42. **Knobbe,C.B., Merlo,A., and Reifenberger,G.** 2002. Pten signaling in gliomas. *Neuro.-oncol.* 4:196-211.
 43. **Konopka,G. and Bonni,A.** 2003. Signaling pathways regulating gliomagenesis. *Curr.Mol.Med.* 3:73-84.
 44. **Kornack,D.R. and Rakic,P.** 1998. Changes in cell-cycle kinetics during the development and evolution of primate neocortex. *Proc.Natl.Acad.Sci.U.S.A* 95:1242-1246.
 45. **Kowalczyk,A., Filipkowski,R.K., Rylski,M., Wilczynski,G.M., Konopacki,F.A., Jaworski,J., Ciemerych,M.A., Sicinski,P., and Kaczmarek,L.** 2004. The critical role of cyclin D2 in adult neurogenesis. *J.Cell Biol.* 167:209-213.
 46. **Kumagai,K., Ando,Y., Kiyosawa,N., Ito,K., Kawai,R., Yamoto,T., Manabe,S., and Teranishi,M.** 2006. Toxicoproteomic investigation of the molecular mechanisms of cycloheximide-induced hepatocellular apoptosis in rat liver. *Toxicology* 228:299-309.
 47. **Kuwajima,T., Taniura,H., Nishimura,I., and Yoshikawa,K.** 2004. Necdin interacts with the Msx2 homeodomain protein via MAGE-D1 to promote myogenic differentiation of C2C12 cells. *J.Biol.Chem.* 279:40484-40493.

-
48. **Liu,N., Scofield,V.L., Qiang,W., Yan,M., Kuang,X., and Wong,P.K.** 2006. Interaction between endoplasmic reticulum stress and caspase 8 activation in retrovirus MoMuLV-ts1-infected astrocytes. *Virology* 348:398-405.
 49. **Lois,C. and Alvarez-Buylla,A.** 1994. Long-distance neuronal migration in the adult mammalian brain. *Science* 264:1145-1148.
 50. **Lothian,C. and Lendahl,U.** 1997. An evolutionarily conserved region in the second intron of the human nestin gene directs gene expression to CNS progenitor cells and to early neural crest cells. *Eur.J.Neurosci.* 9:452-462.
 51. **Lou,H. and Dean,M.** 2007. Targeted therapy for cancer stem cells: the patched pathway and ABC transporters. *Oncogene* 26:1357-1360.
 52. **Nakamura,J.L.** 2007. The epidermal growth factor receptor in malignant gliomas: pathogenesis and therapeutic implications. *Expert.Opin.Ther.Targets.* 11:463-472.
 53. **Nakatomi,H., Kuriu,T., Okabe,S., Yamamoto,S., Hatano,O., Kawahara,N., Tamura,A., Kirino,T., and Nakafuku,M.** 2002. Regeneration of hippocampal pyramidal neurons after ischemic brain injury by recruitment of endogenous neural progenitors. *Cell* 110:429-441.
 54. **Noble,M.** 2000. Can neural stem cells be used to track down and destroy migratory brain tumor cells while also providing a means of repairing tumor-associated damage? *Proc.Natl.Acad.Sci.U.S.A* 97:12393-12395.
 55. **Okano,H., Imai,T., and Okabe,M.** 2002. Musashi: a translational regulator of cell fate. *J.Cell Sci.* 115:1355-1359.
 56. **Parsa,A.T. and Holland,E.C.** 2004. Cooperative translational control of gene expression by Ras and Akt in cancer. *Trends Mol.Med.* 10:607-613.
 57. **Qiu,J., Takagi,Y., Harada,J., Rodrigues,N., Moskowitz,M.A., Scadden,D.T., and Cheng,T.** 2004. Regenerative response in ischemic brain restricted by p21^{cip1/waf1}. *J.Exp.Med.* 199:937-945.

-
58. **Reynolds,B.A. and Weiss,S.** 1992. Generation of neurons and astrocytes from isolated cells of the adult mammalian central nervous system. *Science* 255:1707-1710.
 59. **Sabatti,C., Karsten,S.L., and Geschwind,D.H.** 2002. Thresholding rules for recovering a sparse signal from microarray experiments. *Math.Biosci.* 176:17-34.
 60. **Shapiro,W.R. and Shapiro,J.R.** 1998. Biology and treatment of malignant glioma. *Oncology (Williston.Park)* 12:233-240.
 61. **Sherr,C.J.** 1995. D-type cyclins. *Trends Biochem.Sci.* 20:187-190.
 62. **Shoshan,Y., Nishiyama,A., Chang,A., Mork,S., Barnett,G.H., Cowell,J.K., Trapp,B.D., and Staugaitis,S.M.** 1999. Expression of oligodendrocyte progenitor cell antigens by gliomas: implications for the histogenesis of brain tumors. *Proc.Natl.Acad.Sci.U.S.A* 96:10361-10366.
 63. **Siegenthaler,J.A. and Miller,M.W.** 2005. Transforming growth factor beta 1 promotes cell cycle exit through the cyclin-dependent kinase inhibitor p21 in the developing cerebral cortex. *J.Neurosci.* 25:8627-8636.
 64. **Singh,S.K., Clarke,I.D., Terasaki,M., Bonn,V.E., Hawkins,C., Squire,J., and Dirks,P.B.** 2003. Identification of a cancer stem cell in human brain tumors. *Cancer Res.* 63:5821-5828.
 65. **Singh,S.K., Hawkins,C., Clarke,I.D., Squire,J.A., Bayani,J., Hide,T., Henkelman,R.M., Cusimano,M.D., and Dirks,P.B.** 2004. Identification of human brain tumour initiating cells. *Nature* 432:396-401.
 66. **Staffin,K., Honeth,G., Kalliomaki,S., Kjellman,C., Edvardsen,K., and Lindvall,M.** 2004. Neural progenitor cell lines inhibit rat tumor growth in vivo. *Cancer Res.* 64:5347-5354.
 67. **Stupp,R., Mason,W.P., van den Bent,M.J., Weller,M., Fisher,B., Taphoorn,M.J., Belanger,K., Brandes,A.A., Marosi,C., Bogdahn,U. et al.** 2005. Radiotherapy plus concomitant and adjuvant temozolomide for glioblastoma. *N.Engl.J.Med.* 352:987-996.

-
68. **Sturrock,R.R. and Smart,I.H.** 1980. A morphological study of the mouse subependymal layer from embryonic life to old age. *J.Anat.* 130:391-415.
 69. **Tanaka,T., Serneo,F.F., Tseng,H.C., Kulkarni,A.B., Tsai,L.H., and Gleeson,J.G.** 2004. Cdk5 phosphorylation of doublecortin ser297 regulates its effect on neuronal migration. *Neuron* 41:215-227.
 70. **Tokuyasu,K.T.** 1980. Immunocytochemistry on ultrathin frozen sections. *Histochem.J.* 12:381-403.
 71. **Tokuyasu,K.T.** 1986. Application of cryoultramicrotomy to immunocytochemistry. *J.Microsc.* 143:139-149.
 72. **Tsujimoto,Y. and Shimizu,S.** 2005. Another way to die: autophagic programmed cell death. *Cell Death.Differ.* 12 Suppl 2:1528-1534.
 73. **Vescovi,A.L., Galli,R., and Reynolds,B.A.** 2006. Brain tumour stem cells. *Nat.Rev.Cancer* 6:425-436.
 74. **Wek,R.C., Jiang,H.Y., and Anthony,T.G.** 2006. Coping with stress: eIF2 kinases and translational control. *Biochem.Soc.Trans.* 34:7-11.
 75. **Wick,W., Naumann,U., and Weller,M.** 2006. Transforming growth factor-beta: a molecular target for the future therapy of glioblastoma. *Curr.Pharm.Des* 12:341-349.
 76. **Wolfgang,C.D., Chen,B.P., Martindale,J.L., Holbrook,N.J., and Hai,T.** 1997. gadd153/Chop10, a potential target gene of the transcriptional repressor ATF3. *Mol.Cell Biol.* 17:6700-6707.
 77. **Wyllie,A.H.** 1987. Apoptosis: cell death in tissue regulation. *J.Pathol.* 153:313-316.
 78. **Zhang,H., Vutskits,L., Pepper,M.S., and Kiss,J.Z.** 2003. VEGF is a chemoattractant for FGF-2-stimulated neural progenitors. *J.Cell Biol.* 163:1375-1384.

Acknowledgements

I would like to thank Professor Dr. Helmut Kettenmann for giving me the opportunity to do my PhD in his lab and providing excellent working conditions and lab equipment.

I also thank Dr. Rainer Glass for the valuable help and support he provided for my work. For great technical assistance a very big Thank you to Irene Haupt and Brigitte Gerlach. Many thanks also to Birgit Jarchow for the best help for all matters besides science.

I thank the Graduate Program Berlin „Dynamics and Evolution of Cellular and Macromolecular Processes“ for giving me financial support and also the International Graduate Program Medical Neuroscience of the Berlin Medical University-Charité.

For giving me huge morally support and very often just making my time in – and outside - the lab most enjoyable I would like to thank all of my lab mates, in particular my dear colleagues Sridhar Chirasani and Dr. Darko Marković. A special Thank you to Jochen Müller for going through the three years with me and most of all to my dear friend Giselle Cheung, the statistics and organizing specialist.

Further on, I thank my parents and my brother, who encouraged me in any way.

Not least thank you to my friend Christine Kirsch for long-distance support.

Finally I would like to thank Hannes Kieseewetter for being always there for me.

Curriculum vitae

Mein Lebenslauf wird aus Datenschutzgründen in der elektronischen Version meiner Arbeit nicht mit veröffentlicht.

List of publications

Rainer Glass, Michael Synowitz, Golo Kronenberg, **Joo-Hee Walzlein**, Darko S. Markovic, Li-Ping Wang, Daniela Gast, Jürgen Kiwit, Gerd Kempermann and Helmut Kettenmann. (2005) Glioblastoma-induced attraction of endogenous neural precursor cells is associated with improved survival. *J Neurosci.* Mar 9;25(10):2637-46.

Joo-Hee Walzlein, Michael Synowitz, Boris Engels, Darko S. Markovic, Konrad Gabrusiewicz, Evgeni Nikolaev, Ulrike Harms, Christoph Harms, Matthias Endres, Kazuaki Yoshikawa, Bozena Kaminska, Gerd Kempermann, Wolfgang Uckert, Leszek Kaczmarek, Helmut Kettenmann and Rainer Glass. (2007) The anti-tumourigenic response of neural precursors depends on subventricular proliferation and age. Submitted.

Meetings with poster presentations

May 2005	Euroglia 2005 - VII European Meeting on glial cell function in health and disease, Amsterdam, The Netherlands
August 2005	Graduate program: Dynamics and Evolution of Cellular and Macromolecular Processes, 5 th International Workshop on Bioinformatics and Systems Biology, Berlin, Germany
July 2006	5 th Forum of European Neuroscience 2006, Vienna, Austria
July 2006	Graduate program: Dynamics and Evolution of Cellular and Macromolecular Processes, 6 th International Workshop on Bioinformatics and Systems Biology, Boston, USA
September 2006	8 th MDC/FMP PhD Student Retreat "Walking Molecular Pathways", Motzen, Germany
December 2006	Brain Tumor 2006, Berlin, Germany

Eidesstattliche Erklärung

Ich, Joo-Hee Wälzlein, erkläre, dass ich die vorgelegte Dissertationsschrift mit dem Thema: „Endogenous neural precursor cells suppress glioblastoma“ selbst verfasst und keine anderen als die angegebenen Quellen und Hilfsmittel benutzt, ohne die (unzulässige) Hilfe Dritter verfasst und auch in Teilen keine Kopien anderer Arbeiten dargestellt habe.

Berlin, den

Joo-Hee Wälzlein